**Use of Nano Particles for Stable Pickering Emulsion in
Heavy Oil Recovery**

by

Zhenjie Wang

A thesis submitted in partial fulfillment of the requirements for the degree of

Master of Science

in

Petroleum Engineering

Department of Civil and Environmental Engineering
University of Alberta

Abstract

Emulsion flooding and heavy oil recovery by in-situ emulsion formation have been reported to show great potential in enhancing heavy oil recovery. Emulsion stability is the key issue controlling the success of this process; conventionally, surfactants were used to facilitate emulsification and improve emulsion stability, increasing the cost remarkably. In this study, we explored using nanoparticles as a cost-effective alternative to expensive surfactants to generate stable Pickering emulsions and studied their effects on heavy oil recovery.

Various types of nanoparticles (NPs) have been tested in this study, which can be classified into three main groups: (1) commercial NPs available in market, including cellulose nanocrystals (CNC), silica, alumina, magnetite, and zirconia, (2) natural clay particles existing naturally in the reservoir, including bentonite and kaolinite clays, and (3) natural asphaltenes in heavy crude oil. Heavy oil with a viscosity of 15,640 cP at 21°C from Western Saskatchewan was used in all the experiments except for the asphaltene study, where model oil composed of heavy mineral oil (653 cP) and toluene was used to get a good control over the asphaltene content in the oil. Effects of particle concentration, water salinity, pH, and water to oil ratio (WOR) on emulsion stability were systematically studied through glass vial tests. For clay particles and asphaltenes, sandpack flooding experiments were performed using the formulation which favored the formation of stable emulsions. The effluent samples were analyzed to determine both the emulsion type and the formation of a stable emulsion. The recoveries were monitored and cross-checked with produced effluent samples. In order to visualize the in-situ behavior of clay particles in the porous medium, glass bead micromodels with known amounts of clays were prepared and microscopy images were

taken to monitor the movement of clay particles in pore space. The transparent mineral oil instead of opaque heavy oil was used in these micromodel tests for better visualization results.

The results showed that for commercial NPs, CNC could become an effective O/W emulsifier by either adjusting pH (3 or 11) or salinity (0.1 wt.% NaCl). The salinity had a great impact on the viscosity of the CNC suspension and CNC-stabilized emulsions with an upper salinity limit of 1 wt.% NaCl; the required minimum concentration for CNC to stabilize O/W emulsion was 1 wt.%. Phase inversion from oil-in-water (O/W) to water-in-oil (W/O) emulsions occurred when the oil content was above 0.6. For clay particles, bentonite is more effective than kaolinite in terms of stabilizing O/W emulsions and the required bentonite concentration was 3 wt.%. The upper salinity limit for bentonite to stabilize O/W emulsion was 0.6 wt.% NaCl at neutral pH (i.e., 7) condition. High pH solutions (i.e., 12) further help the bentonite stabilize emulsions through a reduction of interfacial tension (IFT) between oil and water. Besides, the bentonite-stabilized O/W emulsion inverted to W/O emulsion when the oil content was 0.5 and above. The sandpack flooding test showed that the presence of bentonite further improved final oil recovery from 40%—where no clays were added in the sandpacks—to 49% where 5 wt.% of bentonites were present in the sandpack during the low salinity waterflood process (i.e., DIW). For asphaltenes, an optimal concentration of 0.5 wt.% asphaltenes in oil was found to stabilize W/O emulsions with the model oil composed of 70 vol.% heavy mineral oil (653 cP) and 30 vol.% toluene. The emulsion stability was further improved by adding 1 wt.% NaCl or adjusting the water pH to 10 and above. Additionally, in-situ emulsification of W/O emulsions by asphaltenes was observed in the sandpacks initially saturated with model oil containing 0.5 wt.% asphaltenes.

This study promotes an alternative way to generate stable -Pickering- emulsions without using expensive surfactants, a method that will reduce the operational costs and thus favor the field application step of emulsification in heavy-oil recovery.

Acknowledgements

Contents

List of Tables

List of Figures

Chapter 1: Introduction

Introduction

Canada is famous for its heavy-oil reservoirs with oil viscosities ranging from 50 cP to 50, 000 cP under reservoir conditions (Bryan and Kantzas 2009). Due to the high viscosity of the heavy oil, large amounts of oil remain trapped in the reservoir and the primary recovery of these resources is usually very low (around 3 to 8%) (Adams 1982); therefore, most enhanced oil recovery methods focus on reducing the oil viscosity through methods like thermal and solvent injection. However, thermal methods are not applicable to thin reservoirs where there will be a huge loss of heat to the overburden and underburden formations (Arab et al. 2018a), and solvent injection is not economical due to the high costs of solvents compared to the market value of recovered heavy oil (Sarma et al. 1995). Chemical enhanced oil recovery (EOR) is an alternative method to address these technical and economic issues.

One of the main mechanisms used in improving heavy oil recovery by chemical methods is emulsification; both oil-in-water (O/W) and water-in-oil (W/O) emulsions were reported to increase oil recovery (Bryan and Kantzas 2009; Kumar et al. 2012). Chemicals like surfactants are usually expensive and have other issues like chemical retention in the reservoir and thermal degradation under high-temperature conditions (Sharma et al. 2015), further hindering their application in field scale. S. U. Pickering (1907) observed that solid particles can also stabilize emulsions with higher stability than those stabilized by surfactants (soap), since then such emulsions stabilized by solid particles were named Pickering emulsions.

Pickering emulsions are quite stable and can withstand harsh reservoir conditions (i.e., high pressure and high temperature, HPHT) owing to the high mechanical strength of nanoparticles (Agista et al. 2018). Due to their high adsorption energy, the adsorption of nanoparticles can be thought of as irreversible in contrast to surfactant molecules which exist in a kinetic adsorption-desorption equilibrium (Binks 2002). Additionally, their small size (nano scale) enables free movements of NPs in porous oil reservoirs (Zhang et al. 2010). Another advantage of such Pickering emulsion is the low preparation cost in comparison to chemical methods—if the particle

emulsifier can be readily made or abundant in nature. Consequently, many studies have been directed to the applicability of Pickering emulsions in enhanced oil recovery (EOR) (Aveyard et al. 2003; Bragg and Varadaraj 2006; Cheraghian and Hendraningrat 2016; Arab et al. 2018a).

Factors affecting Pickering emulsion stability include but are not limited to particle size and concentration, electrolyte type and concentration, water to oil ratio, oil type, and particle wettability (Binks 2002; Aveyard et al. 2003). Among these parameters, particle wettability is generally regarded as a key parameter controlling the emulsion type and stability. Usually, water-wet (hydrophilic) particles tend to stabilize O/W emulsions and oil-wet (hydrophobic) particles tend to stabilize W/O emulsions (Binks 2002). The emulsion stability is at its maximum when the particle is neutral wet since the adsorption energy of particles is highest when the particle has a contact angle of 90° (Levine et al. 1989).

Many particles were reported to stabilize emulsions, such as silica, magnetic particles, clays, cellulose nanocrystals (CNC), and alumina (Al_2O_3) (Binks et al. 2005; Kalashnikova et al. 2012; Chevalier and Bolzinger 2013; Nallamilli et al. 2015; Xu et al. 2018). Asphaltenes can also act like effective emulsifiers if their properties are appropriately adjusted since they have both polar (e.g., carboxylic acids, -COOH) and non-polar components (e.g., aliphatic chain) (Joonaki et al. 2019) which make them a surface active species able to adsorb at the oil-water interface thus leading to stable emulsions. These particles can be classified into three groups according to their produced sources: (1) commercial NPs which are available in the market, including cellulose nanocrystals (CNC), silica, alumina, magnetite, etc., (2) clay particles existing naturally in the reservoir, including bentonite and kaolinite clays, and (3) asphaltenes existing naturally in heavy crude oil.

This research intends to identify the optimal conditions for each of these three groups of particles to generate stable Pickering emulsions and study their effects on heavy oil recovery through both glass vial tests and sandpack flooding experiments.

1.1 Statement of the Problem

Even though there are a lot of studies on using nanoparticles to generate stable Pickering emulsions, few studies considered their applicability for field application. To the best of our

knowledge, previously reported studies of Pickering emulsions in the petroleum industry still involved surfactants to help nanoparticles stabilize emulsions. Besides, most studies of Pickering emulsions used simple or light oil instead of heavy oil to prepare emulsions, such as decane (Kim et al. 2017; Xu et al. 2017), biodiesel (Pei et al. 2015), hexane, and light crude oil (around 6 cP at 25°C) (Arshad et al. 2018). Therefore, it is worthwhile to explore the possibilities of generating stable emulsions using heavy oil samples, and solely nanoparticles, a method of which has a low preparation cost compared with expensive surfactants. Regarding this aspect, the following questions need to be answered:

1) What kind of nanoparticles can generate stable Pickering emulsions with heavy oil?
2) What are optimal conditions (e.g., water pH, salinity, particle concentration, and asphaltene content) for stable emulsions?
3) Can such emulsions stabilized by asphaltenes be formed in-situ in a porous medium and thus improve recovery?

1.2 Aims and Objectives

This study aims to select nanoparticles as effective emulsifiers, identify the optimal conditions for these nanoparticles to stabilize Pickering emulsions, as well as observe their effects on heavy oil recovery. More specific objectives include:

1) Screen the effective commercial nanoparticles as emulsifiers through glass vial tests. Tested commercial nanoparticles include cellulose nanocrystals (CNC), silica, alumina, magnetite, and zirconia. After screening, investigate how a range of physical parameters, such as particle concentration, water-to-oil ratio (WOR), and temperature affect emulsion stability.
2) Identify the optimal conditions for natural clays (bentonite and kaolinite) to stabilize emulsions and test their capacity of in-situ emulsification through both glass vial tests and sandpack flooding experiments.
3) Activate natural asphaltenes as effective emulsifiers by adjusting both water (salinity, pH, etc.) and oil (asphaltene content) environments through glass vial tests. Also, study their effects on oil recovery through sandpack flooding tests.

1.3 Structure of the Thesis

This paper-based thesis contains five chapters. Chapters 2 and 3 contain two papers which were previously published in two research journals. Chapter 4 consists one paper that has been submitted to a research journal for peer review.

Chapter 1. This chapter introduces the research background of this thesis which covers the definition of Pickering emulsion, their advantages over surfactant-stabilized emulsions, and their applications in EOR area. The challenges of applying this new technique (Pickering emulsions) in the field are stated along with the aims and objectives of this research.

Chapter 2. This chapter presents a laboratory study of screening commercial nanoparticles for generating stable Pickering emulsions. Methodologies for evaluating emulsion type and stability were established. Five nanoparticles—including cellulose nanocrystals (CNC), silica, alumina, magnetite, and zirconia—were tested through glass vial tests regarding their emulsification capacity with a Western Saskatchewan heavy crude oil sample (15,640 cP at 21°C); the screening parameters are water salinity and pH. After identifying the most effective emulsifier, effects of particle concentration, WOR, and temperature on nanoparticle-stabilized emulsions were investigated. The emulsion stabilization mechanisms were studied through an epi-fluorescent transmitted microscope. The rheological properties of NP-stabilized emulsions were also measured under various salinity conditions.

Chapter 3. After establishing methodologies for evaluating NP-stabilized emulsions, this chapter explores and presents the possibilities of activating naturally occurring nanoparticles (clays) in the reservoir. The same Western Saskatchewan heavy oil sample (15,640 cP at 21°C) was used to ensure the consistency of the work. Two common clay particles in the reservoir were studied, including bentonite and kaolinite. The generated emulsions by these two clays were evaluated through glass vial tests. Effects of particle concentration, water salinity, and pH—as well as WOR on clay-stabilized emulsions—were investigated. Sandpacks with different clay compositions were prepared and used to simulate the porous medium and flooding tests were run to probe the possibility of in-situ activation of clays as the Pickering agents. In order to visualize the in-situ behavior of clays in the porous medium, glass bead micromodels with known amounts of clays were also prepared and flooded with different water solutions.

Chapter 4. This chapter demonstrates ways to activate another natural particle (asphaltenes) to generate stable Pickering emulsions. Asphaltenes were separated from the heavy oil used in previous chapters. Then model oil was prepared by adding various amounts of asphaltenes into the mineral oil with a portion of toluene, of which helps the dissolution of asphaltene in oil phase. The effects of asphaltene content in oil, water salinity, and pH as well as WOR on asphaltene-stabilized emulsions were systematically studied through glass vial tests to identify the optimal conditions for generating stable emulsions. Sandpack flooding tests were then performed to investigate if the identified optimal conditions can also help asphaltenes generate emulsions in-situ and how will it affect oil recovery.

Chapter 5. This chapter summarizes the conclusions and contributions of this work. The limitations and recommendations on this study are also presented in this chapter for further improvement in future work.

Chapter 2: Preliminary Screening and Formulation of New Generation Nanoparticles for Stable Pickering Emulsion in Cold and Hot Heavy Oil Recovery

This chapter of the thesis is a modified version of a published research paper SPE 200190. The conference paper version SPE-200190-MS was accepted for presentation at the SPE conference at Oman Petroleum & Energy Show held in Muscat, Oman, 9-11 March 2020. The journal version of this research paper SPE-200190-PA has been published in SPE Reservoir Evaluation & Engineering Journal.

2.1 Preface

Injecting water with chemicals to generate emulsions in the reservoir is a promising method in the enhancement of heavy oil recovery, as the formation of oil-in-water (O/W) emulsions reduce oil viscosity significantly. Nanoparticles (NPs) (Pickering emulsions) can be used for this purpose as a cost-effective alternative to expensive surfactants; however, such Pickering emulsions need to be stable for successful applications. The objective of this study is to: (1) screen the effective emulsifier for O/W emulsions from a broad range of solid NPs and identify suitable Pickering emulsifying agents (e.g., adjusting pH or salt concentration) that can render emulsions stable at relevant conditions, and (2) investigate how a range of physical parameters, such as particle concentration, water-to-oil ratio (WOR), and temperature affect emulsion stability.

Five NPs—including cellulose nanocrystals (CNC), silica, alumina, magnetite, and zirconia— were tested on their capability to stabilize O/W emulsions through glass vial screening tests under various pH and salinity conditions. The screening results showed that CNC could become an effective emulsifier by either adjusting pH or salinity. In addition, zeta potential measurements were conducted to explain the observations. The stabilization mechanisms of CNC were studied through an epi-fluorescent transmitted microscope showing that the formation of a dense particle layer around the oil droplets, as well as a network in the continuous phase, were the two main mechanisms accounting for the high stability of the emulsions stabilized by CNC. Effects of particle concentrations on the emulsion stability were studied quantitatively by analyzing the droplet size distributions calculated by the open-source ImageJ software, with the results showing a sharp decrease in droplet size, followed by a smooth change as particle concentration increased. For the WOR effect, phase inversion from O/W to W/O emulsions was observed when the oil content was above 0.6. The thermal stability of emulsions was studied both macroscopically by glass bottle tests and microscopically through a microscope, both of which show that the CNC stabilized emulsions remained thermally stable up to 100°C. The rheological properties of both aqueous dispersions of CNC and the corresponding O/W emulsions were also measured under various salinity conditions. The results showed that the salinity had a great impact on the viscosity of the CNC suspension and the typical shear thinning behavior of Pickering emulsions.

This study provides an option to enhance emulsion stability without surfactants, which will reduce the costs and facilitate field applications of emulsion flooding in heavy oil recovery.

Key words: Pickering emulsion, nanoparticle, CNC, heavy oil recovery, thermal stability, WOR, rheology.

2.2 Introduction

Canada is well known for its heavy-oil reservoirs with viscosities ranging from 50 cP to 50, 000 cP under reservoir conditions (Bryan and Kantzas 2009). Due to the high viscosity of the heavy oil, large amounts of oil remain trapped in the reservoir; therefore, most enhanced oil recovery methods focus on reducing the oil viscosity through methods like thermal and solvent injection. However, thermal methods are not applicable to thin reservoirs where there will be a huge loss of heat to the overburden and under burden formations (Arab et al. 2018a), and solvent injection is not economical due to the high costs of solvents compared to the market value of recovered heavy oil (Sarma et al. 1995). Chemical enhanced oil recovery (EOR) is an alternative method to address these technical and economic issues.

Generation of oil-in-water (O/W) emulsions through ASP (alkaline-surfactant-polymer) flooding can help reduce oil viscosity, thus improving the transportability of heavy oil in reservoirs (Delamaide et al. 2014). Bryan and Kantzas (2009) found that the formation of O/W emulsions by alkali-surfactant (AS) flooding improved sweep efficiency significantly by entrapment and entrainment of oil droplets. For the field applications of emulsions, emulsion stability and costs are key issues, as emulsions stabilized by surfactants are usually not stable at high temperatures due to the thermal degradation of surfactants (Sharma et al. 2015). The costs of surfactants also hinder field applications of emulsions due to the current low oil and gas prices. Therefore, the objective of this project is to generate stable and low-cost emulsions stabilized mainly by nanoparticles (NPs).

Emulsions stabilized by solid particles are also known as Pickering emulsions, named after S.U. Pickering who was thought to be the first to report O/W emulsions stabilized by solid particles adsorbed at the oil-water interface (Pickering 1907). Pickering emulsions are quite stable and can withstand harsh reservoir conditions (i.e., high pressure and high temperature, which we refer to as "HPHT" hereafter.) because of the high mechanical strength of nanoparticles (Agista et al. 2018). Because of the high adsorption energy, the adsorption of nanoparticles can be thought of as irreversible in contrast to surfactant molecules which are in a kinetic adsorption-desorption equilibrium (Binks 2002). The adsorption of NPs at the interface leads to the alteration of boundary conditions from slip to non-slip which slows down the drainage of an intervening film when two droplets approach and try to coalesce and thus improves emulsion stability. Despite their much larger size than surfactants that have been just compared previously, their small size (nano scale) enables free movements of NPs in porous oil reservoirs (Zhang et al. 2010). Consequently, many studies have been directed to the applicability of Pickering emulsions in EOR. Bragg and Varadaraj (2006) showed capabilities of particles with various shapes, such as plate, bar, and spherical shapes to stabilize crude oil in water (O/W) emulsions when combining with pH enhancing agents (i.e., sodium hydroxide NaOH). Good review papers summarized emulsion stabilization mechanisms by nanoparticles (Aveyard et al. 2003), applications of nanoparticles in EOR (Cheraghian and Hendraningrat 2016), and possible synergistic effects between surfactants and nanoparticles (Arab et al. 2018a). Pei et al. (2015) showed that synergistic effects between silica nanoparticles and cationic surfactant such as Cetyl Trimethyl Ammonium Bromide (CTAB) on improving O/W emulsion stability existed and observed marked increase of heavy oil recovery by core flooding and micromodel methods. Arab et al. (2018b) found negatively charged silica nanoparticles helped anionic surfactant stabilize heavy oil-in-water emulsions with oil viscosity of 14,850 cP at 25°C. Our previous core flooding tests (Lee and Babadagli 2018) also showed that adding silica nanoparticles to surfactant solutions, such as Dodecyl Trimethyl Ammonium Bromide (DTAB) and CTAB could significantly improve the recovery of heavy oil with a viscosity of 4,812 cP at 25°C.

However, to the best of our knowledge, previously reported studies of Pickering emulsions in the petroleum industry still involved surfactants to help nanoparticles stabilize emulsions. Besides, most studies of Pickering emulsions used simple or light oil instead of heavy oil to prepare emulsions, such as decane (Kim et al. 2017; Xu et al. 2017), biodiesel (Pei et al. 2015), hexane,

and light crude oil (around 6 cP at 25°C) (Arshad et al. 2018). Therefore, it is worthwhile to explore the possibilities of preparing stable heavy oil-in-water emulsions stabilized solely by nanoparticles. For nanoparticles to be effective emulsifiers, the wettability is a key parameter and should be neutral (i.e., around 90°), since their adsorption energy becomes a maximum under neutral wettability condition (Levine et al. 1989). The corresponding adsorption energy can be on the order of 103kT and hence the adsorption can be regarded as irreversible (Aveyard et al. 2003). The wettability of colloidal particles has been reported to be related to their surface charge which renders the surface hydrophilic. Reducing the surface charge therefore renders the surface less hydrophilic (more neutral wetting) (Binks et al. 2008). Adding an opposite charge (by pH adjustment or electrolyte) to the surface of the nanoparticles can adjust the surface charge (Binks and Lumsdon 1999). Therefore, in this paper, we aim to find effective nanoparticles that can work as emulsifiers for stabilizing heavy oil-in-water emulsions by adjusting the pH and the salinity conditions of the aqueous phase.

Many types of particles can stabilize O/W emulsions as long as they fulfill the partial wetting condition of oil and water (Cheraghian and Hendraningrat 2016). These particles include silica (SiO_2)–which is the most studied particle due to their low cost and abundance (Arab et al. 2018a), cellulose nanocrystals (CNC)–which is environmentally friendly (Kalashnikova et al. 2012) and have been tested in core flooding (Pandey et al. 2018), alumina (Al_2O_3) (Xu et al. 2018), iron (II, III) oxide (Fe_3O_4) (Nallamilli et al. 2015), and zirconia (ZrO_2) (Agista et al. 2018). In this study, we examined capabilities of these nanoparticles to stabilize heavy oil-in-water emulsions through glass vial tests and microscopic study. First, different nanoparticles were screened under various pH (3-11) and salinity (2-175 mM NaCl) conditions through glass vial tests of which were followed by zeta potential measurements. Then the stabilization mechanisms of nanoparticle acting as effective emulsifier were studied through microscope study. Finally, the effects of nanoparticle concentration, water to oil ratio (WOR) and temperature on emulsion stability were examined for the applicability to oil field application. Rheological properties of both the aqueous dispersions and the Pickering emulsions of these nanoparticles were also studied.

2.3 Experimental

Materials. Heavy oil (15,640 cP at 21°C) from Western Saskatchewan was used for all the experiments. The mean total acid number (TAN) of the heavy oil was 2.21 mg KOH/g. The saturates, aromatics, resins, and asphaltenes (SARA) components of the heavy oil were as follows: saturates (29.75%), aromatics (23.32%), resins (29.83%), and asphaltenes (15.35%). Transparent mineral oil (poly-butene) (15,800 cP at 20°C) was used for fluorescent visualization tests. Deionized water (DIW) was used for all the experiments and pH of DIW was around 7 (i.e., 6.80). Silica (SiO_2 10-20 nm), alumina (Al_2O_3 50 nm), iron (II, III) oxide (Fe_3O_4 50 nm), and zirconia (ZrO_2 <100 nm) were purchased from commercial sources, Canada. Sulfated cellulose nanocrystals (CNC 70 nm by DLS) was obtained in a salt form with $Na+$ as the counter-ion and used as received. All the nanoparticles mentioned above were provided in powder forms. Sodium chloride (NaCl, 99%) was used to adjust aqueous salinity conditions. Hydrochloric acid solution (HCl, 1 N) and sodium hydroxide (NaOH, ≥ 97.0%) were used to adjust pH conditions. Calcofluor white stain (CFW M2R, 1 g/l, Evans blue 0.5 g/l) was used to dye CNC to enhance contrast of some images.

Aqueous dispersion of nanoparticles. First, aqueous solutions of different salinities (e.g., 2, 17, and 175 mM NaCl) were prepared using sodium chloride (NaCl) and deionized water. The pH of the solutions was adjusted by adding hydrochloric acid (HCl) or sodium hydroxide (NaOH) into deionized water (DIW) and was measured by a pH meter. Then nanoparticles were dispersed in aqueous solutions by sonicating for two minutes to prevent aggregation. The power of sonication was kept constant for all samples at 75% of the maximum capacity.

Formulation of Pickering emulsion. The heavy oil or mineral oil was mixed with aqueous solutions of NPs at 1:1 volume ratio (5 ml oil: 5 ml aqueous solution) unless otherwise stated (e.g., 2/8, 4/6, 6/4, and 8/2 for studying water to oil ratio effects) by using a homogenizer (the Polytron PT 10-35 GT). The mixture was homogenized for two minutes at a speed of 10,000 rpm. All the experiments were performed at room temperature (21°C) unless otherwise stated. The particle concentration was 1 w/v% for most experiments unless otherwise stated (e.g., 0.02, 0.1, 0.5, and 1 w/v%) for studying particle concentration effects.

Emulsion characterization. The emulsion type was deduced first from looking at the appearance. For example, easy flows suggested low viscosities and vice versa. Since the viscosity of the heavy oil is much higher (15,640 cP at 21°C) than that of water, the difference in the viscosity between

O/W emulsions and W/O emulsions must be large. Then, this first deduction was further confirmed by microscopic observations.

The emulsion stability was evaluated by direct visual inspection of the phase separation at different times (right after the sample preparation and 24 hours later) through glass vial tests.

Microscopy images of emulsions were recorded by a high-speed CMOS camera which was connected to a transmitted light microscope with epi-fluorescent function. Emulsion droplet size distribution was calculated by ImageJ software. At least 300 droplets were chosen for droplet size analysis. In ImageJ software, the average droplet radius was calculated based on an area average method as shown by Eq. 1, where D_{ave} is the average droplet diameter, A_i is the area of ith droplet and n is the number of total droplets chosen for analysis.

$$D_{ave} = \sqrt{(\frac{4\sum_{i=1}^{n} A_i}{n \times \pi})} \tag{1}$$

Zeta potential measurement. The Zeta potential and the particle size of nanoparticle dispersions under different pH and salinity conditions were measured by a Malvern® Panalytical® Zetasizer® Nano (Malvern Panalytical Limited, Worchestershire, UK) instrument. The Zeta potential was determined by measuring the electrophoretic mobility first and then converting it to the zeta potential by the Henry equation (Eq. 2) and Smoluchowski approximation. The particle size was determined from dynamic light scattering (DLS). The particle concentration was maintained at 0.25 w/v% and an average of three measurements for each sample was reported.

$$U_E = \frac{2\varepsilon z f(ka)}{3\eta} \tag{2}$$

Where U_E is electrophoretic mobility, z is the zeta potential, ε is the dielectric constant, η is the viscosity of the dispersant, and $f(ka)$ is Henry's functions (approximated with Smoluchowski model as 1.5 in aqueous media).

Rheology measurement. The viscosity of both the aqueous dispersions (without oil) and the Pickering emulsions (with oil) under various salinity conditions was measured by a cone and plate viscometer over a wide range of shear rates.

Thermal study. The Pickering emulsions right after homogenization were heated in a water bath to two temperatures (one batch to 80°C and another to 100°C) for 10 minutes. Another batch of the same emulsion sample was kept at room temperature (21°C) without heating for control. The temperature was controlled by a hot plate and monitored by a thermometer. After the emulsion samples were heated in water bath for 10 minutes, they were transferred to graduated glass bottles for the observation of emulsion stability (phase separation over time) at room temperature. Next, the rheology of the emulsions 24 hours after the preparation was measured at room temperature and compared. The samples were also observed under the microscope.

2.4 Results and Discussion

2.4.1 Glass vial screening tests of various nanoparticles by adjusting pH

Five NPs (CNC, SiO_2, Al_2O_3, Fe_3O_4, and ZrO_2) were tested for their capabilities to stabilize O/W emulsions under various pH conditions without any addition of surfactants or salts. The particle concentrations were kept at 1 w/v% for all samples. **Table 1** shows the experimental parameters of these screening tests. The results of the glass vial tests for various nanoparticles are shown in **Fig. 1**.

Table 1-Experimental scheme for screening different NPs by adjusting pH.

Form	Particle Concentration, w/v%	Salinity, w/v% (NaCl)	WOR	NP type	pH
				CNC	3, 5, 7, 9, 11
				SiO_2	3, 5, 7, 9, 11
Solid Powder	1	0	1:1	Al_2O_3	3, 5, 7, 9, 11
				Fe_3O_4	3, 5, 7, 9, 11
				ZrO_2	3, 5, 7, 9, 11

Fig. 1a shows that at pH=3 and pH=11 conditions, CNC could form and stabilize O/W emulsions, as confirmed by visual inspections of easy flows of the emulsion phase by tilting the glass vial and the microscopic observations that less oil and water separated from the emulsion phase compared to other cases. It is noteworthy that the interface between the upper emulsion phase and the lower water phase was flat at pH=3 and 11, while the interface was curved at the other pH conditions (5,

7, and 9). This is because the interfacial tension (IFT) between the O/W emulsion phase and the water phase below was lower compared with that between pure oil and water or between a W/O emulsion and water, since the continuous phase of an O/W emulsion is water. Therefore, when the O/W emulsion contacted with an excess water phase, the flat interface would be expected. The emulsion was most stable at pH=3 where all the oil was emulsified into water and minimum water separated from the emulsion 24 hours after the homogenization. At pH=11, in contrast, some oil separated as shown on the top layer in the rightmost glass vial (three layers: oil, O/W emulsion, and water from top to bottom as indicated by red arrows) in **Fig. 1a**. For all the other nanoparticles, almost complete water-oil phase separation occurred within 24 hours after the homogenization and the water-oil interface was curved which indicated the high IFT between the two phases. Here, the lower phase was water and the upper phase was either oil or a W/O emulsion phase (where oil is the continuous phase), as confirmed under a microscope (**Figs. 1b–e**). Therefore, by comparison, CNC was the best choice in terms of both formation and stabilization of O/W emulsions by adjusting pH among all other nanoparticles tested (SiO_2, Al_2O_3, Fe_3O_4, and ZrO_2).

To explain why CNC was an effective emulsifier at certain pH conditions (pH=3 and pH=11), the zeta potential and the z-average diameter of aqueous dispersions of CNC (without oil) were measured as shown in **Fig. 2**. The measurements were performed without addition of background electrolyte (NaCl), so the ionic strength difference between the samples with various pH only resulted from the pH determining ions (e.g., H^+, Cl^- from HCl and Na^+, OH^- from NaOH). **Fig. 2** shows that the CNC suspension was stable under pH conditions between 3 and 11, since the particle size (Z-average diameter) was similar under all pH conditions tested, around the original size of 65 nm, which is close to 70 nm as provided by the supplier. Zhong et al. (2012) also observed stable CNC suspensions between pH 2 and 11. The absolute value of zeta potential was maximum (62 mV) at pH=7 which was the pure DIW condition without addition of pH adjusting ions (e.g., HCl and NaOH) or any electrolytes. This indicates that the surface charge was not screened by any cations and was expected to be high. As the pH was lowered from 7 to 3 by adding HCl solution (0.1 M), the absolute value of zeta potential decreased to 45 mV meaning less negatively charged, which may be due to the protonation of sulfate group ($-O-SO3^-$) on CNC (Hubbe et al. 2017). As the pH was raised from 7 to 11 by adding NaOH, there was also a decrease in the absolute value of zeta potential (from 62 mV to 50 mV). This was because the Na+ introduced by the NaOH would cause electrostatic screening effect where the diffuse layer

thickness or Debye length was compressed by counterion (Na+ here) and makes CNC less negatively charged (Zhong et al. 2012). Prathapan et al. (2016) also observed similar trends of zeta potential versus pH where the absolute value of the zeta potential was maximum at neutral pH and reduced as pH deviated from neutral. Combining the results from Kalashnikova et al. (2012), who observed that: (1) reduced surface charge due to desulfation or electrostatic screening by addition of counter-ions lead to a weaker zeta potential of CNC, (2) the reduced surface charge or electrostatic force lead to the weaker electrostatic repulsions which make the hydrophobic plane ((200)β/(220)α plane) of CNC accessible to oil, corresponding to CNC becoming more neutral wetting (contact angle closer to 90º) when an oil is present, and (3) a contact angle closer to 90º is expected to improve the stability of O/W emulsions. It is reasonable to observe that CNC stabilized O/W emulsions at pH=3 and 11 where the electrostatic repulsion was low as indicated by zeta potential (**Fig. 2**).
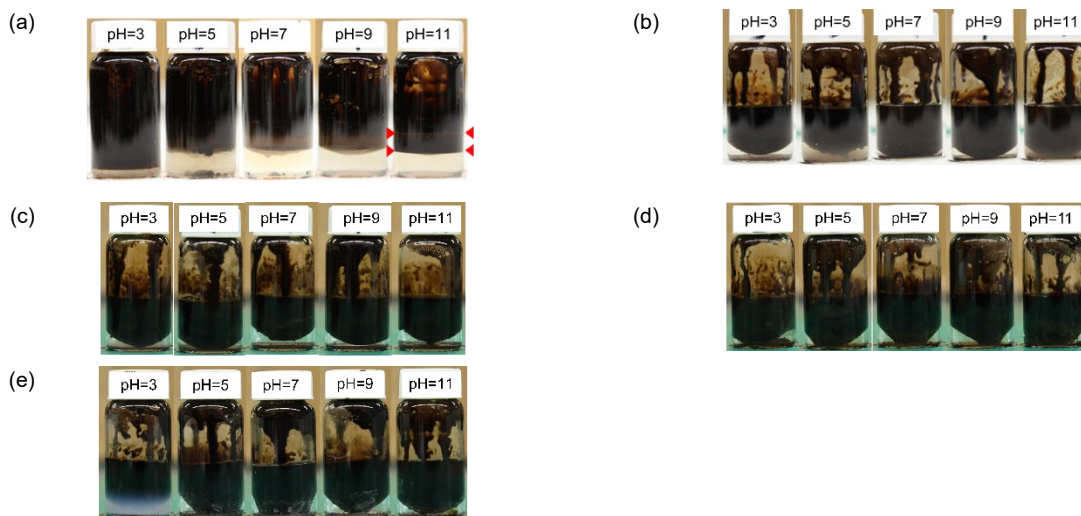
Figure 1—Glass vials 24 hours after homogenization containing heavy oil and dispersions of various nanoparticles under different pH conditions: (a) CNC, (b) SiO$_2$, (c) Al$_2$O$_3$, (d) Fe$_3$O$_4$, and (e) ZrO$_2$.
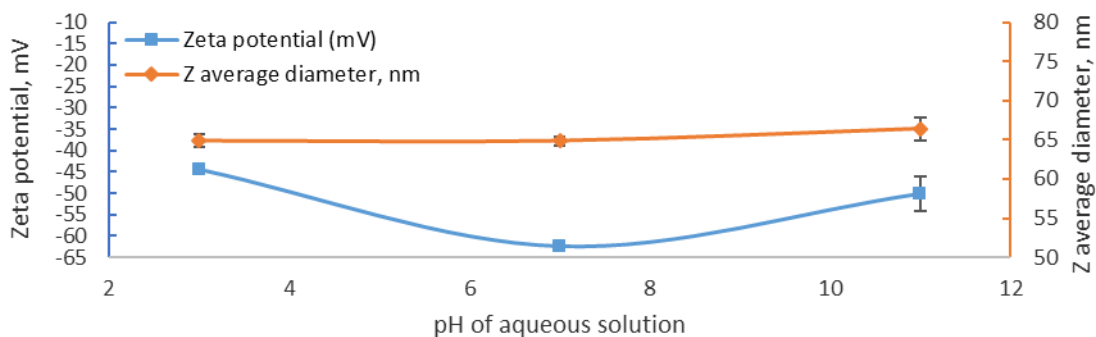
Figure 2—Zeta potential and z-average diameter of 0.25 w/v% CNC dispersed in aqueous solution with various pH and without addition of background electrolyte.

2.4.2 Glass vial screening tests of various nanoparticles by adjusting salinity

Five NPs (CNC, SiO$_2$, Al$_2$O$_3$, Fe$_3$O$_4$, and ZrO$_2$) were tested for their capabilities to stabilize O/W emulsions under various salinity (NaCl) conditions at pH=7. Since the cellulose nanocrystals were provided by CelluForce Inc. in a salt form with Na+ as the counter ion (see above), it is logical to use a strong electrolyte that has Na+ as the cation. Generally, multiple counter ions can dissociate off a single polyelectrolyte or a colloidal particle (including a nanoparticle) and the dissociation constant is a function of pH, so the system pH needs to be controlled. Since we used HCl and

NaOH for the pH adjustments, it is logical to use NaCl as the salt in this study. And the range of salinities was set between 2 mN (100 ppm) and 175 mM (10,000 ppm) in order to study the emulsion behavior under relatively broad salinity conditions. The emulsions became unstable above the NaCl condition of 10, 000 ppm and CNC suspensions also aggregated significantly above this salinity. The particle concentrations were kept at 1 w/v% for all samples. **Table 2** shows the experimental scheme for these screening tests. Results of glass vial tests for various nanoparticles are shown in **Fig. 3**. **Fig. 3a** shows that adding a small amount of NaCl (e.g., 2 mM) helps CNC stabilize the O/W emulsion but the emulsion was not stable to creaming; when the NaCl concentration was above 17 mM, the emulsions were very stable without any oil/water separated from the emulsion phase 24 hours after emulsion preparation. For other nanoparticles (e.g., SiO_2, Al_2O_3, Fe_3O_4, and ZrO_2), it was even hard to mix the heavy oil and the aqueous phase when preparing emulsions by homogenization and most, if not all, complete phase separation was observed for all samples 24 hours after emulsion preparation (**Figs. 3b–e**). Note that for some glass vial pictures, such as **Figs. 3b** and **3d**, the phase separation was not clearly visible due to adhesion of oil onto the walls of the glass vials. Thus, the upper phase of all samples shown in **Figs. 3b-e** was examined by observing the flows of the fluid under a microscope. The upper phase was either oil or W/O emulsion. Both had high viscosities and therefore are undesirable for the flow in porous medium.

Therefore, CNC was chosen as an effective emulsifier for further analysis. In order to study the effects of salinity on CNC dispersion, zeta potential measurements were performed on CNC suspension under various salinity conditions.

Table 2—Experimental scheme for screening different NPs by adjusting salinity.

Form	Particle Concentration, w/v%	pH	WOR	NP type	Salinity, mM (ppm) NaCl
Solid Powder	1	7	1:1	CNC	2 (100), 17 (1,000), 175 (10,000)
				SiO_2	
				Al_2O_3	
				Fe_3O_4	
				ZrO_2	

Fig. 4 shows that the zeta potential became weaker and the particle size of the aqueous dispersions of CNC (without oil) increased with increasing salt concentration. The electrostatic force between CNC particles weakened (less negative zeta potential) and the nanoparticles aggregated, as expected from the addition of NaCl which would screen the electrostatic repulsion between the CNC particles (Tang et al. 2014). When the electrostatic repulsion between CNC particles was reduced, the CNC would be wetted by both oil and water (Kalashnikova et al. 2012) because the hydrophobic crystalline plane ((200)β/(220)α) of CNC will become more accessible by oil making it more oil wet (Cherhal et al. 2016). This neutral wetting stabilized the emulsions as shown in **Fig. 3a**. Also, the aggregation of CNC will form a network in the continuous phase which will improve the emulsion stability to creaming by modifying its rheological property, which will be explained in the stabilization mechanism and rheological property sections later (Sections 2.4.3 and 2.4.7). What is more, according to the adsorption energy (E) of a particle at the oil-water interface as expressed in Eq. 3, which measures the energy required to remove the particle to either the water (negative sign) or the oil phase (positive sign), larger particle size (r) leads to higher adsorption energy (E) and thus generating more stable Pickering emulsions (Binks 2002).

$$E = \pi r^2 \gamma_{ow}(1 \pm \cos\theta)^2 \tag{3}$$

Where E is adsorption energy, r is particle radius, γ_{ow} is interfacial tension between oil and water phase, and θ is water contact angle of the particle.
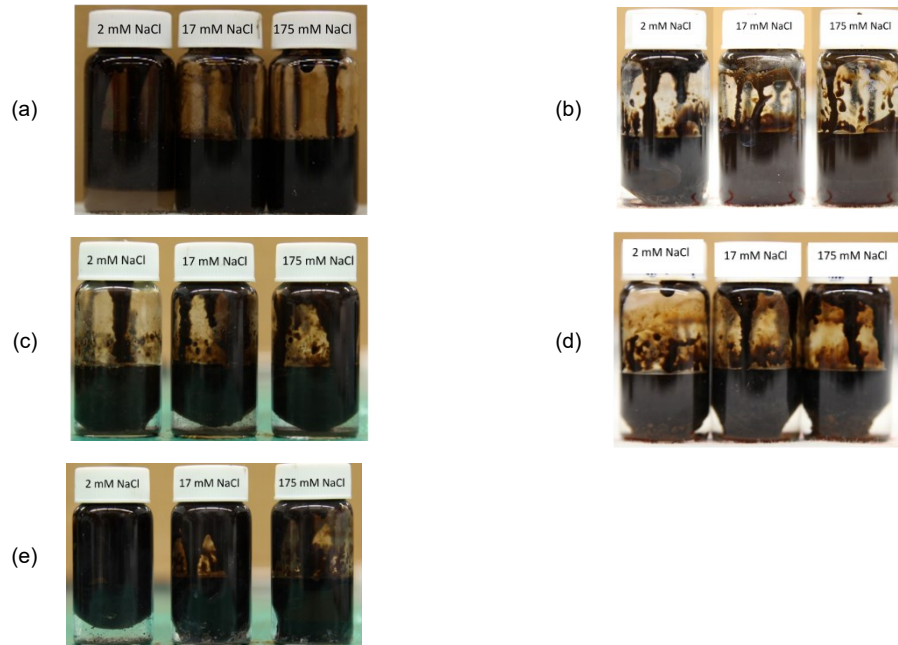
Figure 3—Glass vials 24 hour after homogenization containing heavy oil and dispersions of various nanoparticles under different salinity conditions: (a) CNC, (b) SiO$_2$, (c) Al$_2$O$_3$, (d) Fe$_3$O$_4$, and (e) ZrO$_2$.
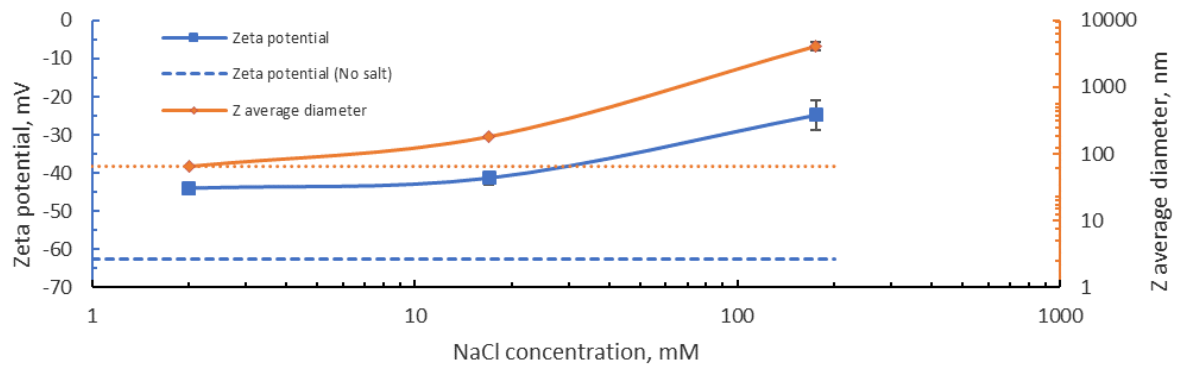
Figure 4—Zeta potential and z-average diameter of 0.25 w/v% CNC dispersed in aqueous solution with various salinity (NaCl) at pH=7.

2.4.3 Stabilization mechanisms of emulsions by CNC

Emulsion stabilization mechanisms of CNC were studied microscopically under both low (17 mM NaCl) and relatively high (175 mM NaCl) salinity conditions through an epi-fluorescent microscope. CNC was dyed with Calcofluor white (CFW).

O/W emulsions were prepared with heavy oil and then observed under a microscope. **Fig. 5a** shows that at low-salinity (17 mM NaCl) conditions, some CNC particles were able to adsorb onto the water-oil interface and form a dense layer, shown as the bright blue layer around the black oil droplets indicated by red arrows. This layer prevented the coalescence of the oil droplets since no oil separation was observed in glass vial tests, as shown in **Fig. 3a**. The blue aqueous phase background under fluorescent light means that the excess CNC particles were fully dispersed in the aqueous phase as indicated by the red arrow in **Fig. 5a**, because the CNC particles were dyed with CFW, which will show as blue under fluorescent light. The zeta potential of CNC was -41 mV, as shown in **Fig. 4**, and the strong electrostatic repulsion kept the suspensions stable (Zhong et al. 2012). Therefore, the main stabilization mechanism of the CNCs under the low salinity conditions was the formation of dense CNC particle layers around the oil droplets which impeded the coalescence between droplets. At a higher salinity condition (175 mM NaCl), **Fig. 5b** shows that the CNC particles still formed dense layers around droplets. In addition, the excess CNC in the continuous water phase formed a network through aggregation due to the weaker zeta potential (e.g., -25 mV), as shown in **Fig. 4**, under which circumstance attractive van der Walls force and the hydrophobic force became dominant. The formation of a network will increase the effective viscosity of the continuous phase, as will be shown later in the rheological property section (Section 2.4.7). When such a continuous phase is an aqueous phase, as in O/W emulsions, such network can trap oil and further improve the emulsion stability to creaming and coalescence, (Tang et al. 2014; Nallamilli et al. 2015). In addition to the developed CNC network, the larger particle size at relatively high-salinity condition (175 mM), as indicated in **Fig. 4**, leads to higher adsorption energy E, as discussed in the Glass Vial Screening Test section (Eq. 3). The particle size will also improve emulsion stability and, thus the droplet size looks smaller at 175 mM NaCl condition compared to that at 17 mM condition as shown in **Figs. 5** and **6** because of the improved emulsion stability.

Next, in order to obtain better visualization results of the emulsion structure under fluorescent light, emulsions were prepared with mineral oil having a similar viscosity to the heavy oil and were observed under a microscope as shown in **Fig. 6**. Under low salinity condition (17 mM NaCl), **Fig. 6a** shows particle layers around the droplets as the bright blue layers and the surplus CNC dispersed in the aqueous phase as the blue background. **Fig. 6b** shows the same location as **Fig. 6a**, but with overlaid fluorescent and bright field light for comparison. **Fig. 6c** shows both the CNC layer around oil droplets and aggregated network in the continuous aqueous phase under a relatively high salinity condition (175 mM NaCl), which further improved emulsion stability to creaming and coalescence. **Fig. 6d** shows the same location as **Fig. 6c**, but again with overlaid fluorescent and bright field light. The preceding observations with the mineral oil were consistent with the heavy oil samples. The CNC will form a dense layer around the oil droplets and be fully dispersed in water phase under low salinity condition (17 mM NaCl) while aggregated under the relatively high salinity condition (175 mM NaCl).

To summarize, at the low salinity conditions, CNC formed dense layers around oil droplets impeding droplet coalescence, while at the relatively high salinity conditions CNC formed both dense layers around oil droplets and a network in the continuous water phase further improving the emulsion stability to creaming and coalescence.

(a)   (b)
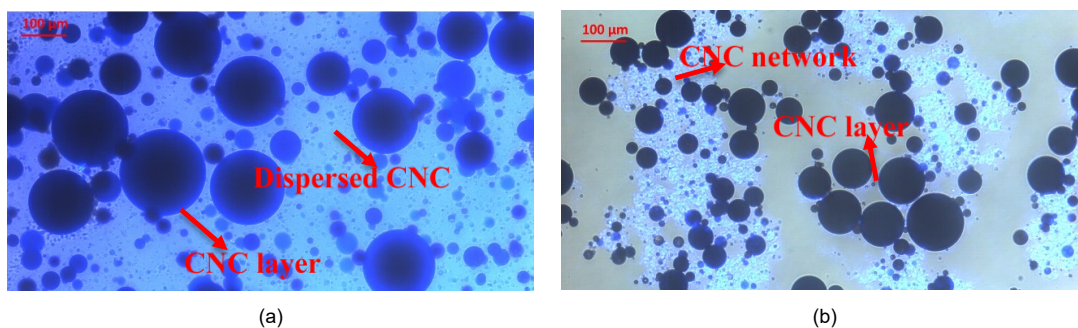
Figure 5—Overlaid fluorescent and bright field microscopy images of heavy oil in water emulsions under (a) 17 mM NaCl, and (b) 175 mM NaCl conditions. Concentration of CNC was 1 w/v% for both samples.
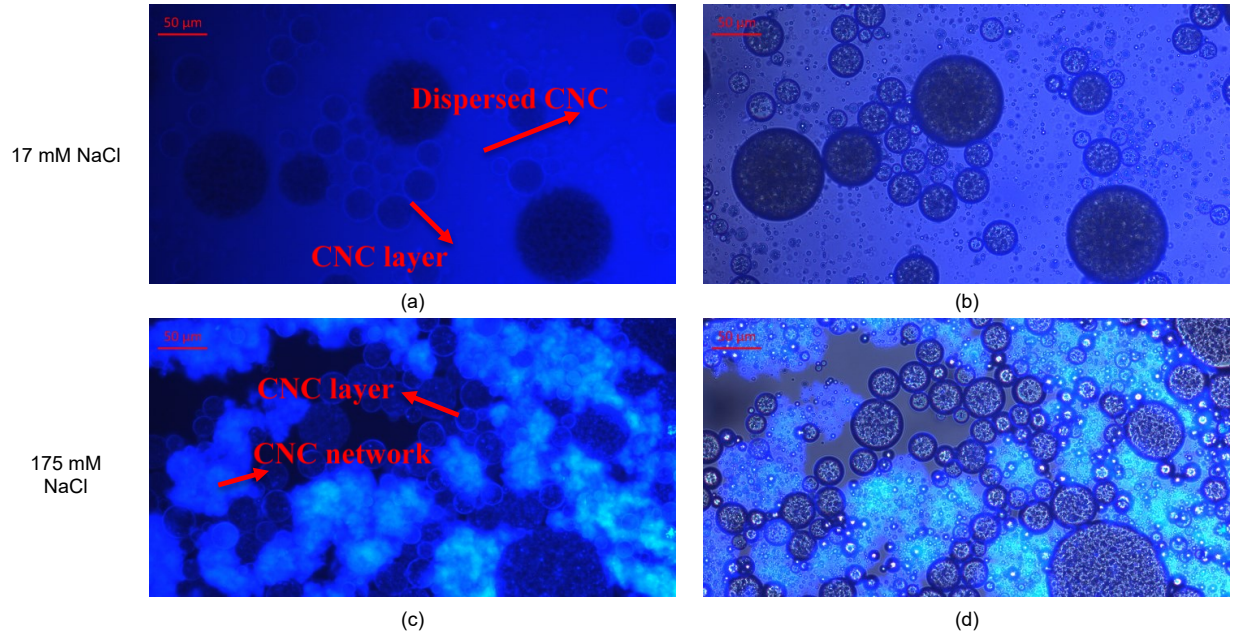
Figure 6—Microscopy images of mineral oil in water emulsions under 17 mM NaCl condition (a) Fluorescent light solely (b) Overlaid fluorescent and bright field light; and under 175 mM NaCl condition (c) Fluorescent light solely (d) Overlaid fluorescent and bright field light. Concentration of CNC was 1 w/v% for all samples.

2.4.4 Effect of CNC Concentration on the Stability of Emulsions.

We studied the effect of CNC concentration on the emulsion stability to find any possible threshold value. **Table 3** shows the experimental scheme of studying the effect of particle concentration (C).

Table 3—Experimental scheme of studying CNC concentration effect on emulsion stability.

pH	Particle Concentration (C), w/v%				Salinity (NaCl), mM	WOR
7	0.02	0.10	0.50	1.00	17 and 175	1:1

Fig. 7a shows that at a low salinity condition of 17 mM NaCl, the suspension of CNC was very stable and shown as a clear phase even at 1 w/v% of particle concentration. This result can be attributed to the high electrostatic repulsion between CNC particles being largely unscreened under the low salinity condition, as shown in **Fig. 4. Fig. 7b** shows that the emulsion was stable to both creaming and coalescence at 1 w/v% of the CNC while at 0.5 w/v% concentration the emulsion was unstable to coalescence. An oil layer separated from the emulsion 24 hours after

homogenization at 0.5 w/v% concentration, as indicated by the red arrows in **Fig. 7b**, and complete oil-water separation was observed when the CNC concentration was below 0.5 w/v%.

Fig. 7c shows that the suspensions of CNC became turbid at a relatively high salinity condition of 175 mM NaCl as a result of particle aggregation due to screening of the electrostatic repulsion. As the CNC particle concentration increased (above 0.5 w/v%), suspensions showed a gelling-like character, possibly indicating that the formation of a CNC network in the aqueous phase increased the viscosity of the aqueous phase and thus improved the emulsion stability to creaming. As shown in **Fig. 7d** when the salinity was at or above 0.5 w/v%, there was no water separation from the emulsions which means high emulsion stability to creaming. This observation was also consistent with the previous conclusion in Section 2.4.3 that states the formation of a CNC network in the continuous phase will further improve the emulsion stability to creaming.
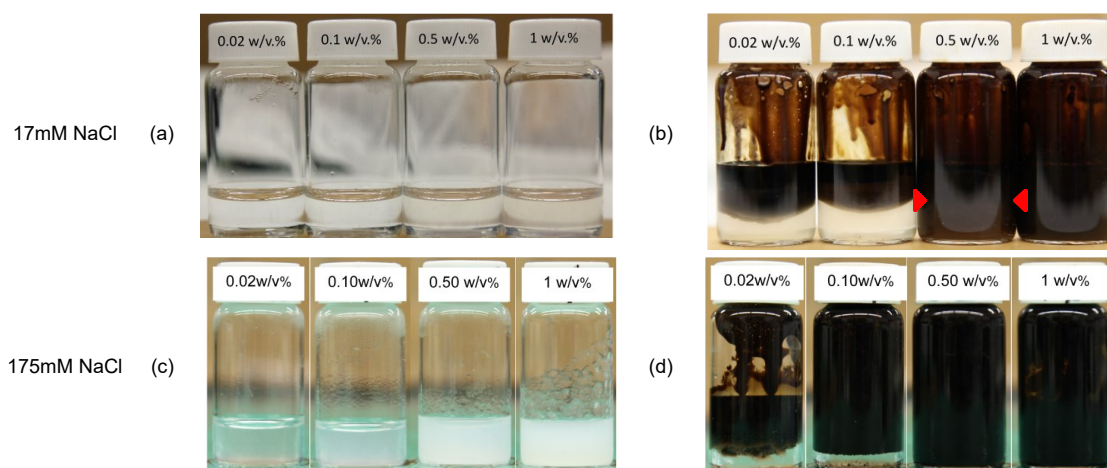
Figure 7—Glass vial tests of aqueous dispersions of different concentrations of CNC as indicated on bottle caps (a, c) and O/W emulsions 24 hours after homogenization (b, d) at both low (17 mM NaCl) and relatively high (175 mM NaCl) salinity conditions.

For a quantitative study of concentration effects, emulsion droplet size distributions with different CNC particle concentrations were obtained using ImageJ software, as described in the experimental section (Section **Emulsions characterization**). For this study, only samples under 175 mM NaCl condition and the CNC particle concentrations of more than 0.02 w/v% were analyzed because the emulsions were relatively stable for 24 hours under these conditions without

significant phase separation, as shown in **Fig. 7d**. The results are shown in **Figs. 8** and **9**. Both show that the droplet diameter decreased with increasing CNC concentrations, but **Fig. 9** shows the average droplet diameter becoming almost constant once the CNC concentration exceeded 0.5 w/v%.
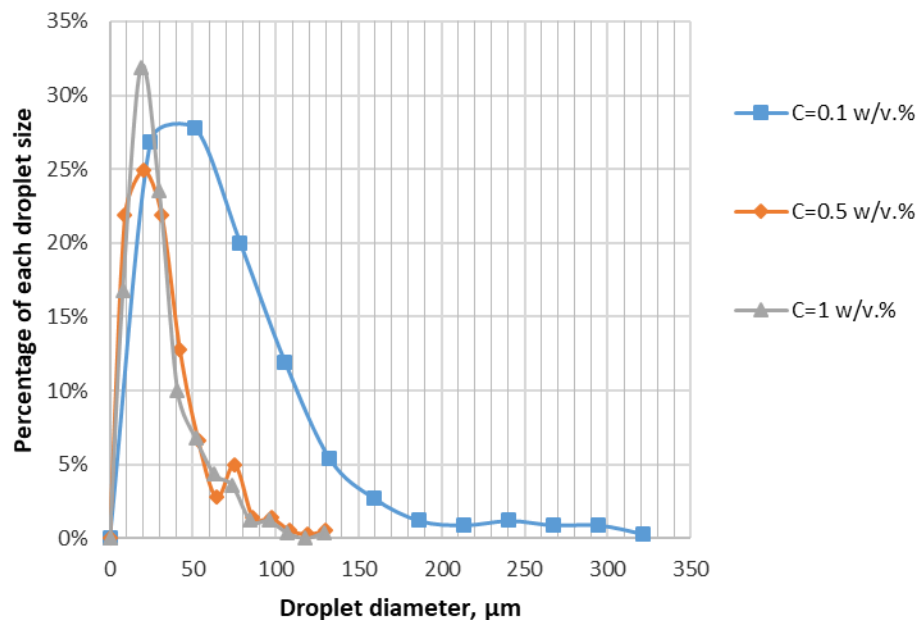
Figure 8—Droplet size distribution with different concentrations (C) of CNC under 175 mM NaCl condition.

This observation is consistent with the limited coalescence theory, which states that when the number of nanoparticles (concentration) is not enough to cover the water-oil interface, the oil droplets coalesce to reduce the total interfacial area until the surface coverage by the nanoparticles reaches a certain degree. This statement relates the small droplet size (larger interfacial area) to a high surface coverage of nanoparticles on the droplet (Arditty et al. 2003). When the nanoparticle concentration increased from 0.5 w/v% to 1 w/v%, the droplet diameter stopped decreasing and the average diameter became around 40 μm. Droplet coalescence stopped due to the sufficient surface coverage of the droplets by the nanoparticles (Chevalier and Bolzinger 2013; Tang et al. 2014) and the excess particles dispersed in the water phase as observed previously in **Figs. 5** and **6**. Therefore, we conclude that at least 1 w/v% of CNC particles were required to generate stable oil-in-water emulsions under a low salinity condition (17 mM NaCl) and this value can be reduced to 0.5 w/v% under a relatively high salinity condition (175 mM NaCl), since the salt (NaCl here) will make CNC particles more effective as an emulsion stabilizer (around neutral wettability) by

decreasing their electrostatic repulsive force thus the amounts required to stabilize emulsions were lowered at relatively high salinity condition.
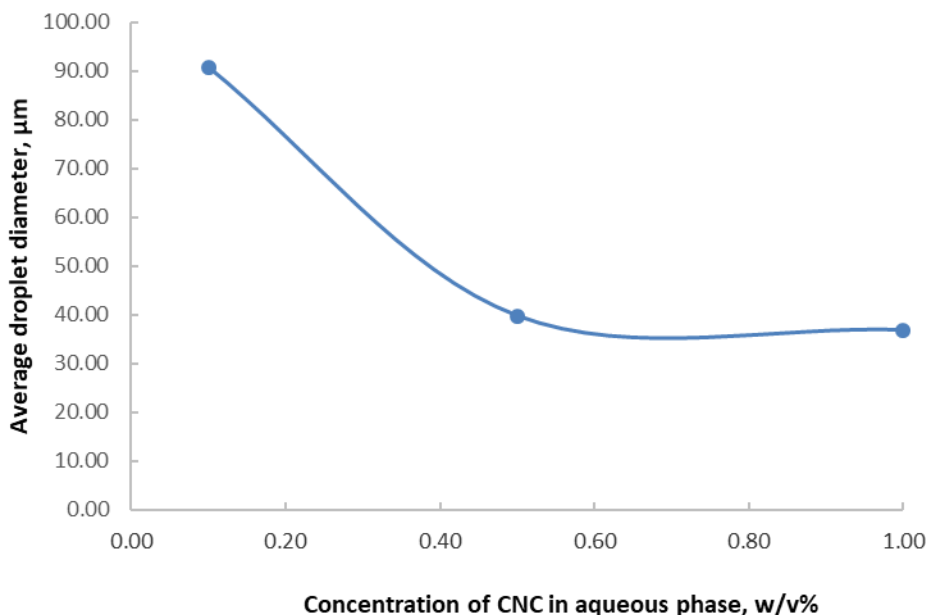
Figure 9—Average droplet diameter versus CNC concentration under 175 mM NaCl condition.

2.4.5 Effects of water to oil ratio (WOR) on stability of emulsions stabilized with CNC

The effects of water to oil ratio (WOR) or oil content on the emulsion stability and type were studied. In all these experiments, the total volume of mixture of oil and water was kept constant at 10 ml for each sample. **Table 4** shows the experimental scheme for this WOR study.

Table 4—Experimental scheme of studying WOR effects on emulsion stability.

CNC concentration, w/v%	Salinity (NaCl), mM	WOR (Oil content)				
1	17 and 175	8:2 (0.2)	6:4 (0.4)	5:5 (0.5)	4:6 (0.6)	2:8 (0.8)

Fig. 10 shows that under both salinity conditions, the emulsion type was O/W when the oil content was 0.6 or less and the oil became the continuous phase when the WOR was 0.8. This phase

inversion induced by the increase of the dispersed phase (oil) volume is called catastrophic inversion which usually occurs when the dispersed phase volume fraction is near 0.7 (Binks and Lumsdon 2000). The volume fraction of 0.7 is near the limit of the close packing of spherical dispersed phase where these spheres are under compression and easily coalesce. The salinity did not affect the phase inversion volume fraction (when the oil content was 0.6) in this study.
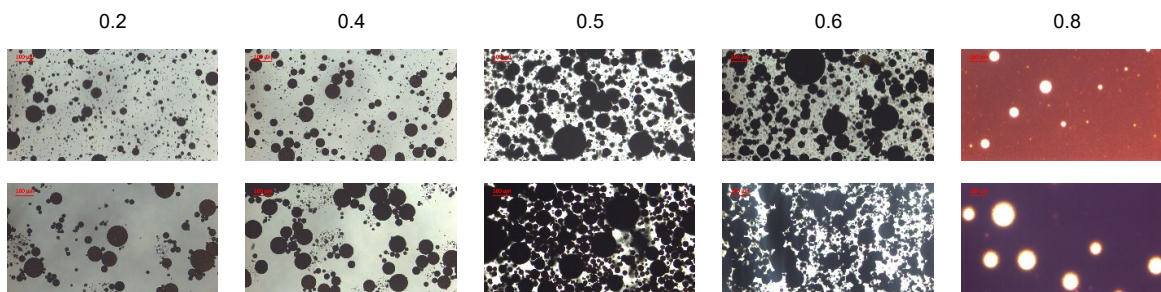
Figure 10—Microscopy images of emulsions prepared with different oil contents (WOR) as indicated on top of images under 17 mM NaCl (upper) and 175 mM NaCl (lower) conditions.

2.4.6 Effects of temperature on the CNC stabilized emulsions

Here, the effects of temperature on the emulsion stability are studied and reported as described in the experimental section (Section **Thermal study**). The salinity was kept at 175 mM NaCl, the CNC concentration at 1 w/v%, and the WOR at 1:1.

Fig. 11 shows that even after heating to 100°C for 10 minutes, the CNC stabilized emulsion did not phase separate for 24 hours after the preparation of the emulsion. The results suggest high thermal stability of these emulsions, which is good for field applications of this technique in relatively high-temperature reservoirs.

Fig. 12 shows that temperature had marginal effects on the emulsion viscosity, indicating that a change in temperature did not induce any phase separation. We note at this stage that the rheological properties of all the emulsion samples was measured at room temperature, and the indicated temperature here is the water bath temperature that heated the emulsion samples, as described in section **Thermal study**. The samples displayed similar shear thinning behaviors at all temperatures. This shear thinning is a typical characteristic of Pickering emulsions that contain

flocculated droplets (Winuprasith and Suphantharika 2015) and suggests that our samples may also contain flocculated droplets. This hypothesis was confirmed by the microscopy visualization of the emulsion droplet structure. **Fig. 13** shows flocculated oil droplets and formation of a CNC network in the continuous aqueous phase at all temperatures. This thermal stability can be attributed to the high surface coverage of oil droplets by the CNC particles as predicted by the limited coalescence theory (Sharma et al. 2014, 2015) and the much higher adsorption energy (E) of these particles, as expressed in Eq. 3, compared to thermal energy which can be as high as 2750 times the thermal energy (kT) when the contact angle is 90°C (Binks 2002).
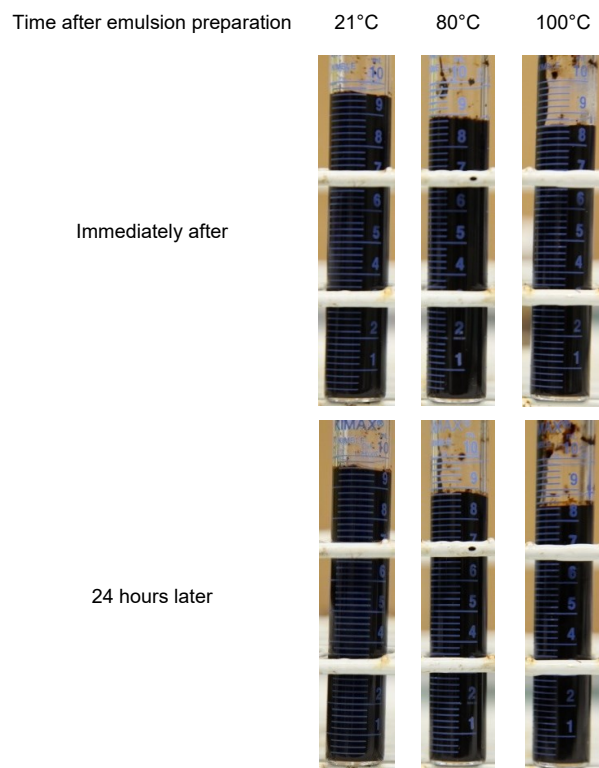
Figure 11—Graduated glass bottles containing O/W emulsions stabilized with 1 w/v% CNC under 175 mM NaCl condition after heated at different temperatures as indicated on top of bottles for 10 minutes in water bath: immediately after (upper) and 24 hours after (lower) emulsion preparation.
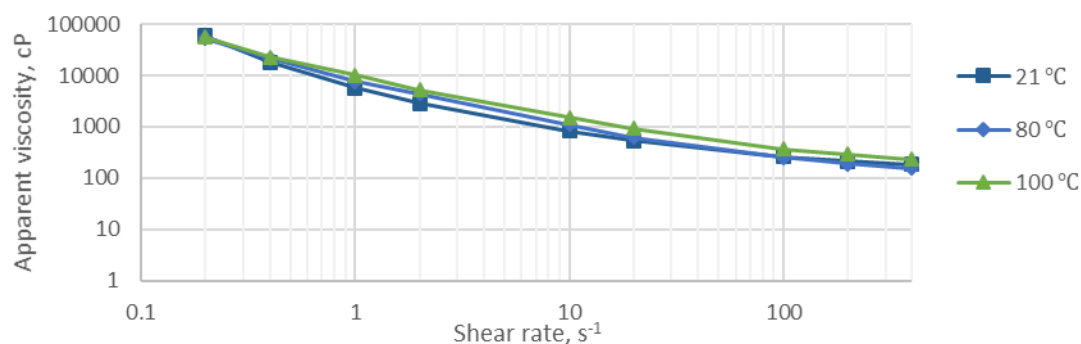
Figure 12—Apparent viscosity of O/W emulsions 24 hours later of preparation versus shear rate after heated at various temperatures for 10 minutes in water bath.
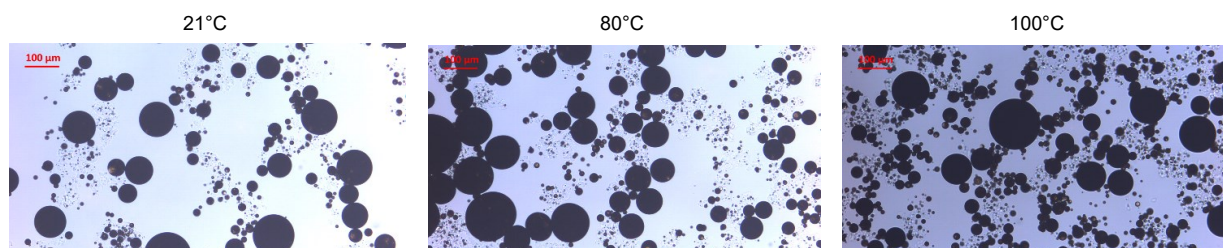
Figure 13—Microscopy images of O/W emulsion samples heated at different temperatures as indicated above each image 24 hours after emulsion preparation.

2.4.7 Rheological properties of aqueous dispersions of CNC and emulsions with CNC

The rheological properties of both aqueous dispersions of CNC and CNC-stabilized emulsions were studied under various salinity conditions. The CNC particle concentration was kept constant at 1 w/v% s and the WOR at 1:1.

Fig. 14a shows that when the NaCl concentration was below 17 mM (e.g., 0 and 2 mM), the CNC suspensions displayed a Newtonian behavior where the shear stress versus shear rate was a straight line passing through the origin and the apparent viscosity was independent of the shear rate, as shown in **Fig. 14b**. When the NaCl concentration was at or above 17 mM, there was a yield stress on the shear stress curve, as shown in **Fig. 14a**, and the suspension showed a shear thinning behavior, as shown in **Fig. 14b**. The shear thinning behavior indicates a flocculated structure of the CNC in the aqueous dispersion (Oguzlu et al. 2017). This finding is consistent with our

28

previous observation that adding NaCl would decrease the absolute value of CNC zeta potential (**Fig. 4**), which would then reduce the electrostatic repulsion between particles and cause particle aggregation at a relatively high salinity condition, as observed in **Fig. 5**. The observed shear thinning behavior of CNC suspension is good because, on the one hand, during the injection of CNC the viscosity will be reduced due to the high shear rate in wellbore, and on the other hand, the sweep efficiency of oil in the reservoir away from the wellbore will be improved. Because the shear rate is lower than the rate near wellbore—according to the Darcy equation—a higher viscosity of CNC suspensions can be expected.
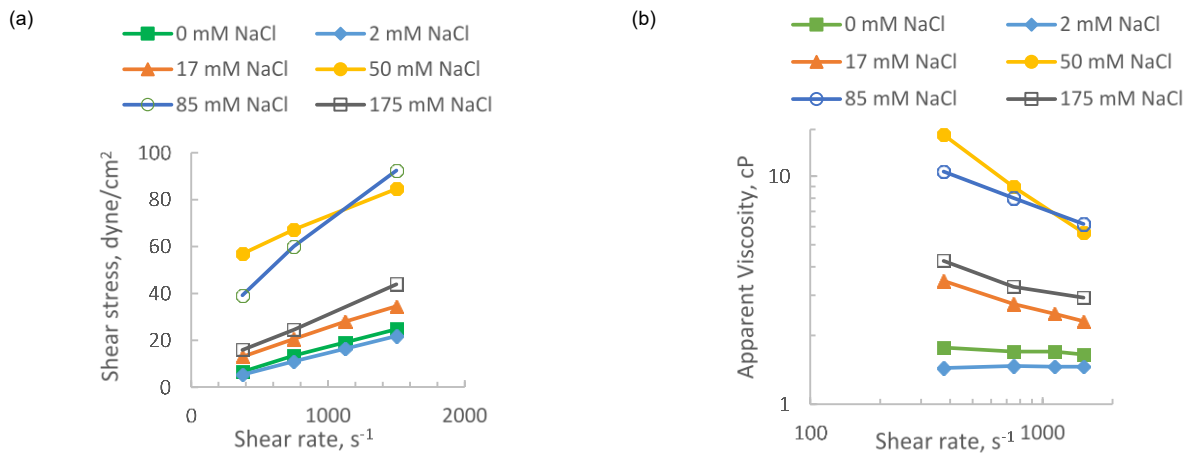
Figure 14—Variation in shear stress (a) and apparent viscosity (b) with shear rate for aqueous dispersions of 1 w/v% of CNC under various salinity conditions.

Another interesting observation here is that the apparent viscosity changed with salinity at the same shear rate. For better visualization of this change, the data in **Fig. 14b** was re-plotted as apparent viscosity versus salinity under various shear rate (SR) in **Fig. 15**, of which shows three regions of the low, intermediate, and high salinity regions. In the low salinity (0-2 mM NaCl) region, the viscosity of the CNC suspension decreased as the salinity increased because the effective thickness of the electrical double layer of the CNCs was compressed by NaCl (Shafiei-Sabet et al. 2014) and therefore reduced the electro-viscous effect, which is the increase of

suspension viscosity due to the ionic charges on the surface of suspended particles (Hubbe et al. 2017). In the intermediate-salinity region (2-50 mM NaCl), the viscosity increased as the salinity increased, which could be attributed to the aggregation of CNC particles induced by the addition of NaCl (Shafiei-Sabet et al. 2014). In the relatively high-salinity region (50-175 mM NaCl), the viscosity decreased again as the salinity increased, which may be attributed to the formation of a space-filling model. Space-filling model postulates an amorphous and turbid gel structure, where the packing of blobs has an intermediate fractal dimension between 1 and 3, induced by high electrolyte concentrations (Oguzlu et al. 2017) and when no more volume is available for extensive aggregated particles to fill in this space-filling model, the viscosity decreases (Hubbe et al. 2017).
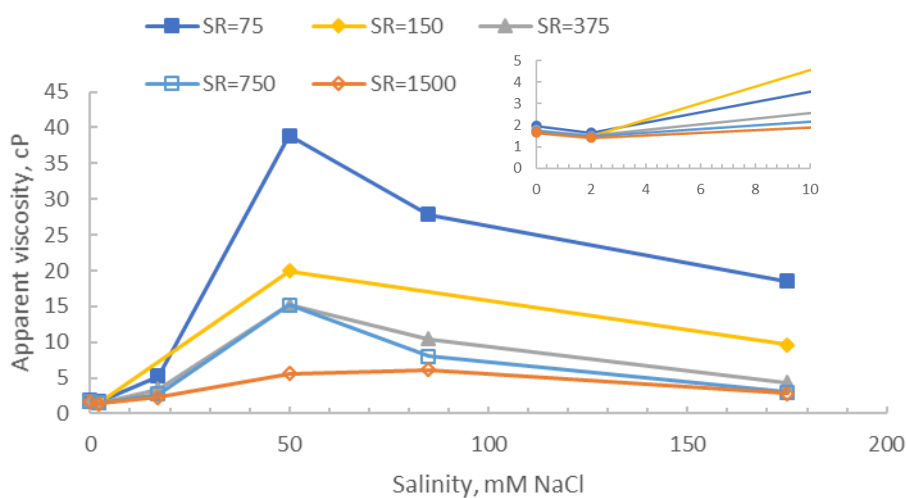
Figure 15—Apparent viscosity of aqueous dispersions of 1 w/v% of CNC versus salinity under different shear rate (SR). The inset was the magnification of the low salinity region (between 0 and 10 mM NaCl) for clarity.

Fig. 16a shows that, for the O/W emulsions stabilized by the CNC particles, the shear stress was almost constant over a small range of shear rates (around 20 s^{-1}) followed by a steady increase at higher shear rates, which was also observed by other authors (Binks et al. 2005; Sharma et al. 2014) for Pickering emulsion systems. **Fig. 16b** shows that the O/W emulsions stabilized by the CNCs displayed a shear thinning behavior which is typical of Pickering emulsions (Winuprasith and Suphantharika 2015) and has been linked to droplet flocculation (Binks et al. 2005). The shear thinning behavior of emulsions improves the mobility ratio in the reservoir away from wellbore

and thus increases the sweep efficiency; it is also desirable for the production and transportation of oil where the shear rate would be higher than that in a reservoir and thus lower viscosity would be expected. In comparison to the information in **Fig. 14**, we can see that the viscosity of the emulsions at any given shear rate was much higher than that of the particle dispersions, due to both the addition of the heavy oil and the general rule that emulsion viscosity will be higher than that of the continuous phase (Arab et al. 2018a). Compared to the original oil viscosity of 15,640 cP under all shear rates at 21°C (pure oil is a Newtonian fluid), the viscosity of O/W emulsions stabilized by CNC can be as low as around 100 cP, under certain shear rates (e.g., 400 s-1) and 175 mM NaCl condition, since the oil phase was dispersed in the water phase in a droplet form. Also, the formation of emulsions by adding oil leads to, on one hand, the yield stress and the shear thinning behavior even at 2 mM NaCl condition; on the other hand, the almost overlapping viscosity and shear stress curves when the salinity was above 50 mM NaCl. The mentioned observations may be attributed to the effects of both oil droplets interaction and flocculated CNC structure. The formation of oil droplets accounts for the yield stress and shear thinning behavior at 2 mM NaCl condition. And when the salinity was above 50 mM NaCl, the effect of oil droplet interaction may become more dominant, thus the difference of viscosity and shear stress caused by the flocculated CNC was reduced, resulting in the overlapped curves.
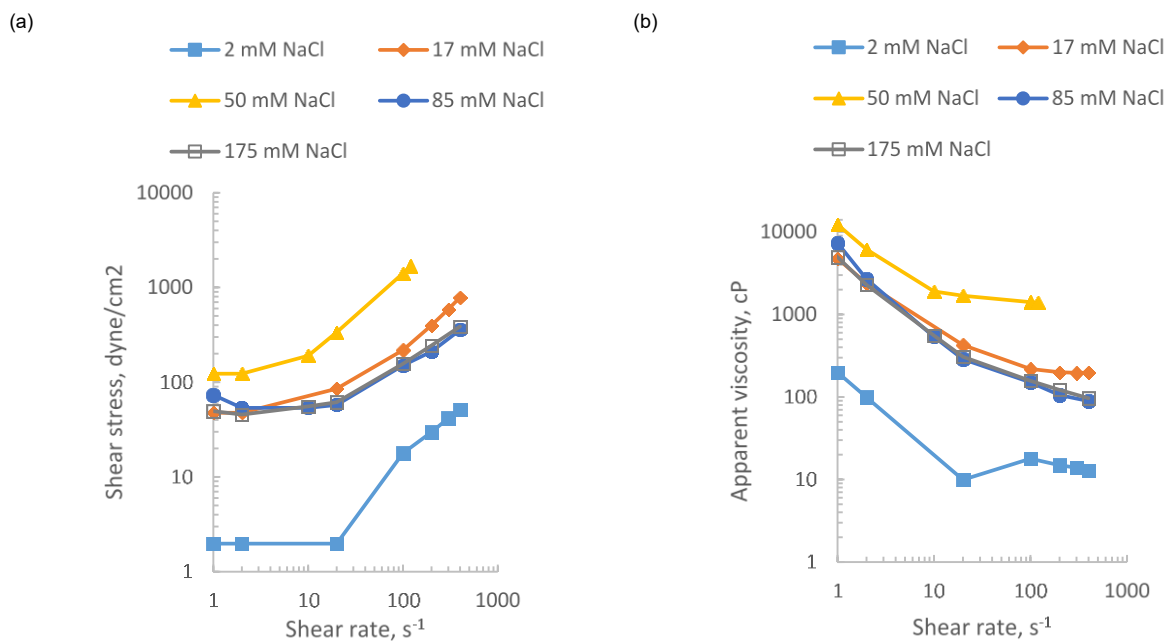
2.4.8 Discussions for future field application

The findings from this work show a very promising prospect of using nanoparticles, CNC in particular, as an emulsion stabilizer in place of surfactants to enhance the heavy oil recovery in field applications for the following reasons:

- The cost of CNC is relatively low since it can be produced from natural sources (trees) which are abundant and environmentally friendly.

- The viscosity of oil can be reduced significantly from around 15,000 cP to as low as 100 cP through the emulsification of heavy oil into water, which enables the easy flow of oil in the reservoir toward production wells. What is more, such Pickering emulsions stabilized by the CNCs have high thermal stability due to the strong adsorption energy of solid particles; therefore, this formulation can also be used in hot water injection processes to further improve the heavy oil recovery through emulsification in addition to the reduction of oil viscosity by high temperature. Another possible application of this technology is alkaline flooding where the high pH environment would be expected, helping the CNCs stabilize O/W emulsions as found in this paper.

Because this research focuses on the preliminary tests of potential nanoparticles to be used in heavy-oil recovery, it is still in its early stages. Further investigations towards field-scale applications are needed as discussed below:

- Flow experiments of both CNC suspensions and Pickering emulsions in porous media need to be executed in order to figure out the magnitude of enhanced oil recovery potential that can be achieved, whether the particle will be retained in the porous medium or not, as well as the formation damage during the flooding process. A limited number of researchers reported relevant information on this matter. For example, Pandey et al. (2018) carried out sandpack flooding experiments successfully using both 2 w/v% of CNC and the pre-prepared O/W emulsion stabilized by chemically modified CNC, observing minimal CNC retention around 12% after 3.6 pore-volume injection. However, in their case, they used

32

chemically treated CNC and light oil (dodecane) to prepare emulsions, hence it is still worthwhile to perform similar studies by using the formulation discovered in this paper for heavy-oil recovery.

- In-situ formation of O/W emulsions stabilized by CNC needs to be achieved at reservoir conditions. In order to create a Pickering emulsion, a large interfacial area should be generated first in order for the particles to adsorb. One solution is to reduce the interfacial tension (IFT) to some extent so that it would be easier to create a large interfacial area even at low shear condition. However, unlike surfactants, the adsorption of solid particles on the interface between water and oil would not usually reduce the IFT. Vignati et al. (2003) measured the IFT between isooctane droplets stabilized by modified silica versus at various particle concentrations using the micropipette tensiometer method and found that the IFT did not change a lot with increasing particle concentration. Another option is to adjust the injection rate, which would increase the shear rate applied by the flowing fluid, and thus help create more interfacial areas between oil and water. Therefore, the flow rate needs to be optimized when designing the flowing experiments in porous medium like sandpack or sandstone rock.

- Effective methods to break up the generated Pickering emulsion should be developed. A stable O/W emulsion is good for the displacement and sweep of oil in the reservoir, but undesirable for transportation through pipelines. Therefore, the break-up strategy for the formulated Pickering emulsion needs to be further investigated in future work. The results from this paper can be used as a foundation for such studies since the stabilization mechanisms are already known and can also be used to de-stabilize emulsions, such as by changing pH, salinity, or WOR—all of which were found to be main parameters affecting the emulsion stability.

- Effects of brine composition and high salinity should also be further studied. NaCl was chosen in this paper for the preliminary study; however, in a real reservoir, divalent cations such as Ca^{2+} and Mg^{2+} also exist, which may have great impact on the colloidal stability. Therefore, the brine composition also needs to be further investigated. Besides, the salinity limit of 175 mM (around 10,000 ppm) found in this work is considered at a low side for field application, which is one of many main challenges (e.g., high salinity, high temperature, high pressure) for using nanoparticles in oil fields as pointed out by Patel et

al. (2017), who found that 5000 ppm NaCl is the salinity limit for hydrophilic silica nanoparticles to stabilize emulsions. The limit of 10, 000 ppm NaCl in this work shows a further improvement of nanoparticle dispersion stability to salinity in this regard. Therefore, future work needs to address the stability of nanoparticle system to high salinity condition in order to be considered for filed application.

Considering both the opportunities and challenges that CNC brings, the findings from this paper can be regarded as preliminary results for finding the optimal formulation of nanoparticles in field applications.

2.5 Conclusions

In this study, screening tests were first conducted on various nanoparticles (e.g., CNC, SiO_2, Al_2O_3, Fe_3O_4, and ZrO_2) by adjusting the pH and the salinity of the aqueous phase followed by zeta potential measurements. It was found that CNC could be an effective emulsifier under appropriate pH or salinity conditions. Next, the emulsion stabilization mechanism of CNC was studied microscopically as well as the effects of particle concentration, water to oil ratio (WOR), and temperature on the emulsion stability. The detailed conclusions can be drawn as:

1) CNC could act as an effective emulsifier for O/W emulsions either by adjusting the pH (3 or 11) or by adding an appropriate amount of salt (17 mM NaCl); although, the emulsion was not stable to creaming if only the pH was adjusted.

2) Zeta potential measurements showed that addition of salt (NaCl) screened the electrostatic repulsion between the CNC particles due to the compressed Debye length by counterions (Na^+) and induced particle aggregation at relatively high salinity conditions (175 Mm NaCl).

3) Two stabilization mechanisms account for the emulsion stability with the CNC; one is the formation of a dense particle layer around oil droplets impeding droplet coalescence, the second is the formation of a CNC network structure in the continuous aqueous phase induced by relatively high salinity condition (175 mM NaCl).

4) The droplet size decreased sharply as the CNC concentration increased from 0.1 to 0.5 w/v%, then became almost constant at a higher CNC concentration from 0.5 to1 w/v%.

5) Catastrophic phase inversion was observed when the oil content increased from 0.6 to 0.8 when the O/W emulsion was inverted to a W/O emulsion.

6) Emulsions stabilized with the CNCs were thermally stable up to 100°C.

7) Salinity had a great impact on the viscosity of the suspensions of the CNC, and O/W emulsions stabilized by the CNC displayed a shearing behavior showing yield stress due to droplet flocculation.

8) The salinity limit of 175 mM (10,000 ppm) is considered low for field application, which is a common challenge for using nanoparticle in oil fields, therefore, future work needs to improve the stability of both CNC suspensions and emulsions to high salinity conditions for the consideration of field application.

Chapter 3: Can We Generate Stable Pickering Emulsions Activating Naturally Occurring Nanoparticles in the Reservoir for Cost Effective Heavy-oil Recovery?

This chapter of thesis is a modified version of a published research paper Fuel 283 (2021) 118916. The conference paper version SPE-200880 was accepted for presentation at the 2019 SPE Western Regional Meeting held in Bakersfield, CA, USA, 27 April to 1 May 2020. The journal version is a substantially revised and improved version of this conference paper and has been published in Fuel journal.

3.1 Preface

Activating naturally occurring nanoparticles in the reservoir (clays) to generate Pickering emulsions results in low-cost heavy oil recovery. In this study, we tested the stability of emulsions generated using different types of clays and performed a parametric analysis on salinity, pH, water to oil ratio (WOR), and particle concentration; additionally, we report on a formulation of injected water used to activate the clays found in sandstones to improve oil recovery.

First, oil-in-water (O/W) emulsions generated by bentonite and kaolinite clays were prepared for bottle tests and zeta potentials of clay suspensions were measured, then the stability of dispersion was measured under various conditions (pH, salinity and WOR). Heavy crude oils (15,640 cP) were used for all experiments. Second, sandpacks with different clay compositions were saturated with heavy-oil samples. Aqueous solutions with various salinity and pH were injected into the oil-saturated sandpacks with a pump. The recoveries were monitored while analyzing the produced samples. Third, glass bead micromodels with known amounts of clays were also prepared to visualize the in-situ behavior of clay particles under various salinity conditions. The transparent mineral oil instead of opaque heavy oil was used in these micromodel tests for better visualization results.

The bottle tests showed that 3% bentonite stabilized O/W emulsions under a high WOR (9:1) condition. The addition of 0.04% of NaOH further improved the emulsion stability which was attributed to the reduction of interfacial tension (0.17 mN/M) between the oil and alkali solution. The sandpack flood experiments showed an improved sweep efficiency caused by the swelling of bentonite when injecting low salinity fluid (e.g., DIW). The micromodel tests indicated a wettability change to be more oil-wet under high salinity conditions, and the swelling of bentonite would divert incoming water flow to other unswept areas thus improving sweep efficiency.

This paper presents new ideas and recommendations for further research as well as practical applications to generate stable emulsions for improved waterflooding as a cost-effective approach.

Key words: Pickering emulsion, nanoparticle, cost effective heavy oil recovery, activation of clay particles.

3.2 Introduction

Canada hosts the third-largest proven oil reserves in the world with total estimated reserves amounting to 171.0 billion barrels. Most of these reserves (more than 95%) are heavy oil and oil sand deposits located in western Canada (Arab et al. 2018). These heavy oil and oil sand resources are usually deposited in unconsolidated sandstones with high porosity, permeability, and almost zero tensile strength (Dusseault, 2001). Due to the high oil viscosity, low gas to oil ratio (GOR), and low reservoir pressure, the primary recovery of these resources is usually very low (around 3 to 8%) (Adams 1982). Also, conventional waterflood technologies usually fail when it comes to heavy oil due to the severe adverse water-oil mobility ratio owning to the high oil viscosity (Miller 2006). Therefore, large amounts of heavy oil resources remain underground encouraging the development of various enhanced oil recovery (EOR) methods in past years to reduce oil viscosity and thus increase oil recovery. These methods can be classified—roughly—into three categories: (1) thermal methods, (2) solvent methods, and (3) chemical methods. Thermal methods, such as steam-assisted gravity drainage (SAGD) and cyclic steam stimulation (CSS), work well in shallow and thick formations, but they will lose efficiency in thin and deep formations because of the heat loss to the adjacent formations (Arab et al. 2018). The solvent injection method is limited by the high cost of material, solvent loss, and the availability of solvent/gas—considering the current low oil price (Babadagli 2020). Chemical method can be another option to enhance the heavy oil recovery. Chemical additives, such as alkali (A), surfactant (S), polymer (P), or the combination of these three (ASP) are usually injected into the reservoir in this process, where the polymer helps to increase the water viscosity thus improving the mobility ratio between water and oil. Surfactants will reduce the interfacial tension (IFT) between oil and water, facilitating the formation of emulsions whether it be oil-in-water (O/W) or water-in-oil (W/O), thus leading to higher displacement and sweep efficiency (Delamaide et al. 2014). Alkali is reported to react with acidic components in heavy oil—as reflected in the total acid number (TAN)—to release natural surfactants which further helps reduce IFT and accelerates emulsification (Mandal 2015).

One of the main mechanisms used in improving heavy oil recovery by chemical methods is emulsification; both O/W and W/O emulsions were reported to increase oil recovery. For O/W emulsions, the viscosity is lower than that of pure heavy oil, and thus can be easily transported in

the porous medium along with the water (entrainment); besides, the oil droplets may plug some of the rock pores and improve the sweep efficiency of waterflooding (entrapment) (Bryan and Kantzas 2009). For W/O emulsions, the viscosity of the emulsion is usually higher than that of the oil since the water droplets are dispersed in the continuous oil phase. Large amounts of oil were consistently produced in this W/O emulsion stage accompanied by high displacement pressure, a phenomenon resulting from the high viscosity of the emulsion as reported by Kumar et al. (2012). The high oil recovery through the formation of W/O emulsion can be attributed to the high emulsion viscosity—which is favorable for mobility control and the semi-miscible displacing process enabled by the external oil phase nature in W/O emulsion (Fu et al. 2012). The successful field application of emulsions on enhancing heavy oil recovery lies on emulsion stability and chemical costs. Chemicals like surfactants are usually expensive and have other issues like chemical retention in the reservoir and thermal degradation under high-temperature conditions (Sharma et al. 2015), further hindering their application in field scale. S. U. Pickering (1907) observed that solid particles can also stabilize emulsions with higher stability than those stabilized by surfactants (soap). This observation is very attractive since emulsion stability was improved without using surfactants, which reduces the cost of preparing emulsions. Since then, such emulsions stabilized by solid particles were named after S. U. Pickering, i.e., the Pickering emulsions, which have attracted a lot of research attention.

Factors affecting Pickering emulsion stability include but are not limited to: particle size and concentration, electrolyte type and concentration, water to oil ratio, oil type, and particle wettability (Binks 2002; Aveyard et al. 2003). Among these parameters, particle wettability is generally regarded as a key parameter controlling the emulsion type and stability. Usually, water-wet (hydrophilic) particles tend to stabilize O/W emulsions and oil-wet (hydrophobic) particles tend to stabilize W/O emulsions (Binks 2002). The emulsion stability is at its maximum when the particle is neutral wet since the adsorption energy of particles is highest when the particle has a contact angle of 90° (Levine et al. 1989). The adsorption energy can be interpreted as the energy required to remove the particle from the water-oil interface to either oil or water phase and the emulsion stability is usually at the maximum when the adsorption energy is highest (Aveyard et al. 2003). For applications in the porous medium, the size of particles should be small enough to be transported at the pore scale. Nanoparticles (NP) with a diameter smaller than 100 nm fulfill this requirement because their small size makes possible the free movement of particles in the

porous medium (Zhang et al. 2010). Many particles were reported to stabilize emulsions, such as silica (Binks et al. 2005), magnetic particles, and clay (Chevalier and Bolzinger 2013). Among these particles, clay particles were the target of this paper because they are abundant in reservoir formations, especially in western Canadian formations.

Clays are a wide group of minerals with a sheet-like geometry perceived as repeated aluminosilicate layers composed of octahedral and tetrahedral sheets, often referred to as phyllosilicates (Uddin 2008). It was reported that the average clay content in Alberta oil sand deposits is around 10 wt.% with main clay minerals of kaolinite, illite, montmorillonite and chlorite (Bayliss and Levinson 1976). If these clay particles can be activated in-situ to generate stable Pickering emulsions, the cost will be reduced significantly. Also, clays are natural to the reservoir whereas chemicals like surfactants are foreign to the reservoir. Another interesting point about clays is that their size can be reduced from micro scale (usually less than 2 μm) to nano scale (nanoclay, 1 nm in thickness) through a delamination process where the swelling clay (e.g, bentonite) was broken into individual 1 nm thick layers by adsorbing water (Bragg and Varadaraj 2006). When the bentonite is fully hydrated and dispersed as colloidal particles, a large surface area will be available, in turn forming a thin film around oil droplets and thus improving the emulsion stability (Clem and Doehler 1961). Therefore, the objective of this work is to explore the possibility of utilizing the naturally occurring clay particles in the reservoir to form stable emulsions and investigate the effect of said emulsions on heavy oil recovery. Kaolinite and bentonite, both rich in montmorillonite with 10 to 20 percent of other minerals like silica, gypsum, calcite, and feldspar (Uddin 2008), were chosen in this study because they are the main clay minerals in western Canadian formations and possess two different unique properties of clay: swelling (bentonite) and non-swelling (kaolinite). Both types of clay (kaolinite and bentonite) were reported to stabilize emulsions in laboratory conditions. Abend et al. (1998) reported heterocoagulation of bentonite (negatively charged) and layered double hydroxide (positively charged) can stabilize paraffin in water emulsions through the formation of three-dimensional networks. Later, Abend and Lagaly (2001) found that bentonite type clay also had an impact on emulsion stability, where the Wyoming bentonite was more effective than Turkish sample as an emulsion stabilizer and Na-montmorillonite separated from bentonite played an important role in stabilizing emulsions. Yan and Masliyah (1993) observed that the wettability of kaolinite can be tuned by the adsorption of bitumen asphaltene leading to stable O/W emulsions. They also reported

the minimum diameter of emulsion droplets when the contact angle of kaolinite is 65° which is a balance between the surface coverage and positioning of clay particles at the water-oil interfaces (Yan and Masliyah 1995).

From these published pieces of literature, clays—especially bentonite (montmorillonite) and kaolinite—show potential to be effective emulsion stabilizers once their physicochemical properties were adjusted properly. Previous reports used light oil such as paraffin oil (Abend et al. 1998), and mineral oil (Yan and Masliyah 1995) to prepare emulsions. Few studies have been reported using heavy oil, to the best of our knowledge. Therefore, in this work, we performed a systematic study about the effects of clay particles (bentonite and kaolinite) on the emulsion formulation with heavy oil (15,640 cP at 21°C). First, glass vial tests were done to evaluate the emulsion type and stability under various pH (2-12), salinity (0 to 1.75 wt.%), water to oil ratio (WOR), and particle concentration (1 to 5 wt.%) conditions. Then flooding experiments in the porous medium were performed in sandpacks prepared with sand (250 to 500 μm) and clay particles (bentonite and kaolinite) to probe the possibility of in-situ activation of clays as the Pickering agent.

3.3 Materials and Experimental Setup

Materials. For all the glass vial tests and sandpack flooding experiments, heavy oil with a viscosity of 15,640 cP at 21°C from Western Saskatchewan was used for all the experiments. **Table 5** summarizes the properties of this heavy oil. Deionized water (DIW) with pH around 7 (i.e., 6.8) was used to prepare desired solutions with various salinity and pH. Hydrochloric acid solution (HCl, 1 N, Fisher Scientific, U.S.A.) and sodium hydroxide (NaOH, Fisher Scientific, U.S.A., $\geqslant$ 97.0%) were used to adjust pH conditions. For a better dispersion of clay particles (e.g., sodium bentonite) better, sodium chloride (NaCl, Research Products International, U.S.A., 99%) was used to adjust aqueous salinity conditions. Wyoming sodium bentonite with a particle size around 1.5 μm measured from dynamic light scattering (DLS) technique was purchased in powder form from BAROID (AQUAGEL). Pure kaolinite (1-1.8 μm) was purchased from ACROS ORGANICS and was provided in powder form. TARGET Filter Silica sands purchased from TARGET Products Limited were used to prepare the sandpacks.

Table 5—Properties of the heavy oil from Western Saskatchewan.

Properties	Value
Viscosity at 21 °C, cP	15,640
Density, g/cm^3	0.9792
Total acid number (TAN), mg KOH/g	2.21
Saturates (S), wt.%	29.75
Aromatics (A), wt.%	23.32
Resin, wt.%	29.83
Asphaltene, wt.%	15.35

Preparation of clay particle dispersions. For glass vial tests, dispersions of clay particles were prepared by the sonification method to prevent any particle aggregation. Firstly, water solutions with various salinities (e.g., 0, 10(0.06), 100(0.60) and 300(1.75) mM(wt.%) NaCl) and pH values (2-12) were prepared. A pH meter (Five Easy, METTLER TOLEDO) was used to measure the pH of solutions. Next, clay particles were dispersed in aqueous solutions by sonicating for 2 mins (Misonix MICROSON XL 2000). The input intensity of sonication was kept the same for all the samples by fixing the sonication amplitude at 75% of the maximum capacity.

Preparation of Pickering emulsion. Since O/W viscosity is lower than heavy oil viscosity, which is desired in reservoir conditions for the easy flow of fluids, a high WOR (e.g., 9/1) was applied in most experiments to generate O/W emulsions if possible. More specifically, the heavy oil was mixed with clay particle dispersions at a volume ratio of 9/1 (9 ml water: 1 ml oil) unless otherwise stated (e.g., 1/9, 5/5, and 7/3 for studying WOR effects) by using a homogenizer (the Polytron PT 10-35 GT). The mixture was homogenized for 3 min. at a speed of 10,000 rpm. All the experiments were performed at room temperature (21°C). The particle concentration was 3 w/v.% for most experiments unless otherwise stated (e.g., 1, 3, and 5 w/v.%) for studying particle concentration effects.

Emulsions characterization. The following procedure was used to determine the emulsion type. First, the viscosity of the fluid mixture was checked by observing the flow of fluids in a tilted glass vial where easy flows indicate low viscosities and vice versa. Since the viscosity of the heavy oil is much higher (15,640 cP at 21°C) than that of water, the difference in the viscosity between O/W emulsions and W/O emulsions must be large. Then, this first deduction was further confirmed by microscopic observations, where microscopy images of emulsions were recorded by a high-speed CMOS camera (Lumenera's Lt225) which was connected to a transmitted light microscope (Axiostar plus).

The emulsion stability was evaluated by observing the phase behavior (e.g., phase separation) of emulsions at different times (right after the sample preparation and 24 hours later) through glass vial tests.

Zeta potential measurement. A Malvern Zetasizer Nano (UK) instrument was used to measure Zeta potential and size of clay particles in dispersions under various conditions. First, the electrophoretic mobility was measured and then converted to the zeta potential by the Henry equation (Eq. 1) and Smoluchowski approximation. The size of the clay particles was determined by using a dynamic light scattering (DLS) technique with the same instrument. The particle concentration was maintained at 0.1 w/v% and an average of five measurements for each sample was reported. 10 mM NaCl was added into the aqueous solution as a background electrolyte to measure such properties (e.g., Zeta potential, particle size).

$$U_E = \frac{2\varepsilon z f(\kappa a)}{3\eta} \qquad (1)$$

U_E: Electrophoretic mobility; z: Zeta potential; ε: Dielectric constant; η: viscosity of the dispersant; *f(ka)*: Henry's functions (Approximated with Smoluchowski model as 1.5 in aqueous media).

Interfacial tension (IFT) measurement. The heavy oil has a relatively high total acid number (TAN, 2.21) as shown in **Table 5**, meaning acid components are rich in this heavy oil. These components can be activated by an alkali like NaOH to generate soap or natural surfactants (e.g., carboxylic surfactant) (Tamiz Bakhtiari 2015). And it has been reported that these released carboxylic surfactants can make clay less hydrophilic and thus more easily attached to bitumen (Tamiz Bakhtiari et al. 2015). As described earlier in **Section 3.2: Introduction**, the wettability of clay particles affects Pickering emulsion stability, therefore, NaOH was used to activate natural surfactants in heavy oil to make clay particles effective emulsion stabilizers if possible. IFT between heavy oil and alkali solutions with different concentrations of NaOH was measured based on the pendant drop method using the Rame-Hart tensiometer accompanied by DROPimage software. To simply describe the measurement process, firstly, the chamber of tensiometer was filled with the desired aqueous solution, and then the pendant oil drop was generated by injecting the oil to the chamber slowly from the bottom. Next, the DROPimage software will calculate the interfacial tension between aqueous solution and oil by analyzing the shape of oil drop based on the Young-Laplace equation. The IFT between the measured aqueous solution and heavy oil was taken when the reading was stabilized indicating that the equilibrium was reached.

Sandpack floods. The sandpack flooding experiments were performed to simulate the flow in porous medium conditions and study the clay effects on emulsion generation, pressure, as well as oil recovery under different conditions (pH, salinity). To prepare the sandpack, silica sands were first sieved through two standard sieves (ASTM E-11) with mesh size No. 60 (<250 μm) and No. 35 (<500 μm) to obtain sands with sizes between 250 μm and 500 μm, this was done to mimic the unconsolidated sand formation with high porosity and high permeability. Then, the sieved sands were saturated with heavy oil by mixing the sands with oil using a stainless stirrer bar. Next, the mixture of sands and oil was packed into a sleeve within a core holder. The sleeve is 5 in. long with an inside diameter of 1.5 in. When simulating a porous medium with a certain type of clay (either kaolinite or bentonite), the sieved sands were first mixed with weighted clays (5 wt.%), the remaining procedures were the same. **Table 6** shows the properties of the prepared sandpacks. The porosity was approximately 0.35. The permeability was measured by flowing the brine solutions

to the dry sandpack and recording the pressure difference across the length of sandpack using a pressure transducer. **Table 6** summarizes the sandpacks used for flooding experiments. As can be seen from the **Table 6**, the permeabilities of sandpacks with the addition of clay (SP4 to SP9) are much lower compared to those of pure sandpacks (SP1 to SP3), while the porosities are same. This is because the size of clay particle is much smaller (around 2 μm) than that of sand grains (250 μm to 500 μm), which leads to a lower permeability, but does not affect porosity a lot.

The injected fluids were pumped to the sandpack by using an Isco pump at a constant flow rate (0.2 ml/min), which was found to be the optimal flow rate in our previous study (Lee and Babadagli 2018). Another Isco pump was used to apply the overburden pressure to prevent the water channeling during the sandpack flooding process.

Table 6—Properties of sandpacks for flooding experiments.

Sandpack (SP) number	Clay composition in SP	Porosity	Permeability, Darcy	Injected solution	Clay production in flood experiments	Recovery factor
SP1	No clay	0.35	9.3	DIW	No	0.40
SP2				1.75 wt.% NaCl	No	0.33
SP3				10 wt.% NaCl	No	0.33
SP4	5 wt.% bentonite (B)	0.35	NA*	DIW	Yes (A few)	0.49
SP5			0.2	1.75 wt.% NaCl	No	0.35
SP6			0.4	10 wt.% NaCl	No	0.30
SP7	5 wt.% kaolinite (K)	0.35	0.5	DIW	Yes	0.40
SP8			1.2	1.75 wt.% NaCl	Yes	0.30
SP9			1.3	10 wt.% NaCl	Yes	0.31
SP10	No clay	0.35	Not measured	DIW+0.04 wt.% NaOH	No	0.78
SP11	5 wt.% bentonite (B)				Yes	0.38
SP12	5 wt.% kaolinite (K)				Yes	0.38

NA*: The pressure data was unstable and kept decreasing when injecting DIW due to the continuous production of clay.

Micromodel tests. To visualize the in-situ behavior of clay effect on oil recovery, micromodel tests were performed using mineral oil (poly-alpha-olefin) with a medium viscosity of 644.7 cP at 20 ℃ in a Hele-Shaw micromodel. The Hele-Shaw micromodels were prepared by first putting either a single layer of oil-saturated glass beads or a mixture of glass beads and clay on top of one microscope glass slide. The glass slide had a width and length of 25 and 75 mm, respectively, a thickness of 1-1.2 mm, and the glass beads used had a diameter of 1 mm. The oil-saturated glass

beads with a known amount of clay were prepared similar to the oil-saturated sands in the sandpack experiments, where a certain amount of glass beads-clay mixture was mixed with the mineral oil using a stainless stirrer bar. Next, another microscope slide with the same dimensions but with two through holes drilled was put on top of the glass beads-clay mixture. The two through holes enable the production and injection of fluids while using this model. Finally, the gaps near glass edges between the two glass sides were glued using epoxy resin, which includes two long sides and two short sides to prevent the spill of injected fluids. The spaces in the center part were filled with oil-saturated glass beads—kept intact with glue. Two luer adapters were glued onto the two through holes to enable the injection and production via a syringe pump.

The fluids with a high (10 wt.% NaCl) and low (DIW) salinity were injected into the prepared micromodels at a constant flow rate of 0.2 ml/min with a syringe pump. The initial and residual oil distribution was recorded using a transmitted light microscope.

3.4 Results and Discussion

3.4.1 Effects of particle concentration on emulsion formulation

Glass vial tests. Particle concentration is an important parameter controlling Pickering emulsion stability. Usually, the size of the emulsion droplets decreases initially and then remains almost unchanged as particle concentration increases. This change is because the surface coverage of solid particles initially increases with particle concentration thus improving emulsion stability. However, when the particle concentration is above a certain point, the droplet surface becomes fully saturated with particles, making any further addition a surplus and thus not making any difference in terms of droplet size reduction (Chevalier and Bolzinger 2013). Therefore, various concentrations (1, 3, and 5 w/v.%) of clay particles (bentonite and kaolinite) were tested through glass vial tests to study their effects on emulsion stability. These experiments were performed at a high WOR (9/1) to generate O/W emulsions, and the water used was de-ionized water (DIW). The experimental scheme for studying clay concentration effects is summarized in **Table 7**. The results of these glass vial tests are shown in **Fig. 17**.

Fig. 17a and **17b** show that when the bentonite concentration was 3 w/v.% or above, stable O/W emulsions were formed. However, **Fig. 17c** and **17d** show that kaolinite was not able to stabilize emulsions even at a high particle concentration (e.g., 5 w/v.%) and complete phase separation was observed with sedimented kaolinite at the bottom. The reasons for such observations are explained in the following section.

Table 7—Experimental scheme for studying clay concentration effects on emulsion stability.

Clay type	Particle concentration, w/v.%			Salinity, wt.% NaCl	pH	WOR
Bentonite	1	3	5	0	7	9:1
Kaolinite						
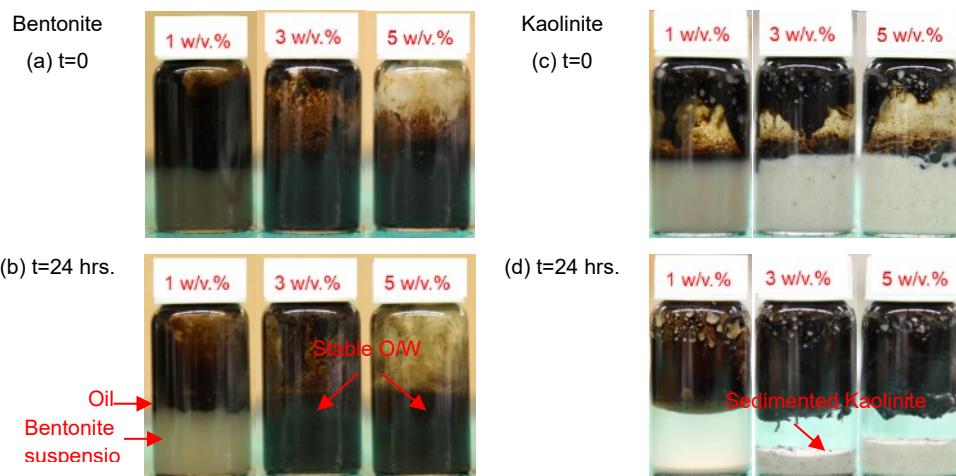
Figure 17—Glass vials containing 1 ml heavy oil and 9 ml aqueous clay dispersions with various particle concentrations as labeled in red fonts on the caps at different times after emulsion preparation: (a, b) bentonite, t=0 and 24 hrs, (c, d) kaolinite, t=0 and 24 hrs respectively.

Stabilization mechanisms. As shown in **Fig. 18a**, the bentonite particle was fully dispersed in water with smaller particle size, whereas significant kaolinite particle aggregation was observed in the aqueous phase leading to large, flocculated particle size as shown in **Fig. 18b**—even though their original size was quite similar in powder form (e.g., around 2 μm). The small size of bentonite particle gives it a high specific surface area, like nanoparticle, enabling it to be an effective emulsion stabilizer since the clay flakes would form a thin film around oil droplets given sufficient particle concentration (e.g., 3 w/v.%) as shown in **Fig. 19**. Additionally, the high surface area of bentonite helps the entrapment of droplets when they were broken down during the homogenization process (Clem and Doehler 1961). When significant particle aggregation happened, the particle failed to be an emulsion stabilizer due to its tendency to sediment at the bottom in the aqueous phase as shown in **Fig. 17d**, instead of being adsorbed onto the oil-water interface. A similar phenomenon was also observed by Binks and Lumsdon (1999), who found that extensive flocculated silica destabilized emulsions.

The size difference between these two clay particles when dispersed in water is attributed to the strong swelling capacity of bentonite, as kaolinite is a non-swelling clay. Usually, bentonite contains 70-90 wt.% of sodium montmorillonite (Au and Leong 2013), which is responsible for the high swelling capacity. The lattice of clays like montmorillonite and kaolinite are permanently negatively charged due to the isomorphous replacements of ions (Clem and Doehler 1961) which is the substitution of an element with higher valance by an element with lower valance, such as

Si^{4+} replaced by Al^{3+} in the tetrahedral sheet or the Al^{3+} substituted by Mg^{2+} or Fe^{2+} in the octahedral sheet (Uddin 2008). These negatively charged basal surfaces were balanced by cations (e.g., Na^+, Ca^{2+}) which are adsorbed on the surface of clay sheets and these cations can be readily exchanged (Clem and Doehler 1961) as described by the cation exchange capacity (CEC) of clay. When the clay contacted with water, the osmotic pressure drove water molecules into the interlayers between basal surfaces of clay particles and hydrated those exchangeable cations like Na+, causing the swelling of the clay (Au and Leong 2013). Bentonite is well known for its strong swelling capacity, which can expand 10 or more times to its dry volume, owning to the high CEC which is usually higher than 100 meq/100 g in comparison to the 5 meq/100 g of kaolinite (Uddin 2008). When the bentonite was fully swollen, the average size of clay particle decreased because of the delamination of clay; the interlayer spaces between clay sheet units expanded due to the adsorption of water molecules leading to the breaking of clay particles into fundamental particles with 1 nm thickness (Lagaly 2006).

(a) 3 w/v.% of bentonite in DIW   (b) 3 w/v.% of kaolinite in DIW
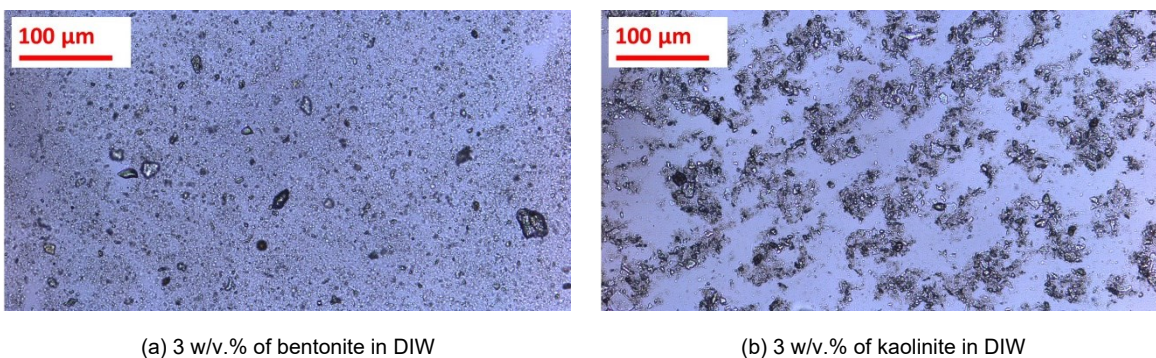
Figure 18—**Microscopy images of clay dispersions in de-ionized water (DIW): (a) 3 w/v.% bentonite, (b) 3 w/v.% of kalinite.**

Fig. 19 shows that as the concentration of bentonite increases, the surface coverage of oil droplets by clay particles increases, helping to stabilize O/W emulsions. When the particle concentration was low (e.g., 1 w/v.% in **Fig. 19a**), a severe coalescence of oil droplets happened due to the insufficient coverage of the oil-water interface by clay particles, which leads to the destabilization of emulsions as shown previously in **Fig. 17b**. When the clay concentration was 3 w/v.% and above (**Fig. 19b** and **19c**), a thin film of bentonite particles as indicated by the red arrow and circle formed around the oil droplets, preventing the coalescence of droplets, and thus improving emulsion stability. Also noted in **Fig. 19b** and **19c** is that the aqueous phase looks more viscous compared to that in **Fig. 19a**, which is caused by the excess bentonite particles when the

49

concentration was above 1 w/v.% (e.g., 3 and 5 w/v.%). This observation was confirmed by measuring the clay suspension viscosity under various particle concentrations as shown in **Fig. 20**, where the average viscosity of three measurements for each sample was plotted against clay particle concentration and the error bars were added based on the standard deviation. Note that most of the error bars were too small (close to 0) to be observed except for the sample of 3 w/v.% of bentonite, which has a slightly larger deviation of 0.19. The viscosity was measured by using a cone and plate viscometer (Brookfield, DV2T) at a fixed shear rate. As shown in **Fig. 20**, the viscosity of bentonite dispersions in DIW increases with increasing particle concentration due to swelling, while that of kaolinite dispersion remains almost unchanged and close to the viscosity of water (1 cP). This increase in bentonite viscosity suspension also helps stabilize emulsions because the coalescence rate of oil droplets will be slowed down by the viscous aqueous phase. To summarize, there are mainly two mechanisms accounting for the improved emulsion stability by adding bentonite. On one hand, bentonite particles swell a lot in DIW which reduces the size of particles to nanoscale owing to the delamination of particles, and these smaller particles form a thin layer around oil droplets, protecting them from coalescence; on the other hand, the swelling of bentonite also increases the viscosity of aqueous phase, which further slows down the coalescence rate.
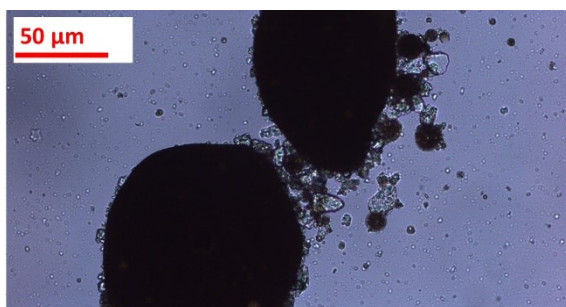
(a) 1 w/v.% of bentonite
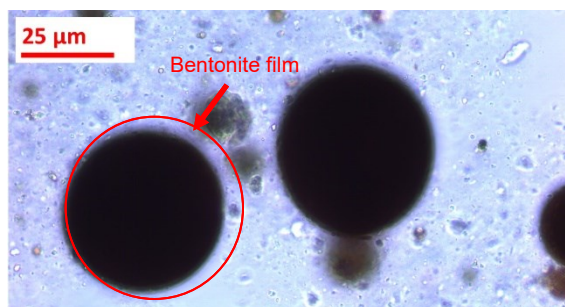
(b) 3 w/v.% of bentonite
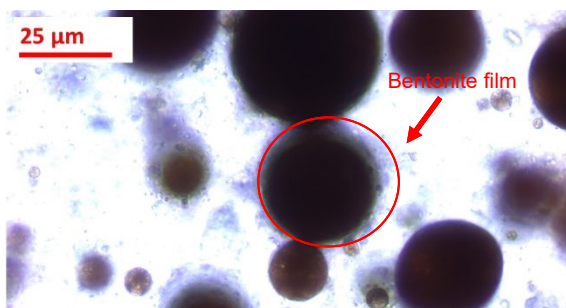
(c) 5 w/v.% of bentonite
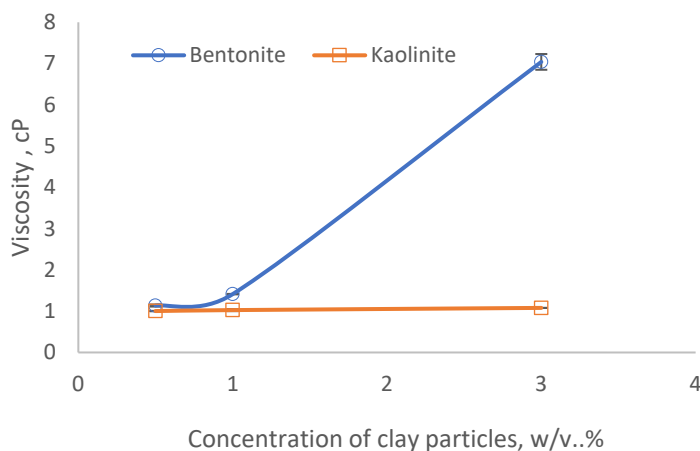
Figure 20—Viscosity of clay dispersions (bentonite and kaolinite) in DIW versus concentrations of clay particles.

3.4.2 Effects of pH on emulsion formulation

Clay particles have permanent negative charges on surfaces, which are not pH-dependent, due to both isomorphous substitutions as described earlier and pH-dependent charges at the edges (Lagaly 2006). pH is an important parameter affecting Pickering emulsion stability because pH will affect the zeta potential of solid particles dispersed in water. When the net charge of the particle is reduced to zero potential (e.g., isoelectric point, iep), particles flocculate to some extent, which can yield stable emulsions (Binks et al. 2008). Therefore, broad pH environments ranging from 2 to 12 were examined to see the pH effect on emulsion stability. High pH values of 10 and 12 were also chosen because the tested heavy oil has a high acid number (TAN=2.21 mg KOH/g) and the alkali environment helps release the natural surfactants (soap) by reacting with acid components in heavy oil (Mandal 2015). This occurrence was reported to be favorable for clay adsorption on heavy oil (Tamiz Bakhtiari et al. 2015) and thus improves emulsion stability.

Glass vial tests. Fig. 21 shows that bentonite was able to stabilize O/W emulsions when the pH was 4 or above and failed at pH=2 where the black oil just settled at the bottom in the glass vial and was covered by bentonite particles (**Fig. 21a**), whereas the kaolinite failed to stabilize emulsions over all tested pH conditions (**Fig. 21b**). To evaluate the net charge of clay particles

under various pH conditions, zeta potential measurements were performed. As shown in **Fig. 22**, the zeta potential of kaolinite increases with reducing pH and approaches 0 (iep) at pH=2, but it still could not stabilize emulsions even at iep point. With bentonite, the zeta potential was always negative and relatively stable in the pH range between 2 and 10. When the pH was raised to 12, the zeta potential of bentonite became more negative from around -50 mV to -90 mV. The different responses of zeta potential of bentonite and kaolinite to pH changes result from their structure and property difference. The edge of kaolinite was composed of exposed silica and alumina layers which will be positively charged at low pH conditions (Williams and Williams 1978), explaining the more positive zeta potential of kaolinite under low pH values. With bentonite, the contribution from edge charge was less compared to the permanent negative face charge, a result of the delaminated bentonite particles having a thickness around 1 nm—which is far smaller than the double layer length; therefore, the negative electric field generated from the face spills over into the edge zone especially at a low electrolyte condition (e.g., 10 mM NaCl) (Secor and Radke 1985). The high magnitude negative charge of bentonite at pH=12 might indicate some mineralogy change of clay, such as dissolutions of minerals of bentonite. Heikola et al. (2013) observed that due to minerals dissolution, the CEC of bentonite increased at high pH conditions (pH=11.3 and 12), indicating a higher negative layer charge.

 From these results, it can be drawn that bentonite is more effective for stabilizing emulsions when compared to kaolinite, and the emulsion is relatively stable in the pH range between 4 and 12.
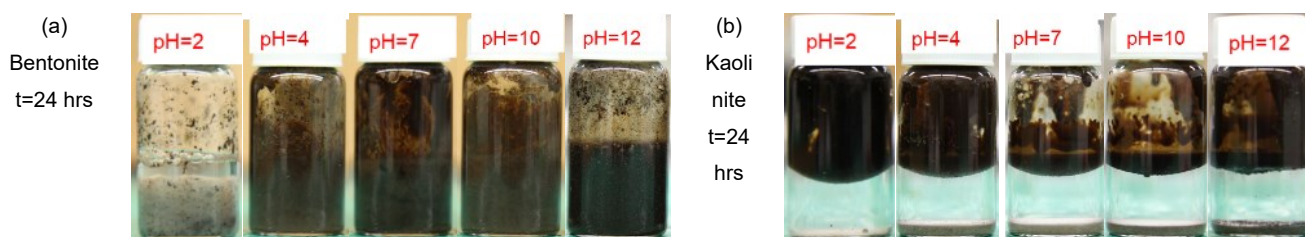
**Figure 21—Glass vials containing 1 ml heavy oil and 9 ml clay dispersion in DIW with various pH values as labeled in red fonts on vial caps 24 hours after emulsion preparation: (a) bentonite and (b) kaolinite. The particle concentration was 3 w/v.%.**
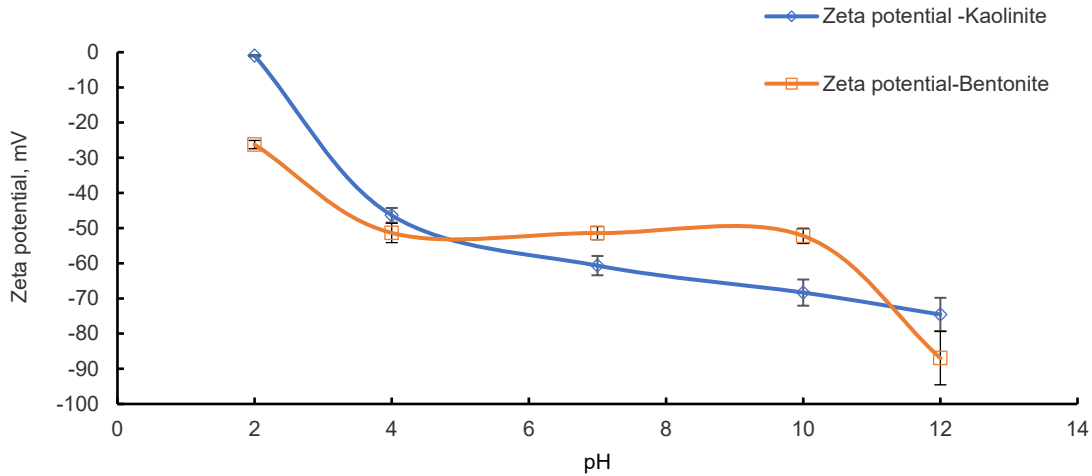
Figure 22—Zeta potential of clay particle dispersions (Kaolinite and bentonite) in 10 mM NaCl solution with various pH values.

Effect of addition of NaOH on emulsion stabilization. To study the emulsion structure (i.e., droplet shape and size) under different pH conditions, emulsion samples taken from glass vial tests as those shown in **Fig. 21a** were checked under a transmitted light microscope (Axiostar plus) and microscopic images were taken. **Fig. 23** shows that the smaller emulsion droplets were stabilized at pH=12 condition in comparison to those under other pH conditions (e.g., pH=4, 7, and 10). This was because, at such a high pH condition, NaOH reacted with acid components in the heavy oil, thus reducing the interfacial tension (IFT) between heavy oil and aqueous solution. This observation can be confirmed by the IFT measurements depicted in **Fig. 24**, which shows that the IFT was reduced from 20.61 mN/m without the addition of alkali to a minimum value of 0.17 mN/m with 0.04 w/v.% of NaOH (pH=12); a further increase of alkali concentration did not reduce IFT.

(a) pH=4
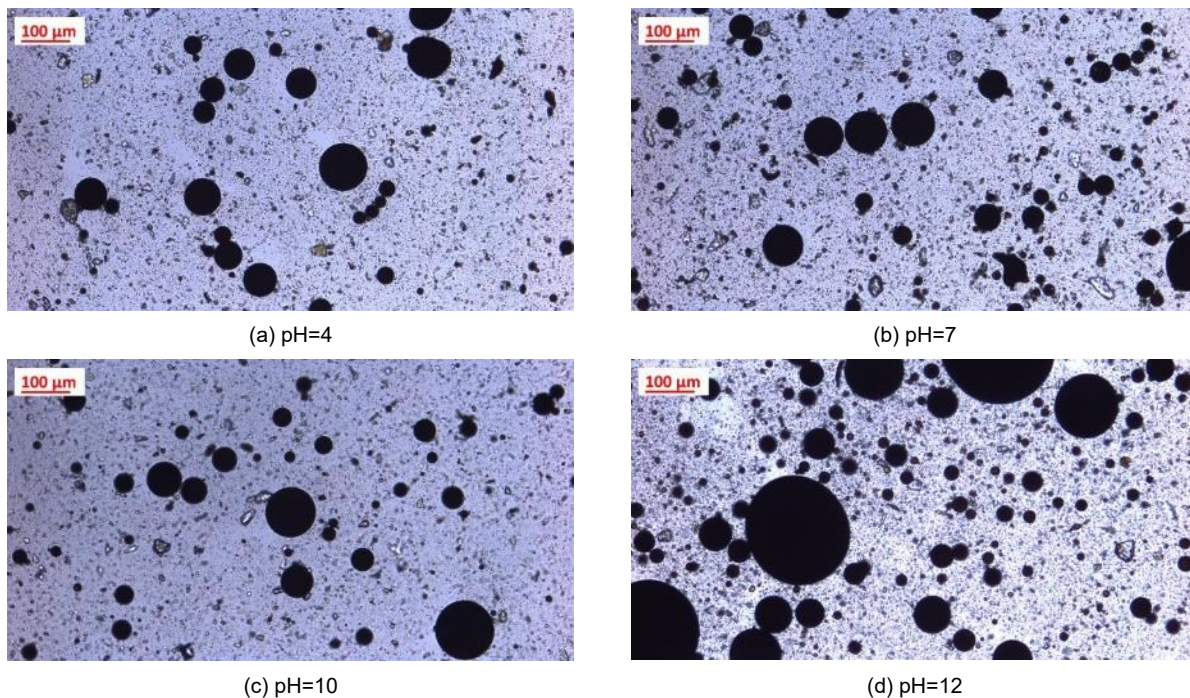
(b) pH=7

(c) pH=10

(d) pH=12

Figure 23—Microscopy images of O/W emulsions stabilized by 3 w/v.% of bentonite dispersions in DIW with various pH values: (a) pH=4, (b) pH=7, (c) pH=10, and (d) pH=12. WOR=9:1.
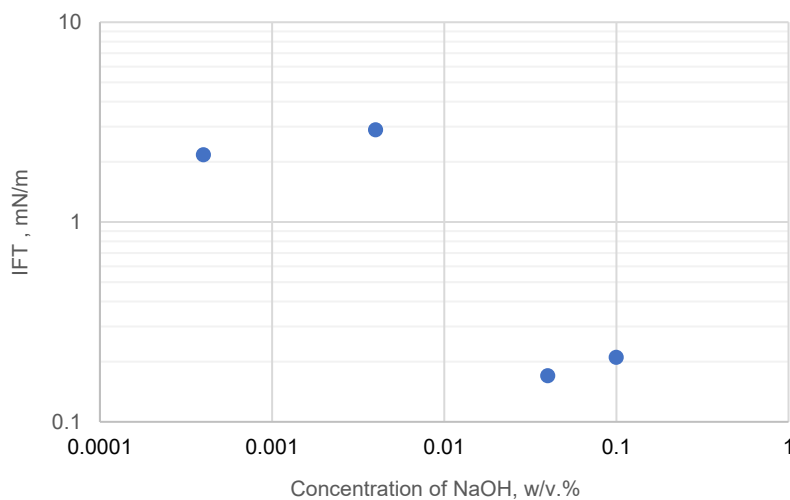
Figure 24—IFT between heavy oil and aqueous solutions with various concentrations of NaOH and 1.75 w/v.% of NaCl.

To determine whether it is NaOH itself or alkali and bentonite together that stabilized emulsions, a controlled experiment was performed. In this experiment, we compared the stability of emulsions prepared with NaOH only, with the stability of emulsions prepared with bentonite and NaOH together. As shown in **Fig. 25**, complete water-oil phase separation was observed in both the base case (**Fig. 25a**) without additives and the alkali only solution (**Fig. 25b**). The stable O/W emulsion

was only generated when both bentonite and NaOH were present. Therefore, it can be concluded that the addition of NaOH further helps bentonite stabilize the emulsion through the activation of natural surfactants in heavy oil.
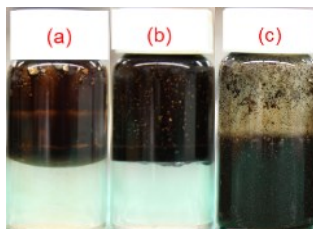
Figure 25—Glass vials containing 1 ml heavy oil and 9 ml aqueous solutions with various composition of NaOH and bentonite: (a) no bentonite and no NaOH, (b) 0.04 wt.% NaOH (pH=12), (c) 0.04 w/v.% NaOH (pH12) and 3 w/v.% bentonite.

3.4.3 Effects of salinity on emulsion stability

Fig. 26 shows that the emulsion stabilized by bentonite became unstable when the NaCl concentration was 300 mM (1.75 wt.%) at pH=7 condition, whereas under high pH (12) condition, the emulsion remained stable at such a high salinity condition. **Fig. 27** shows the microscopic emulsion droplet structure under different salinity and pH conditions. As shown in **Fig. 27**, at neutral pH conditions, a coalescence of oil droplets was observed when the concentration of NaCl was 100 mM and above, leading to the unstable emulsions as shown in **Fig. 26a** (300 mM NaCl); while at alkali condition (e.g., pH=12) the oil droplets remained stable despite the increasing electrolyte concentration. This observation can be explained by the DLVO (named after Derjaguin, Landau, Verwey, and Overbeek) theory in combination with the Ionizable Surface-Group model (Isaacs and Chow 1992). In this case, the oil droplets were treated as negatively charged dispersed particles in aqueous solution due to the dissociation of acid components (e.g., carboxy group) in heavy oil. When the electrolyte concentration increases, the net charge of droplets will reduce since the electrical double layer thickness was reduced, causing a reduction of electrostatic repulsive force. This change makes the Van der Waals attractive force dominant, leading to droplets coagulation. When the pH is raised to 12, functional groups originating in the heavy oil can expect to be dissociated, effectively enhancing the surface charge of oil droplets, providing a higher repulsive force and higher emulsion stability (Isaacs and Chow 1992).
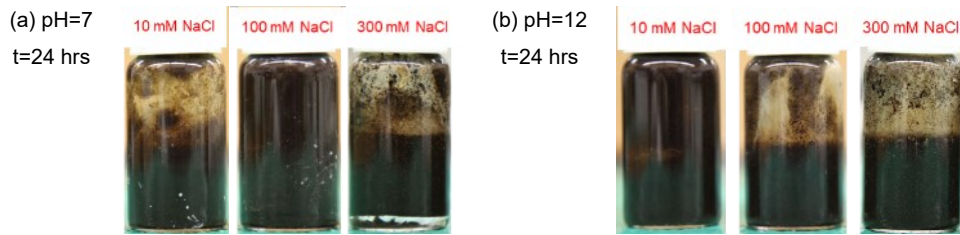
Figure 26—Glass vials containing 1 ml heavy oil and 9 ml NaCl solutions with various concentrations of salt 24 hours after emulsion preparation under different pH conditions: (a) pH=7 and (b) pH=12. Bentonite concentration was 3 w/v.%.
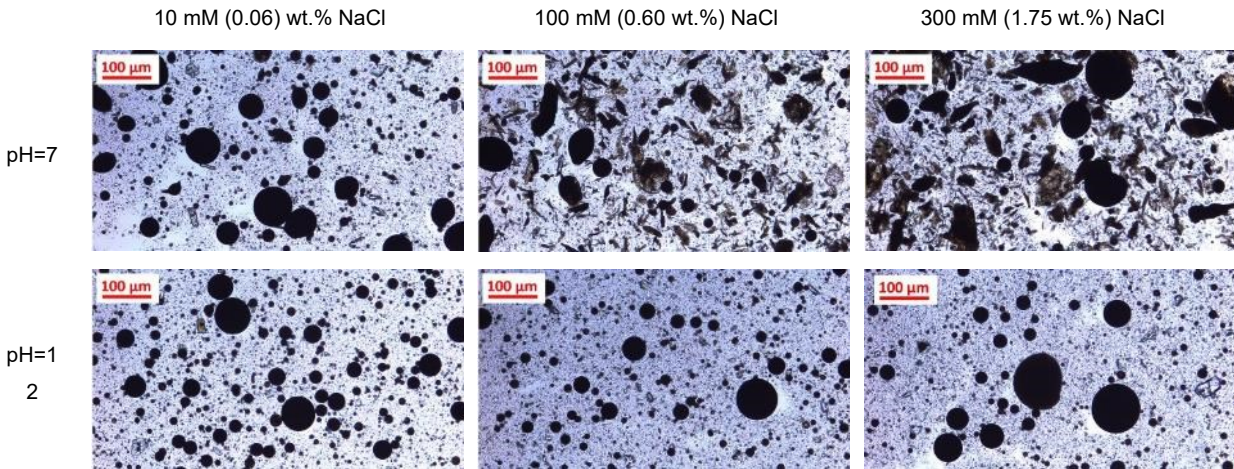
Figure 27—Microscopy images of O/W emulsions stabilized by 3 w/v.% of bentonite under various pH and salinity conditions.

3.4.4 Effects of water to oil ratio (WOR) on emulsion formulation

Fig. 28 shows that as WOR reduced from 9:1 to 5:5, the O/W inverted to W/O emulsion with an inversion point around WOR=7:3. At WOR=7:3, the emulsion was most unstable with both O/W and W/O emulsion observed. The similar emulsion inversion behavior was also observed at high pH (12) condition, where the inversion also happened at WOR=7:3 and above which complete W/O emulsion was formed. This type of phase inversion induced by changing WOR is called catastrophic phase inversion and the emulsion is least stable at the inversion point (Binks and Lumsdon 2000).
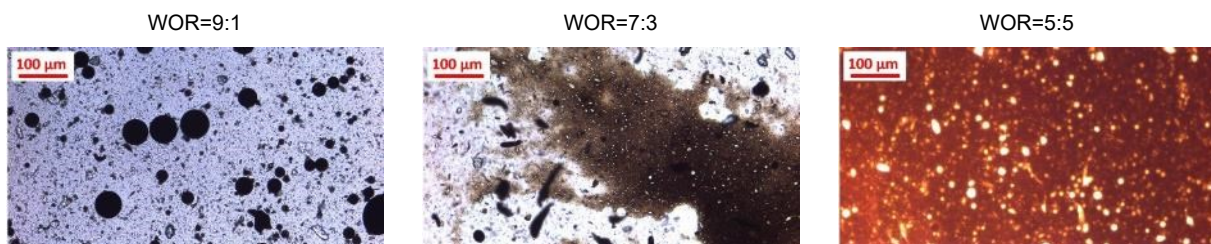
3.4.5 Sandpack (SP) floods

The properties of sandpacks used for the following flood experiments are summarized in **Table 6**. In these flood experiments, the sandpack composition (clay type and content), salinity, and pH were varied to study the effect of clay on the oil recovery and pressure as well as the produced emulsion under various salinity and pH conditions. The tested salinities are 0 (DIW), 1.75 wt.%, and 10 wt.% NaCl, which represent low, medium, and high salinity conditions, respectively.

Floods 1 to 3. These three flood experiments (SP1, SP2, and SP3) were designed to serve as base cases, where the sandpacks were composed of pure sands without clay. The salinity was varied to study its effect on oil recovery. **Fig. 29** shows that in SP1 the pressure increases up to a maximum value of 20 psi at 0.24 pore volume (PV) as fluid was injected into the sandpack, then goes down to 5.6 psi after 2 PV was injected. The final oil recovery factor is 40%, which is the ratio of cumulative produced oil to the original oil in place (OOIP). The water breakthrough, which is the formation of a continuous water path from the injection point to production point, happened at 0.24 PV fluid, where the pressure was maximum because of the single-phase oil flow. After the water breakthrough, the pressure decreases as more water is present in the flow channel. Before water breakthrough, only oil was produced; after breakthrough, W/O emulsion was produced accompanied by excess water. **Fig. 30** shows the microscopy images of pure oil (**Fig. 30a**) and W/O emulsion (**Fig. 30b**) collected from effluent samples before and after water breakthrough. The formation of W/O was probably due to the natural surfactants in heavy oil, which is usually lipophilic (Kumar et al. 2012). The in-situ formation of W/O emulsion in the porous medium was commonly observed during low salinity waterflood process as reported by multiple authors ((Vittoratos and Kovscek, 2019)), which would also help improve the recovery.
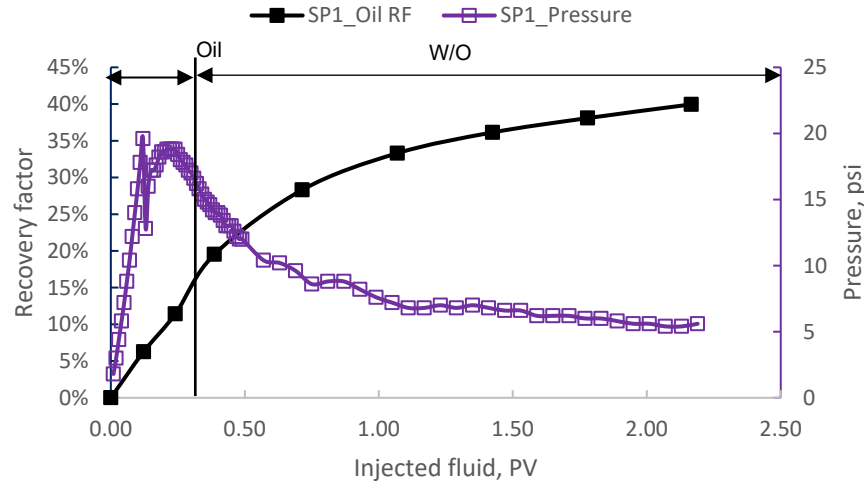
Figure 29—Oil recovery and pressure versus cumulative injected fluid in pore volume (PV) in sandpack flood 1 (SP1): No clay, DIW.
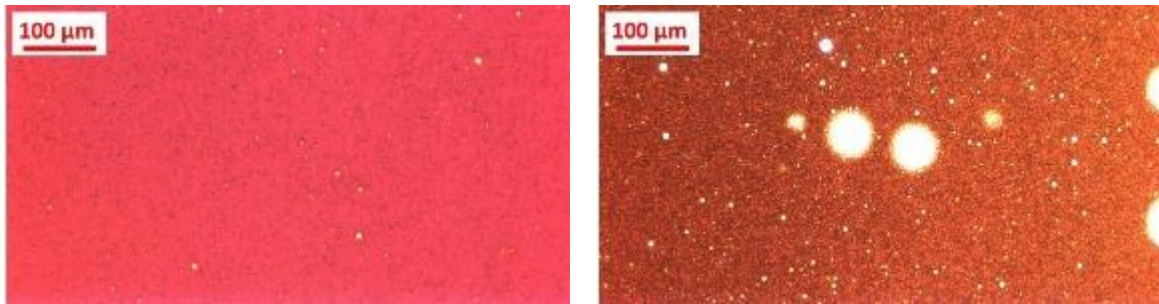
(a) Pure oil before water breakthrough

(b) W/O emulsion after water breakthrough

Figure 30—Microscopy images of effluent during different production stages in SP1: (a) pure oil before breakthrough and (b) W/O emulsion after breakthrough.

The oil recovery profiles from flood 2 (SP2) and flood 3 (SP3) were plotted in **Fig. 31** together with those from flood 1 (SP1) to compare the salinity effect on oil production. The effluent fluids from SP2 and SP3 are similar to those from SP1, where only oil was produced before breakthrough and W/O emulsion was formed after breakthrough. **Fig. 31** shows that the oil recovery profiles of SP2 and SP3 almost overlap and the final recovery is 33%, which is lower than that obtained by injecting DIW (40%). This reduction of oil recovery by injecting salt solutions might be due to the change in the wettability of sand to be more oil wet. The addition of salt will make the sand surface change towards a more positively charged state, as reported by Pratama and Babadagli (2019), who also found that the surface charge of quartz, which is the main mineral in the sand, weakened

58

from -130 mV at 1 mM brine condition to -50 mV at 100 mM (0.6 wt.%) condition. This decrease in the solid surface charge will tend to attract more oil which is usually negatively charged and thus make the sand more oil wet, leading to lower oil recovery. The change of rock wettability to be more water wet was widely reported in the low-salinity-water (LSW) flooding process (Nasralla et al. 2011; Bartels et al. 2019).
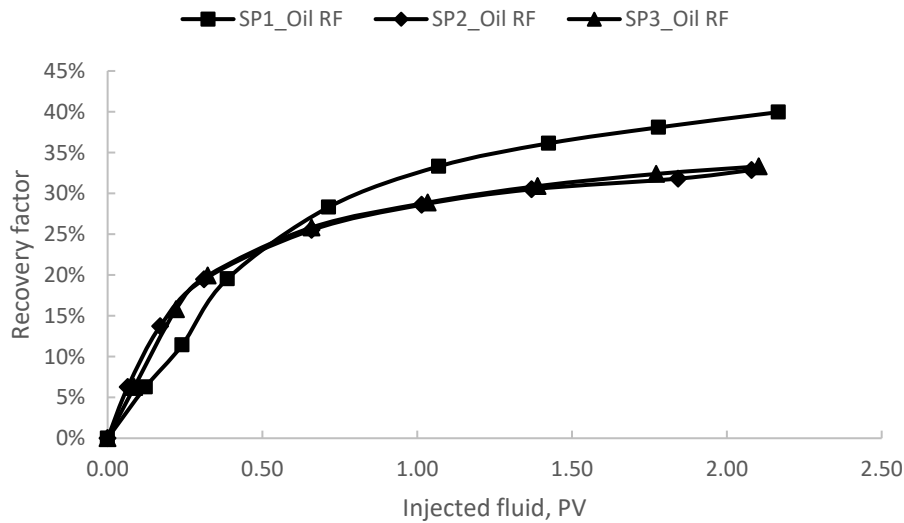
Figure 31—Comparison of oil recovery from pure sandpacks by injecting various salt solutions: (SP1) DIW, (SP2) 1.75 wt.% NaCl (SP3) 10 wt.% NaCl.

Floods 4 to 6. The sandpacks used for floods 4 to 6 are composed of 5 wt.% bentonite and 95 wt.% sands. The salinities of injected fluids were varied: 0 (DIW, SP4), 1.75 wt.% (SP5), and 10 wt.% (SP6). **Fig. 32** shows that the maximum injection pressure reaches around 500 psi, due to the swelling of bentonite when contacted with water, leading to the blockage of pore space and reduction of permeability. After water breakthrough, the pressure went down and stabilized at around 280 psi, indicating that the equilibrium of bentonite swelling might be reached as more fluids are injected. The final oil recovery was 49%, which is higher than that of SP1 (40%). The incremental recovery from SP4 might be attributed to, on one hand, the wettability change caused by low salinity water flooding as described earlier, on the other hand, the improved water sweep efficiency induced by the swelling of bentonite. When the water first meets the bentonite in the porous medium, the dry clay particles will absorb the water and swell, then the hydrated clay will form a low permeability zone and prevent the flow of incoming water (Clem and Doehler 1961),

59

which might divert the flow of water to new channels, and thus improve oil recovery (Bernard 1967).

By checking the effluent fluids under a microscope, it was found that bentonite was produced together with oil before water breakthrough. An example is highlighted in the green rectangle where the bright particles represent bentonite particles and the yellowish parts represent oil (**Fig. 33a**), which makes sense because the bentonite was loosely packed with sands, and when only single-phase oil flows, these fine clay particles will move along with the flowing phase (Muecke 1979). After water breakthrough, W/O emulsion was produced, with the bright parts being water and the dark parts being oil (**Fig. 33b**), like previously observed in pure sandpack experiments. Besides, a small number of bentonite particles attached to a few oil droplets were also observed in the aqueous phase (some examples can be seen in red rectangles in **Fig. 33c**. Bentonite was only produced when the injection fluid was DIW (SP4), and no clay was observed in the effluents from both SP5 and SP6 floods where the salinities were relatively high. This might be because under low salinity condition like DIW, the expanded clay aggregation more easily disengages from the sand surface and deflocculates due to the thickness of the diffuse double layer; both clay and sand increase leading to an enhanced electrostatic repulsion force between these solids (Bennion et al. 1998). No O/W emulsion was observed in the effluent even under high water cut conditions (e.g., above 90%) as shown in **Fig. 34** where 90% of water cut was reached when 1.36 PV fluid was injected in SP4. This might be caused by several factors. Firstly, the shear force induced by fluid flow in a porous medium might not be high enough to create emulsions as compared to the mechanical energy generated by homogenization in glass vial tests. This phenomenon was also observed by Bryan and Kantzas (2009) in an alkali-surfactant flooding process. Secondly, the clay concentration might not be enough to stabilize the emulsion. As found in glass vial tests, the required bentonite concentration to form stable O/W emulsions is 3 w/v.% in water, but the clay concentration in the effluent is far less than 3 w/v.% indicated by the microscopy images of clay suspensions in water as shown in **Fig. 33c** in comparison to that in **Fig. 18a**, which shows 3 w/v.% of bentonite dispersed in DIW. Also, the bentonite particles in the effluent were mostly aggregated, meaning they were not fully swollen, because their size will reduce once fully hydrated as described in section **Stabilization mechanisms**. And these aggregated particles are ineffective in stabilizing emulsions.
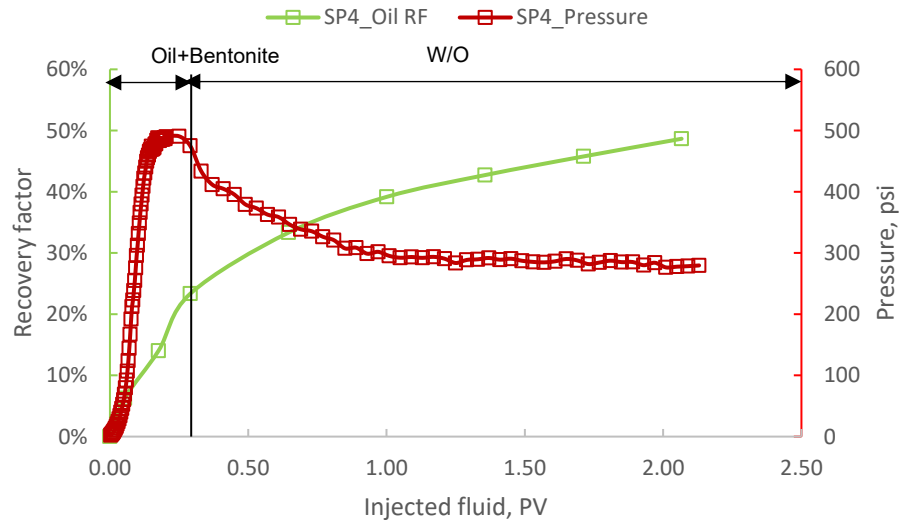
Figure 32–Oil recovery and pressure versus cumulative injected fluid in pore volume (PV) in sandpack flood 4 (SP4): 5 wt.% bentonite, DIW.
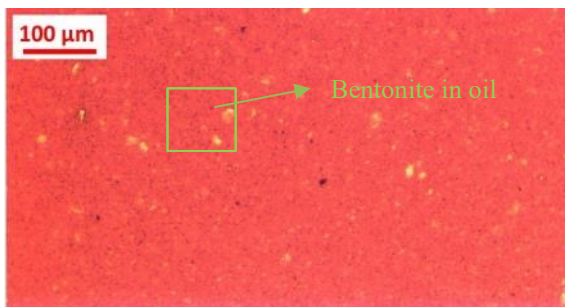
(a) Oil and bentonite particles before water breakthrough
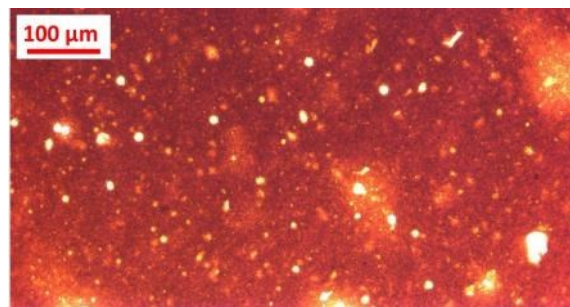
(b) W/O emulsion after water breakthrough
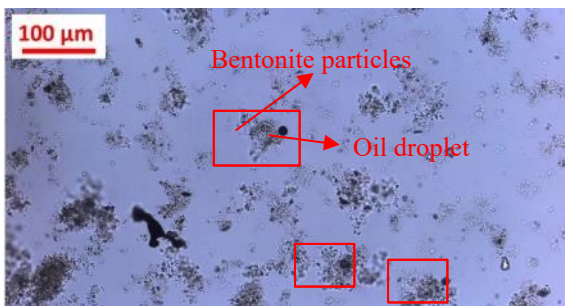
(c) Produced bentonite in the aqueous phase after breakthrough

Figure 33—Microscopy images of effluent during different production stages in SP4: (a) oil and bentonite particles (green rectangle shows an example of bentonite produced with oil) before the breakthrough, (b) W/O emulsion (bright parts-water, dark parts-oil) after breakthrough, and (c) produced bentonite in the aqueous phase after breakthrough (red rectangles show an example of bentonite particles attached to oil droplets).

The oil recovery and water cut profiles from flood 5 (SP5) and flood 6 (SP6) were plotted in **Fig. 34** together with those from flood 4 (SP4). The effluent fluids from SP2 and SP3 were similar to those from SP4, where oil and bentonite particles were produced before the breakthrough and W/O emulsion was formed after breakthrough—except that no clay was observed in the aqueous phase in SP5 and SP6. **Fig. 34** shows that the water cut in SP4 was lower compared to that in SP5 and SP6 after injecting the same amount of fluid, thus explaining the higher oil recovery factor when injecting DIW (SP4). This lower water cut provides additional evidence of improved sweep efficiency by injecting DIW. After salt concentration was increased to 1.75 wt.% (SP5) and 10 wt.% (SP6), the final oil recovery factors (35% for SP5 and 30% for SP6) are quite close and lower than that in DIW (49%, SP4). The reduction of this oil recovery is most probably due to the change of sand wettability toward more oil wet when the salt concentration was increased (Nasralla et al. 2011). Because in all three (SP4, SP5, and SP6) of these flood experiments, the formation damage caused by swelling of clay might be similar as indicated by the similar pressure profiles as shown in **Fig. 35**, therefore, the mechanism about improving sweep efficiency by clay swelling was expected to exist in all three cases. The observation of high injection pressure even when injecting high salinity water (e.g., 10 wt.% NaCl, SP6) in the sandpack flooding experiment was different from that observed in rock (like sandstone) flooding where the clay swelling will be avoided and thus the injection pressure will be low under high salinity condition (Bernard 1967). This might be due to the different clay distribution format in sandpack and real rock, where the clay particles were loosely packed in the sandpack while cemented in the rock, therefore, the accessible clay to water ratio is high in the sandpack, leading to more swelling and formation damage compared to that in rock.
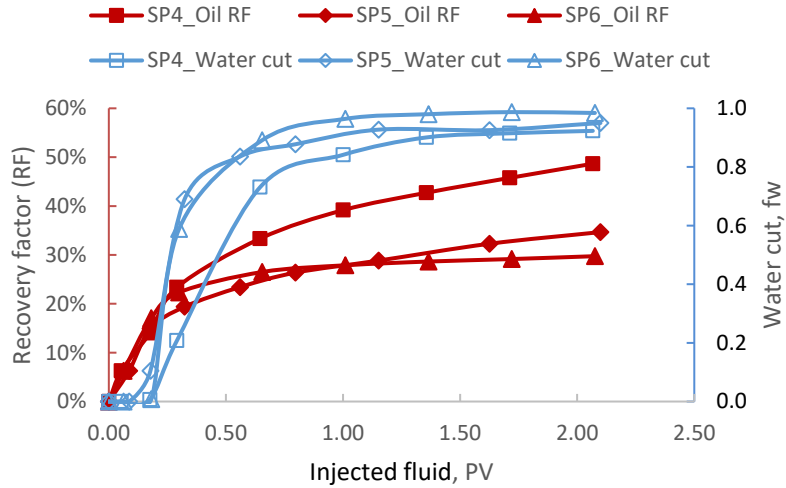
Figure 34—Comparison of oil recovery and water cut from sandpacks with 5 wt.% of bentonite by injecting various salt solutions: (SP4) DIW, (SP5) 1.75 wt.% NaCl, (SP6) 10 wt.% NaCl.
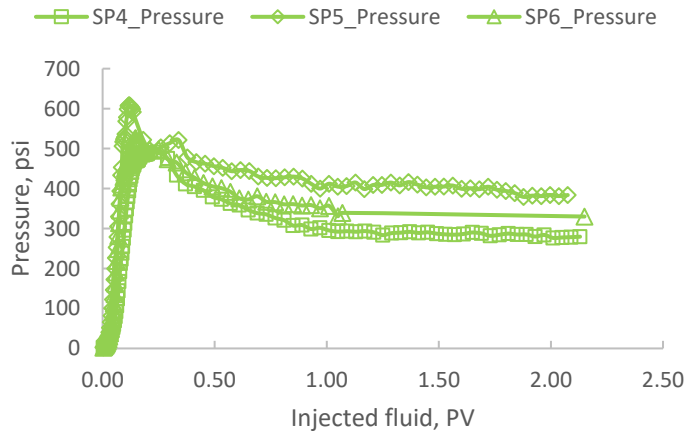
Figure 35—Comparison of pressure profiles from sandpacks with 5 wt.% of bentonite by injecting various salt solutions: (SP4) DIW, (SP5) 1.75 wt.% NaCl, (SP6) 10 wt.% NaCl.

Floods 7 to 9. For these three experiments, the sandpacks were composed of 5 wt.% kaolinite and 95 wt.% sands. The salinities of injected fluids were varied such as 0 (DIW, SP7), 1.75 wt.% (SP8), and 10 wt.% (SP9). **Fig. 36** shows that before the breakthrough, the pressure increases up to a maximum value of around 100 psi before which only pure oil and kaolinite were observed in the effluent sample as shown in **Fig. 37a**, where the green rectangle shows an example of kaolinite particles (bright parts) dispersed in the oil phase (yellowish background). The maximum pressure

63

of 100 psi is lower than 500 psi when the bentonite was present in the sandpack (SP4). This is because kaolinite is a non-swelling clay, and the formation damage is caused by the migration of these fine particles which will bridge and plug the pore throat and thus reduce permeability (Muecke 1979). This type of formation was less harmful compared to that caused by swelling clay, which will plug the hole pore and pore throat due to the expansion of clay. This different formation damage was also reflected by the measured permeability values as shown in **Table 6**, which shows that the permeability values of sandpacks with bentonite (e.g., 0.2 D and 0.4 D) were lower than those of sandpacks with kaolinite (e.g., 1.2 D and 1.3D).

After the water breakthrough, the pressure goes down as water enters more pore space. One interesting finding after breakthrough is that the produced oil phase was not in W/O emulsion form, as observed in previous experiments, instead, the water and oil were separated with highly flocculated kaolinite in the continuous water phase. The produced water also contains suspensions of aggregated kaolinite particles and an example was shown in the red rectangle in **Fig. 37c**. One possible explanation is as follows: W/O emulsion might be originally formed in the oil phase, but since kaolinite is naturally hydrophilic and when both oil and water are present, clay particles tend to stay in water; after they gathered in the water phase, these kaolinite particles are prone to aggregate and settle down as also observed in the glass vial tests in **Fig. 17d** and **Fig. 18b**, therefore, the aggregation of kaolinite particles, such as the example shown in the green rectangle in **Fig. 37b**, destabilized the W/O emulsion leading to the water-oil separation. The destabilized W/O emulsion leads to a lower final oil recovery (40%) compared to that of 49% in SP4. These types of effluent samples before sand after water breakthrough were also observed in SP8 and SP9 floods.
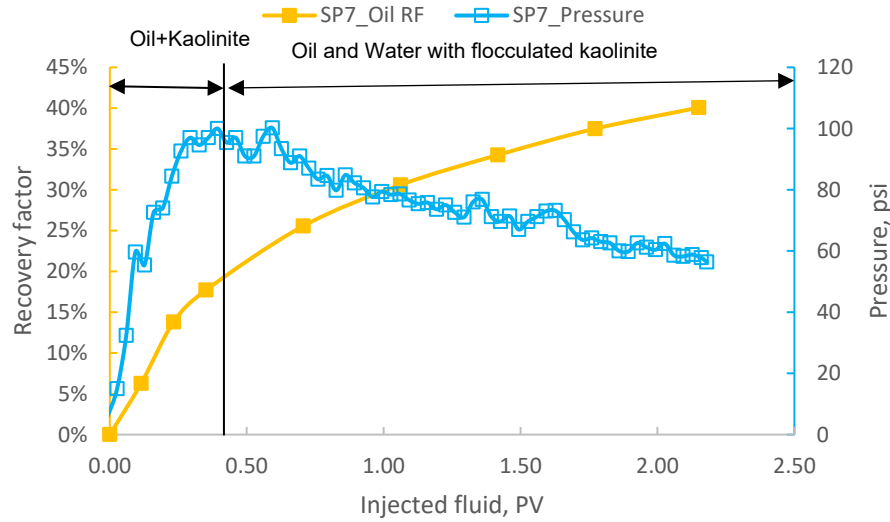
Figure 36—Oil recovery and pressure versus cumulative injected fluid in pore volume (PV) in sandpack flood 7 (SP7): 5 wt.% kaolinite, DIW.

(a) Oil and kaolinite before water breakthrough

(b) Oil and emulsion after water breakthrough

(c) Produced kaolinite in aqueous phase after breakthrough
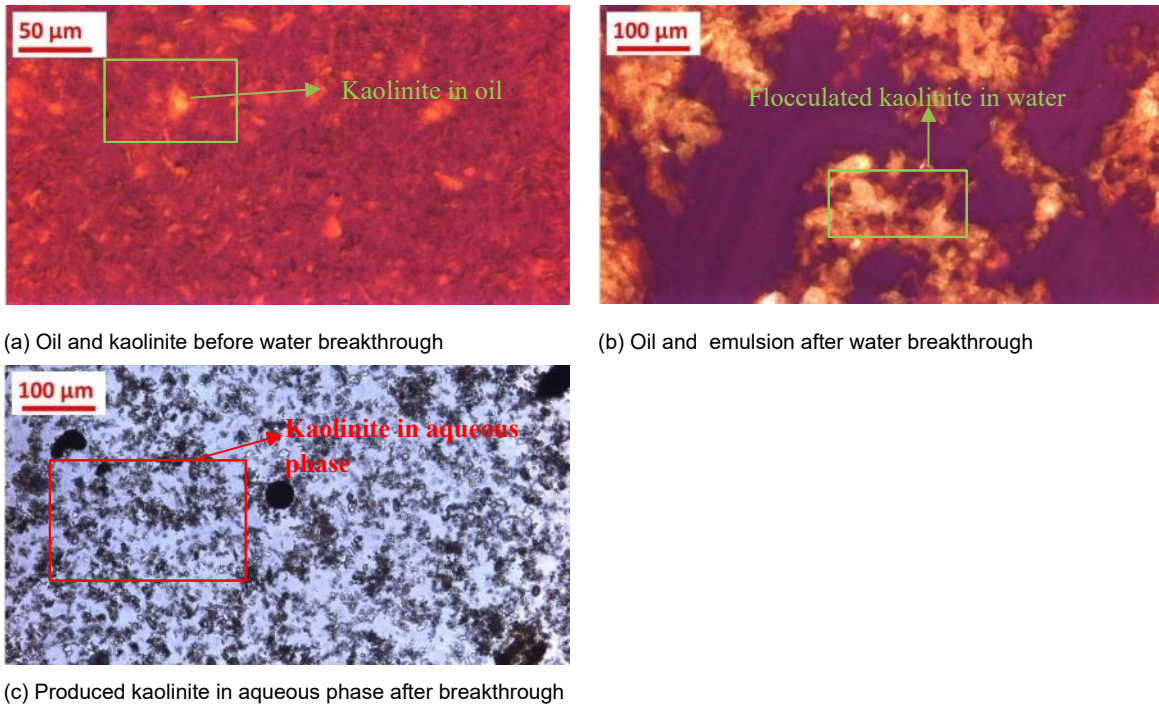
Figure 37—Microscopy images of effluent during different production stages in SP7: (a) oil and bentonite before breakthrough, (b) W/O emulsion after breakthrough, and (c) produced kaolinite in aqueous phase after breakthrough. The rectangles in (a), (b), and (c) show examples of: (a) kaolinite particles (bright parts) dispersed in oil (yellowish background), (b) flocculated kaolinite particles in oil phase of effluent sample where water was present, and (c) flocculated kaolinite particles in aqueous phase of effluent sample.

65

Fig. 38 shows the comparison of oil recovery and pressure from sandpack floods with kaolinite under various salinity conditions. Again, the maximum oil recovery of 40% was achieved by injecting DIW, which might be attributed to the wettability change as described previously in both **section Floods 1 to 3** and **Floods 4 to 6.** When the salinity was 1.75 wt.% and above, such wettability change effects diminished, stopping the salinity from affecting the oil recovery allowing a final recovery of 31% in both SP8 and SP9. The pressure profiles from SP8 and SP9 are similar and lower than that from SP7 (e.g., 20 psi difference in maximum pressure). This might be due to the deflocculation of clay particles in low electrolyte conditions (Lever and Dawe 1987), which will cause more migration of particles and thus more blockage of pore throats leading to lower permeability of 0.5 D when measured with DIW in comparison to that of 1.2 and 1.3 D when measured with 1.75 wt.% and 10 wt.% NaCl respectively as shown in **Table 6**.
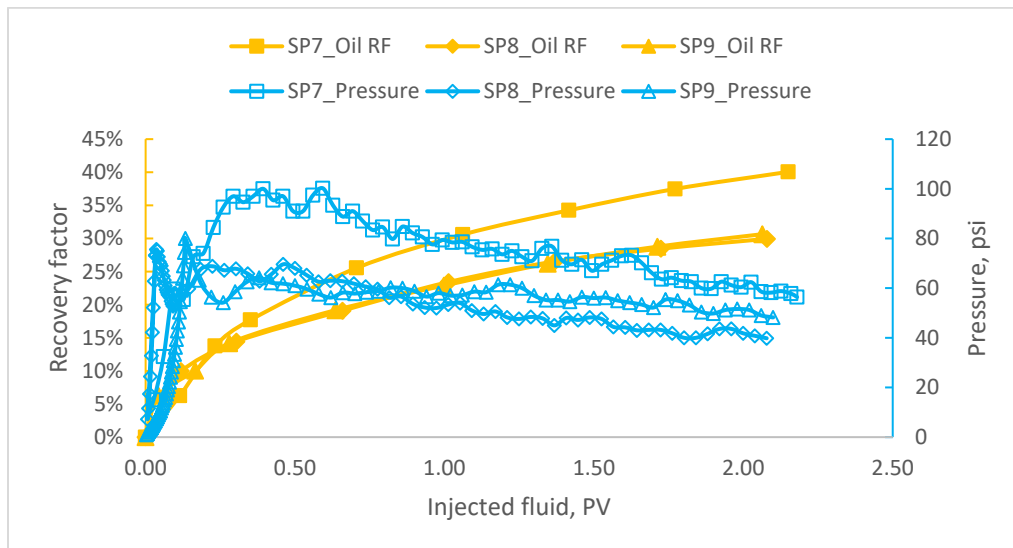
Figure 38—Comparison of oil recovery and pressure from sandpacks with 5 wt.% of kaolinite by injecting various salt solutions: (SP7) DIW, (SP8) 1.75 wt.% NaCl, (SP9) 10 wt.% NaCl.

Floods 10 to 12. For these three experiments, the injected fluid was kept the same: a high pH solution (pH=12) adjusted by adding 0.04 wt.% NaOH in DIW. The sandpack composition was varied as follows: SP10-no clay, SP11-5 wt.% bentonite, and SP12-5 wt.% kaolinite. These experiments were performed to see whether adding alkali will help clay particles stabilize emulsions in a porous medium and assess their effect on oil recovery.

Fig. 39 shows that a maximum final oil recovery of 78% can be achieved by alkali flooding from SP10, where no clay was present. When clay particles, whether bentonite or kaolinite, were present in the sand pack, the oil recovery is lower (38% from both SP11 and SP12). This is because, at such a high pH (12) environment, clay particles will react with NaOH and reduce pH below 12 as observed in **Fig. 39**, which makes the alkali solution less effective and thus lowers oil recovery. Experiments have shown that the significant reaction of NaOH with clay components in some reservoir rocks can be rapid and complete (Jennings Jr. et al. 1974). The pressure profiles as shown in **Fig. 40** show that some significant change in bentonite property might happen as indicated by the abnormal pressure change from SP11, where the sandpack was composed of 5 wt.% bentonite. During the SP11 flood process, a significant amount of bentonite was produced in the aqueous phase of the effluent sample after water breakthrough as shown in the inset picture (left) in **Fig. 40**. This production of bentonite led to the continuous reduction of pressure because the permeability of the sandpack was expected to improve after the clay particles flowed out. However, the oil recovery of SP11 did not improve when significant amounts of bentonite particles were produced. This is because the destabilization of clay particles consumed NaOH which as reflected from the pH change of effluent sample in **Fig. 39**, would make NaOH less effective and thus lead to lower recovery in comparison to SP10. Therefore, during the high pH flooding process such as alkaline flooding, the presence of clay particles would be detrimental. The increase in pressure—after around 1 PV fluid was injected into SP11—was due to the formation of O/W/O multiple emulsions with a high viscosity as indicated in the inset picture (right) in **Fig. 40** where the bright parts are water, and the dark parts are oil. This second increase in pressure did not lead to an improvement in the oil recovery of SP11 as shown in **Fig. 39**, which might be because the water channels were already formed and most oil was bypassed by the injecting fluid or the in-situ formed multiple emulsions. The reason for the large production of bentonite particles under high pH conditions might be the dissolution of some mineral components in bentonite as observed by Heikola et al. (2013), who found that the most significant mineral changes in bentonite occurred at pH=12.
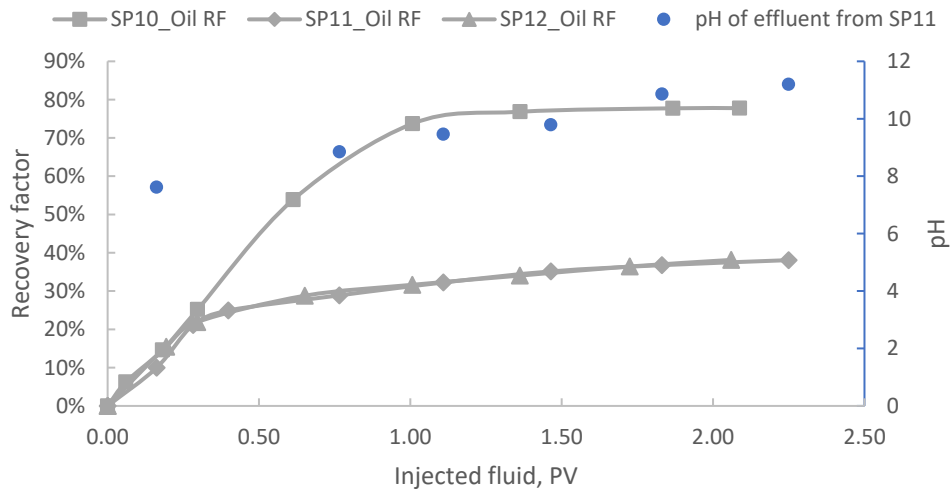
Figure 39—Comparison of oil recovery from sandpacks with various compositions (SP10-No clay, SP11-5 wt.% bentonite, SP12-5wt.% kaolinite) by injecting 0.04 wt.% of NaOH in DIW(pH=12) and the pH change of effluent from SP11.
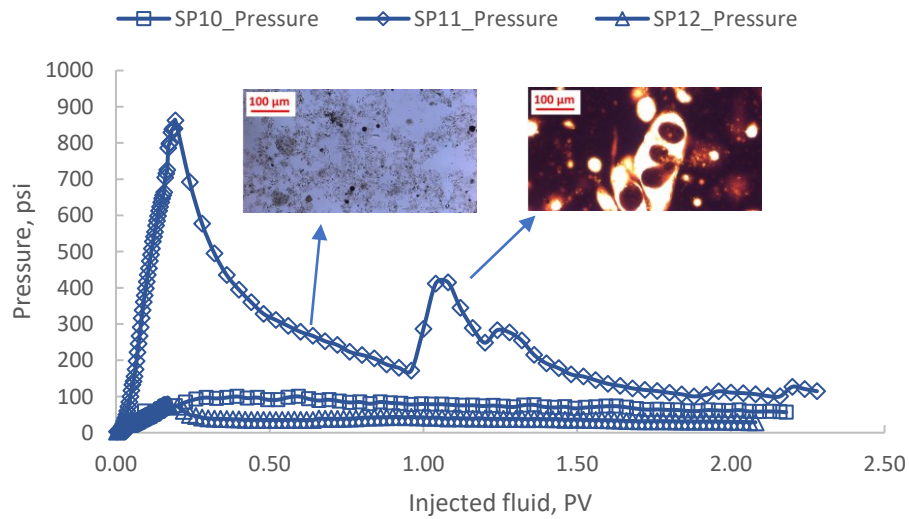
Figure 40—Comparison of pressure from sandpacks with various compositions (SP10-No clay, SP11-5 wt.% bentonite, SP12-5wt.% kaolinite) by injecting 0.04 wt.% of NaOH in DIW(pH=12).

Discussion. By comparing the oil recovery from SP1, SP4, and SP7 (**Fig. 41a**) flood experiments, the addition of bentonite clearly shows higher oil recovery, which is 49% (SP4) in comparison to that of 40% from both SP1 and SP7. Since the injected fluid was DIW in all these three floods, the wettability change induced by the low salinity environment was expected to be similar. Therefore,

the incremental oil recovery (9%) should be attributed to the swelling of bentonite, which might divert the flow of incoming water to new flow channels and thus improve the sweep efficiency. This increase in oil recovery was accompanied by the high displacement pressure resulting from the swelling of clay plugging the pore spaces and reducing permeability significantly.

As the salinity was raised to 1.75 wt.% NaCl (**Fig. 41b**), the oil recovery profiles from SP2 and SP5 were close, with final oil recovery of 33% and 35%, respectively. Oil recovery from SP8 (30%) was slightly lower, possibly due to the destabilized W/O emulsion in SP8 as observed in **Fig. 37b**. Generally, stable W/O emulsion helps improve sweep efficiency and thus improves oil recovery owing to the high emulsion viscosity (Kumar et al. 2012).

As salinity was further raised to 10 wt.% NaCl (**Fig. 41c**), the oil recovery from all the cases (SP3, SP6, and SP9) was close. This effect was likely a result of the wettability change mechanism and swelling of clay effect induced at low salinity condition (e.g., DIW) disappearing under such a high salinity condition.

(a)

(b)
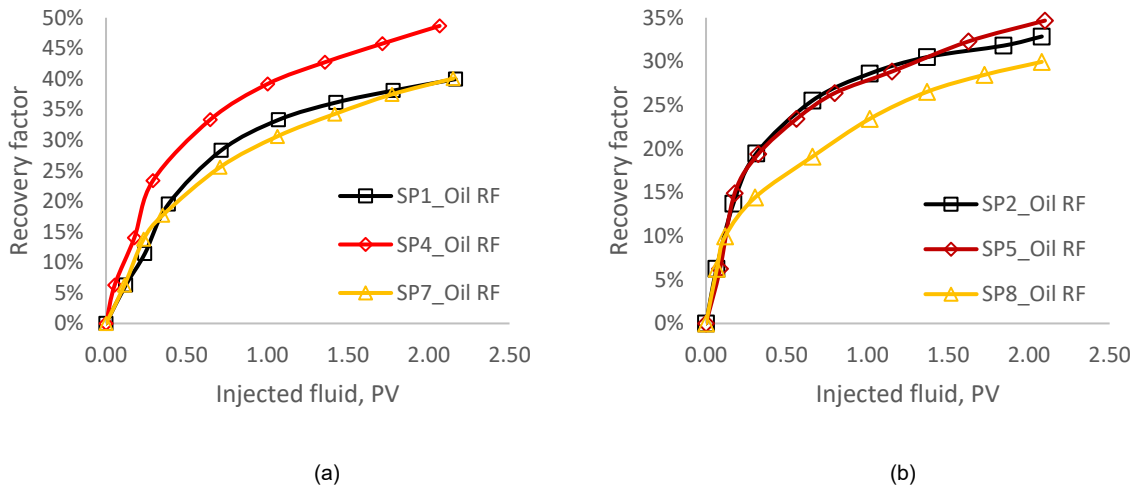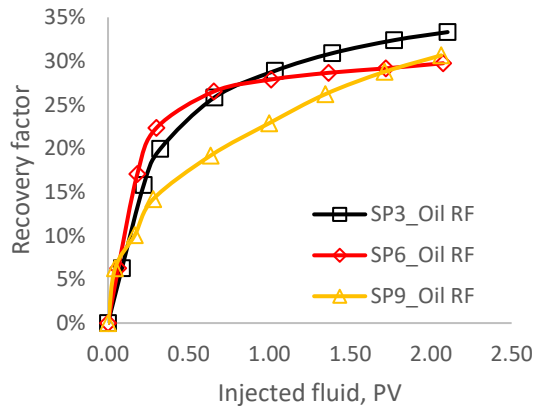
(c)

Figure 41—Comparison of oil recovery from sandpacks with various compositions (SP1, SP2 and SP3-No clay, SP4, SP5 and SP6-5 wt.% bentonite, SP7, SP8 and SP9-5wt.% kaolinite) under different salinity conditions: (a) DIW, (b) 1.75 wt.% NaCl, (c) 10 wt.% NaCl.

3.4.6 Micromodel tests

Low salinity (DIW) floods. In these experiments, DIW was injected into micromodels with and without clays (kaolinite and bentonite) to study the clay effect on residual distribution under low salinity conditions. **Fig. 42** shows the initial (**Fig. 42a**) and residual oil condition (**Fig. 42b**) of the pure glass bead micromodels. **Fig. 42a** shows the model was initially fully saturated with red-dyed mineral oil. **Fig. 42b** clearly shows the spherical residual oil, as highlighted in the yellow square, indicating the glass beads were more water wet. This supports our previous assumption that the sand was more water-wet at low salinity conditions.

a   b
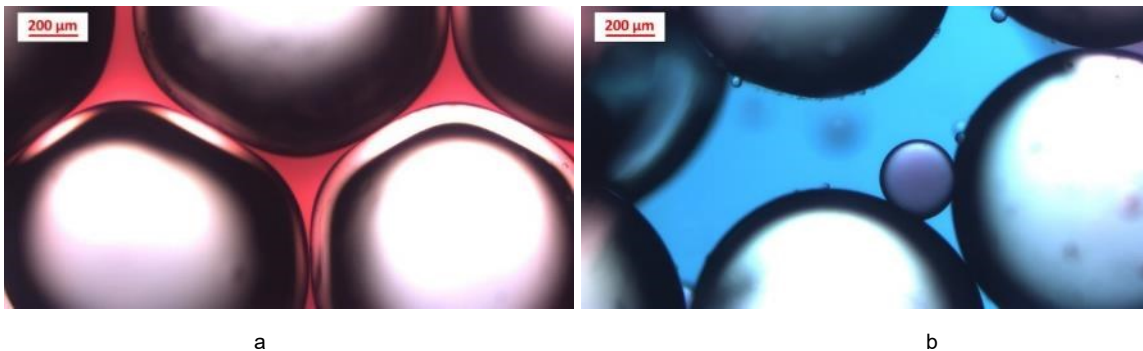
Figure 42—Pure glass bead model without clay at (a) initial condition and (b) residual oil condition (different position) after injecting 9 ml of dyed DIW. The yellow square in (b) shows the spherical residual oil.

Fig. 43 shows the results of DIW flood on the micromodel with 5 wt.% bentonite. **Fig. 43a** shows the initial condition where the bentonite particles were loosely attached on the glass bead surface (an example was shown in the yellow rectangle), which simulates the initial reservoir condition when clays are present. **Fig. 43b** shows a different location at residual oil condition, where many oil droplets stabilized by bentonite were observed as highlighted in the yellow rectangle. This observation is also consistent with our glass vial tests which showed bentonite as an effective emulsion stabilizer. The formed O/W emulsion helps the transportation of oil in the porous medium since the oil viscosity is reduced. The residual oil distribution in **Fig. 43c** shows the glass bead was more water wet as reflected from the spherical residual oil in the yellow rectangle in **Fig. 43c**, which is also consistent with the pure glass bead case as shown in **Fig. 42b**. **Fig. 43d** shows a new observation when bentonite was present, which illustrates the diverted water flow due to the plugging of pore throat caused by swelling of bentonite particles as highlighted in the yellow rectangle in **Fig. 43d**. This supports the previous argument that the incremental oil recovery at low salinity condition was attributed to diverted water flow when bentonite was present in sandpack as described in the **Discussion** section.
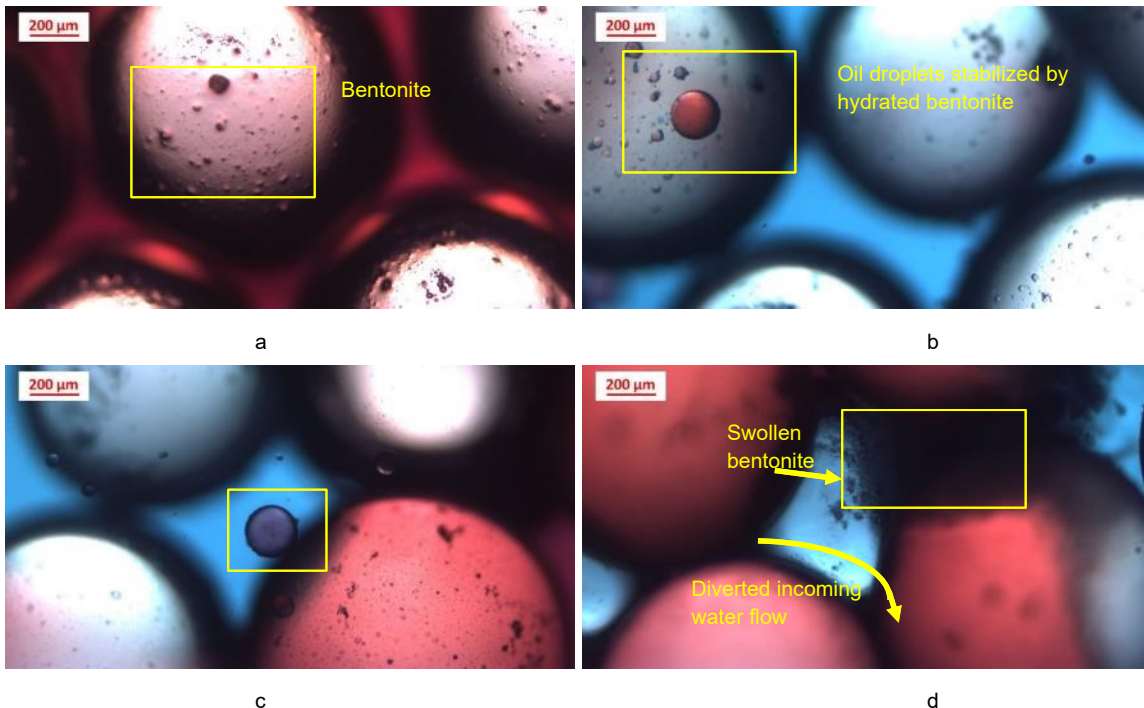
Figure 43—Glass bead model with 5 wt.% bentonite at (a) initial condition and (b-d) residual oil condition after injecting 9 ml of dyed DIW. The yellow rectangles in (a), (b), (c), and (d) show: (a) an example of bentonite particles attached to glass beads, (b) oil droplets stabilized by hydrated bentonite particles, (c) spherical residual oil, and (d) plugging of pore throat by swollen bentonite and the induced diverted incoming water flow.

Fig. 44 shows the results of DIW flood in the micromodel with 5 wt.% kaolinite. Fig. 44a shows the initial condition where the model was fully saturated with oil and kaolinite was attached to the surface of the glass beads (an example was highlighted in the yellow rectangle in Fig. 44a). Fig. 44b shows after injecting 9 ml of DIW, some oil was transported as oil droplets stabilized by kaolinite particles while other oil was retained on the glass bead surface as oil film as shown in the yellow rectangles. This film-like residual oil indicates the glass bead was more oil wet or less water wet. This may explain the low oil recovery at early and middle production periods when kaolinite clay was present as shown in Fig. 41a.

a   b
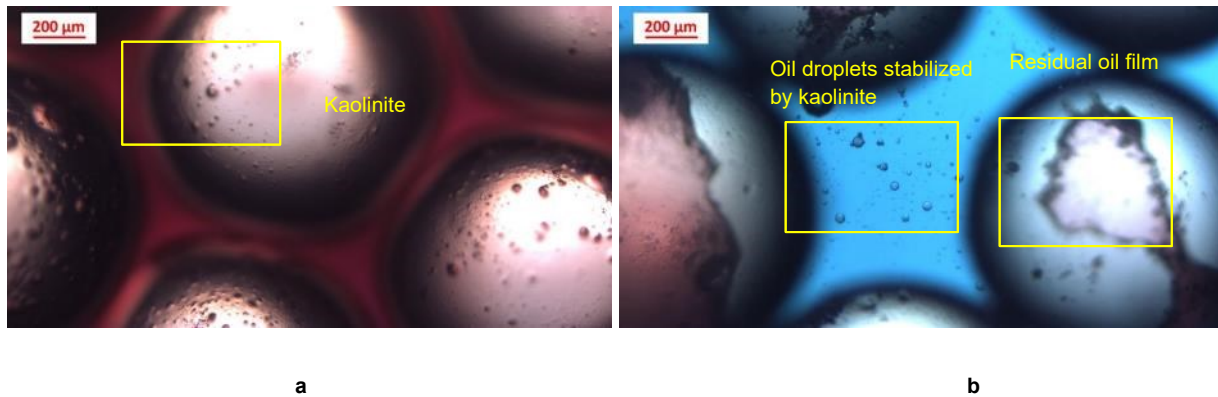
Figure 44—Glass bead model with 5 wt.% kaolinite at (a) initial condition and (b) residual oil condition after injecting 9 ml of dyed DIW. The yellow rectangles in (a) and (b) show: (a) an example of kaolinite particles attached to glass beads, (b) oil droplets stabilized by kaolinite and film-like residual oil on glass beads.

High salinity (10 wt.% NaCl) floods. In these experiments, 9 ml of 10 wt.% NaCl solution was injected into micromodels with known amounts of clays (kaolinite and bentonite) to study the clay effect under high salinity condition. The initial conditions of the glass bead models used in these experiments were like those shown in **Fig. 42** to **44** accordingly. Therefore, for simplicity purposes, the initial conditions were not shown in the following section and only the residual conditions were presented. **Figs. 45** shows the residual oil distribution in the glass bead models with various clay compositions after injecting the high salinity solution.

Figs. 45a shows in the pure glass bead model, the residual oil was in direct contact with glass beads, seen in the bridging of residual oil in the yellow rectangle, indicating a more oil wet condition which contrasted with that shown in **Fig. 42b**.

Fig. 45b shows the residual oil distribution of the model with 5 wt.% bentonite, which also indicates a more oil wet condition since the residual oil was in direct contact with the glass bead surface as highlighted in the yellow rectangles in **Fig. 45b**. The wettability change toward more oil wet under high salinity condition was the main reason leading to the low oil recovery in sandpack experiments as shown in **Fig. 31** and **34**.

Fig. 45c shows when kaolinite clay was present, the glass bead became more strong oil wet as indicated by the strongly bridged residual oil (an example can be seen in the yellow rectangle in **Fig. 45c**). This observation suggests that the glass bead becomes oil wet more easily under high salinity conditions when kaolinite clay was present in comparison to bentonite clay or no clay cases, which might explain the lowest oil recovery in early and middle production periods under high salinity conditions in sandpack experiments when kaolinite particles were present as shown in **Fig. 41c**.

a

b

c
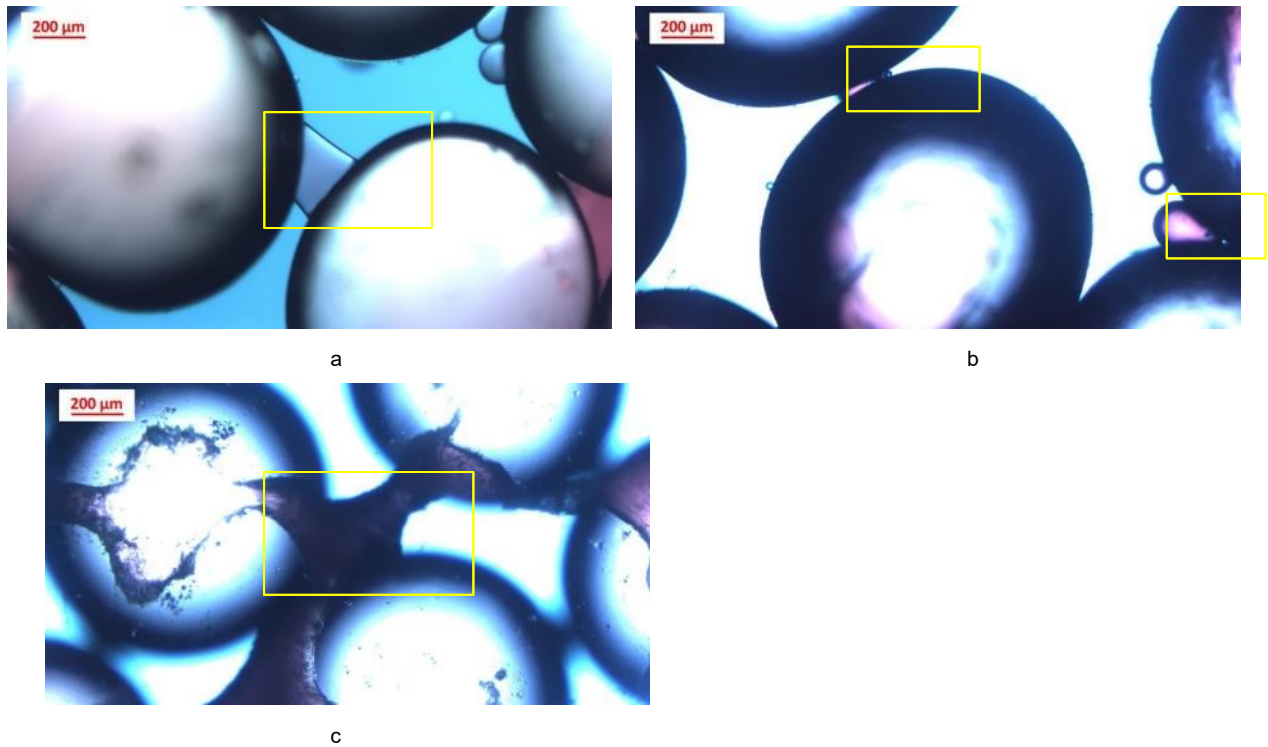
Figure 45—Residual oil condition after injecting 9 ml of 10 wt.% NaCl in glass bead models with various clay compositions: (a) pure glass bead model, (b) 5 wt.% bentonite, (c) kaolinite. The yellow rectangles in (a), (b) and (c) show: (a) the bridging of residual oil, (b) residual oil in direct contact with glass beads, (c) strongly bridged residual oil.

3.5 Conclusions

A systemic study of clay particles (bentonite and kaolinite) effects on oil recovery, pressure, and emulsion generation under various salinity and pH conditions was performed. The following conclusions can be drawn:

1. Stable O/W emulsions can be formed with 3 w/v.% of bentonite particles when the WOR is above 7:3 and the salinity is lower than 0.60 wt.% NaCl.

2. The formation of a thin layer around oil droplets by delaminated bentonite particles and the increase in aqueous phase viscosity by clay swelling are two emulsion stabilization mechanisms.

3. Addition of 0.04 wt.% NaOH (pH=12) further helps bentonite stabilize O/W emulsion due to the release of natural surfactants originating in heavy oil, which reduces the IFT between oil and water.

4. Waterflood experiments in sandpacks show that using low salinity water (e.g., DIW) could recover more oil compared to that when relatively high salinity water (e.g., 1.75 wt.% and 10 wt.% NaCl) was injected. The incremental oil recovery might be due to the wettability change towards more water wet induced by the low salinity environment, as supported by the residual oil distribution under various salinity conditions observed in the glass bead micromodel tests.

5. During the low salinity waterflood process, the presence of bentonite further improves oil recovery. For example, the final recovery increased from 40% without bentonite clay in the sandpack to 49% with 5 wt.% of bentonite accompanied by a high displacement pressure. This improved oil recovery was probably due to the enhanced sweep efficiency caused by the swelling of bentonite when contacted with DIW as shown in the micromodel test.

6. No O/W emulsion was observed in the sandpack experiments despite stable O/W emulsions produced in glass vial tests under appropriate conditions (e.g., WOR and salinity). This observation is most likely because while the activation energy provided by the shear force when fluid is flowing in the porous medium is not high enough to generate O/W emulsion, the bentonite concentration in-situ was not high enough to stabilize O/W emulsion.

7. During the alkaline flood process, the presence of clay (either bentonite or kaolinite) will be detrimental by reacting with NaOH. A high pH (12) solution might cause the dissolution of some clay mineral components, leading to a significant amount of production of clay particles, especially bentonite. However, such a production of clay particles did not lead to improved oil recovery as would be expected, which might be due to the reduced pH of the injected solution and water channeling.

Chapter 4: Generation of Pickering Emulsions by Activating Natural Asphaltenes: An Experimental Analysis for Cost Effective Heavy-Oil Recovery

This chapter of thesis is a modified version of a research paper submitted to SPE Journal for peer review.

4.1 Preface

Enhancing oil recovery through emulsification is possible during both cold and hot production in the heavy oil process. Emulsion stability is the key issue controlling the success of this process; conventionally, surfactants were used to facilitate emulsification and improve emulsion stability, increasing the cost remarkably. This study promotes an alternative way to generate stable - Pickering- emulsions without using expensive surfactants, a method that will reduce the operational costs and thus favor the field application step of emulsification in heavy-oil recovery. Throughout the paper, we explored answers to the following questions: (1) What conditions (asphaltene content) allow asphaltenes to stabilize W/O emulsions? (2) What are optimal aqueous conditions (pH, salinity) for stable emulsions? (3) Can such emulsions stabilized by asphaltenes be formed in-situ in a porous medium and thus improve recovery? These questions were answered through glass vial tests under controlled experimental conditions and sandpack flooding experiments. Finally, recommendations were made for choosing the optimal formulation to help improve heavy-oil recovery.

We started by mixing a heavy-crude oil and excess heptane to separate the asphaltic components. Then, model oil was prepared by adding various amounts of asphaltenes into a mineral oil with a portion of toluene, a component which helps the dissolution of asphaltene in an oil phase. The prepared oil samples with different asphaltic contents were mixed with water solutions to prepare emulsions and study the effect of the amount of both asphaltenes and aqueous conditions (pH, salinity) on emulsion stability. The purpose of this stage of experiments is to establish conditions (asphaltene concentration, salinity, and pH of aqueous phase) under which stable water in oil (W/O) emulsions could be formed. Emulsion stability was evaluated through glass vial tests, and the emulsion structure and type were determined using an optical microscope. Furthermore, sandpack flooding experiments were performed using the formulation which favored the formation of stable emulsions. For example, water solutions with various pH values (i.e., 7, 10, and 12) and salinities (i.e., 0, 1, and 5 wt.% NaCl) were injected into sandpacks initially saturated with model oils containing different amounts of asphaltenes (i.e., 0.25, 0.5, and 1 wt.%). The effluent samples were analyzed to determine emulsion type, asphaltene content, and the formation of a stable emulsion. These characteristics were cross-checked with oil recovery.

4.2 Introduction

Emulsification is an important mechanism used during the chemical enhanced oil recovery (EOR) process, such as alkaline flooding, surfactant flooding, and alkaline-surfactant-polymer (ASP) flooding (Mandal 2015). Both oil-in-water (O/W) and water-in-oil (W/O) emulsions were reported to improve the sweep and displacement efficiency of crude oil and thus enhance oil recovery (Li et al. 2020). However, problems often occur when injecting chemicals underground, such as the plugging of porous medium by polymer, incompatibility of surfactant with high salinity and high temperature conditions, as well as the scaling problem during alkaline flooding (Zhou et al. 2019). Besides, the chemical cost is usually high for field application. One potential solution to address these mentioned problems is the Pickering emulsion.

Pickering emulsions are emulsions either O/W or W/O that are stabilized by solid particles (Chevalier and Bolzinger 2013). It was named after S.U. Pickering (1907) who first observed that such emulsions can be stabilized by fine solid particles. Particle wettability is a key parameter controlling Pickering emulsion type and stability, among other parameters such as particle concentration, salinity, and pH of water phase (Binks and Lumsdon 1999). Water wet particles tend to stabilize O/W emulsions while oil wet particles tend to stabilize W/O emulsions (Aveyard et al. 2003). When the particle is neutral wet, the emulsion exhibits maximum stability owing to the high adsorption energy (Binks 2002). Such high adsorption energy makes the adsorption of particles on the water-oil interface irreversible (Binks 2002) and thus produces very stable emulsions even under harsh conditions, such as high pressure, high temperature, and high salinity conditions (Zhang et al. 2010; Sharma et al. 2015). Another advantage of such Pickering emulsions is the low preparation cost in comparison to chemical methods—if the particle emulsifier can be readily made or abundant in nature. From this motivation, we aim to test the emulsification capability of one type of natural particle existing in crude oil, especially in heavy oil—the asphaltenes.

Asphaltenes are heavy components in crude oil and are usually defined as the oil fractions precipitated out by adding paraffinic solvents such as pentane (C5) and heptane (C7) (Langevin and Argillier 2016). They are surface-active species and can adsorb at the oil-water interface leading to stable emulsions, usually water-in-oil (W/O) emulsions, since asphaltenes have both polar (e.g., carboxylic acids, -COOH) and non-polar components (e.g., aliphatic chain) (Joonaki et al. 2019). Joseph D. McLean and Kilpatrick (1997) studied the effect of asphaltene solvency on the water-in-crude oil emulsion stability, finding that the emulsion stability is controlled primarily by the state of solubility of asphaltenes in oil which is affected by several parameters, such as asphaltene concentration, resin to asphaltene ratio, aromaticity of the oil medium, and the concentration of polar functional groups (e.g., -COOH). Later, they used model oil composed of heptane and toluene (Heptol) to further study the effect of asphaltene aggregation on emulsion stability, concluding that asphaltenes are most surface active when they are near the point of precipitation in the form of fine dispersions (i.e., 1 μm) (Joseph D. McLean and Kilpatrick 1997). The adsorption of these fine asphaltene particles at the oil-water interface has the similar stabilization mechanism of a Pickering emulsion where fine solid particles are collected at the interface and thus provide emulsion stability (Eley et al. 1988). Therefore, asphaltenes can potentially be emulsion stabilizers if their aggregation state was adjusted appropriately. The emulsion stabilization mechanism by asphaltenes was attributed to the formation of a rigid film at the water-oil interface, which acts like a physical barrier for droplet coalescence as confirmed by the interfacial shear rheology measurement (Fan et al. 2010). Compared to the surfactant stabilized emulsions, there are two factors that render Pickering emulsions superior: (1) the irreversible adsorption of solid particles (e.g., asphaltenes) instead of the adsorption-desorption kinetics of surfactant stabilized emulsions slowing the rate of the Ostwald ripening, and (2) the draining of a liquid film between two approaching solid walls is slower than that between two approaching (immiscible) fluid walls (Binks 2002).

For asphaltene-stabilized emulsions, the aqueous environment also has an important effect on emulsion stability, such as pH and salinity. Nenningsland et al. (2011) studied the water pH on water-in-oil emulsions (W/O) stabilized by asphaltenes which was separated from a North Sea crude oil, finding that the emulsion was least stable at an intermediate pH (around 6) and more stable at both lower and higher pH conditions. The reasoning behind this observation was attributed to the amphoteric nature of asphaltenes, since their crude oil sample has a similar amount

of acid and base components as indicated by the total acid number (TAN: 2.15 mg/g) and total base number (TBN: 2.81 mg/g) (Nenningsland et al. 2011). These acid or base functional groups would become charged at high or low pH conditions, leading to increased hydrophilicity and surface activity, respectively, of asphaltenes and thus create more stable emulsions (Poteau et al. 2005). Besides the water pH, the solution salinity also affects emulsion stability. Ling et al. (2018) observed that the stability of water-in-oil (W/O) emulsions increased consistently with water salinity over the tested range of 0 to 1 wt.% NaCl and CaCl2, by using different types of oil samples (i.e., crude oil, crude oil with reduced asphaltene content, paraffin oil, etc.); they concluded that the accumulation of surface-active species (e.g., asphaltenes) at the water-oil interface with increasing salt concentration could be the reason for higher emulsion stability (Ling et al. 2018). While some other authors observed an opposite trend of emulsion stability with increasing salt concentration under high salinity conditions (e.g., sea water). Maaref et al. (2017) observed the W/O emulsion stability decreased with increasing salinity over a range of 4 wt.% NaCl to 14 wt.% NaCl because of the high interfacial tension (IFT), high rate of droplet aggregation, and coalescence under high salinity conditions.

In summary, asphaltenes can potentially be emulsion stabilizers acting like solid particles for Pickering emulsions; the literature reviews suggest that the conditions for stable water in oil (W/O) emulsion stabilized by asphaltenes can be obtained in bottle tests by adjusting either the oil environment (e.g., asphaltene concentration, oil aromaticity, etc.) or water conditions (e.g., salinity and pH). However, few studies were reported on the effect of such parameters (e.g., oil and water environment) on the formation of asphaltene-stabilized emulsions in porous medium, where the rock was present, and the mixing energy induced by fluid flow was low. In this work, we conducted a systematic study on the effect of asphaltene concentration, water pH, and salinity on the stability of asphaltene-stabilized emulsions (W/O) through both glass vial tests and sandpack flooding tests of which simulate the porous medium condition. The asphaltenes separated from the heavy oil sample with a viscosity of 15,640 cP were used for both types of tests. First, optimum asphaltene concentration, salinity, and pH values for stable W/O emulsions were identified through glass vial tests. Then sandpack flooding tests were performed to study the effect of same parameters on the emulsion formation at pore conditions. The effluent samples from sandpack flooding tests were analyzed to examine the emulsion production and oil recovery.

4.3 Experimental

Materials. The model crude oil composed of 70 vol.% heavy mineral oil (653 cP at 20°C, poly-alpha-olefin) and 30 vol.% toluene with different amounts of asphaltene fractions was used for both glass vial tests and sandpack flooding tests in order to get a precise control of asphaltene concentration in the oil medium. The asphaltene fractions were separated from a Western Saskatchewan heavy crude oil sample (15,640 cP at 21°C) used in our previous studies (Wang et al. 2021). Hydrochloric acid solution (HCl, 1 N, Fisher Scientific, U.S.A.) and sodium hydroxide pellets (NaOH, Fisher Scientific, U.S.A., ≥97.0%) were used to adjust water pH. Sodium chloride (NaCl, Research Products International, U.S.A., 99%) was used to adjust water salinity. The deionized water (DIW) with a pH around 7 (i.e., 6.8) was used as the base case. The silica sands that were used to prepare the sandpacks were purchased from TARGET Products Ltd.

Separation of asphaltenes. The asphaltenes were separated from the heavy oil sample by following standard ASTM D656 (2017) processes. Briefly, a test portion of the heavy crude oil sample was mixed with excess heptane and the mixture was heated under reflux, and asphaltenes, waxy substances, and some other inorganic material were precipitated on a filter paper. The waxy substances were then removed by washing with hot heptane in an extractor. After removing waxy substances, the asphaltenes were separated from the inorganic material by dissolution in hot toluene which was later evaporated to obtain the asphaltene fractions.

Preparation of model crude oil. Firstly, a certain amount of solid asphaltenes were weighed and dissolved into 1.5 ml of toluene. The toluene-asphaltene mixture was left standing for at least 24 hours until no solid asphaltene particles could be observed in the toluene solution. Then the toluene-asphaltene mixture was mixed with 3.5 ml heavy mineral oil homogeneously using a stirrer bar. The sample mixture (7/3, 70vol.% mineral and 30 vol.% toluene) would be used as model oil in the following study, also note that it has a lower viscosity in comparison to the original pure mineral oil (653 cP) due to the addition of toluene. **Table 8** shows the viscosity values (at 21°C) of model oil samples containing different amounts of asphaltenes. The viscosity was measured by a cone and plate viscometer (Brookfield, DV2T).

Table 8—Viscosity of model crude oils containing various amounts of asphaltenes.

Asphaltene Concentration, wt.%	0	0.25	0.5	1
Model oil viscosity, cP at 21°C	23	24	25	28

Emulsion preparation and characterization. For the static glass vial tests, 5 ml of prepared model oil was mixed with 5 ml of water solution (water to oil ratio, WOR=1:1) by using a homogenizer (the Polytron PT 10-35 GT) at a speed of 10,000 rpm for 3 minutes to prepare the emulsions. Then the water-oil-emulsion mixture was transferred to a graduated glass vial to evaluate the emulsion stability. Water solutions with different salinities (0, 1, and 5 wt.%) and pH values (pH=2, 4, 7, 10, and 12) were prepared by adding various amounts of NaCl and pH adjusting agents (i.e., HCl and NaOH) into DIW (pH=7). A pH meter (Five Easy, METTLER TOLEDO) was used to read the pH values.

The emulsion structure (i.e., droplet size) and type were determined by using a transmitted light microscope (Axiostar plus) and microscopic images were taken with a high-speed CMOS camera (Lumenera's Lt225) connected to the microscope.

Sandpack floods. The dynamic sandpack flooding experiments were performed to investigate the emulsification behavior of asphaltenes in porous medium condition. The procedures to prepare sandpacks were described in detail in our previous work (Wang et al. 2021). Briefly, silica sands were first sieved through two sieves with No. 60 and No. 35 mesh sizes to obtain the sands with sizes between 250 μm and 500 μm. Then, a certain amount of the sieved sand was weighed and mixed with model crude oil homogeneously by using a stainless stirrer bar to achieve the initial 100% oil saturation in the sandpack. Next, the sand-oil mixture was loosely packed into a rubber sleeve placed inside a steel core holder. The sleeve dimensions measure 5 inches in length and 1.5 inches in diameter. The sandpack porosity was approximately 0.35. **Table 9** summarizes the properties of sandpacks (SP) used for flooding experiments.

An Isco pump was used to inject the water solutions into the sandpacks at a constant flow rate (0.2 ml/min), which was identified as the optimal flow rate in our previous work (Lee and Babadagli 2020). A second Isco pump was used to generate an overburden pressure of 200 psi to prevent water channeling during the flooding tests.

Table 9—Properties of sandpacks for flooding tests.

Sandpack (SP) number	Testing parameter	Parameter values	Injected solution
SP1	Asphaltene concentration in model oil	0.25wt.%	DIW (pH=7)
SP2		0.5 wt.%	
SP3		1 wt.%	
SP4	Water pH	pH=10	DIW with pH=10
SP5		pH=12	DIW with pH=12
SP6	Water salinity	1 wt.% NaCl	1 wt.% NaCl
SP7		5 wt.% NaCl	5 wt.% NaCl

4.4 Results and Discussion

4.4.1 Static glass vial tests

Effect of asphaltene concentration. In these tests, various amounts of asphaltenes (0, 0.25, 0.5, 1, and 1.5 wt.%) were added into the model oil to study the effect of asphaltene concentration on emulsion stability. The water solution was DIW with a pH of 7; the WOR was 1:1 (i.e., 5 ml oil:5 ml water). **Fig. 46** shows the differences in phase separation when different amounts of asphaltenes were added into model oil one day after emulsion preparation. The red lines in **Fig. 46** indicate the interfaces between different phases, such as excess oil phase (O), W/O emulsion phase (E), and excess water phase (W). As can be seen from **Fig. 46**, complete phase separation happened when the model oil did not contain any asphaltenes (0 wt.%), and the oil was transparent—since only transparent mineral oil and toluene were used in this case. As the asphaltene concentration increased from 0.25 wt.% to 1.5 wt.%, Winsor type III (three phases system) (Kale and Deore 2016) emulsions were observed where the W/O emulsion phase (E) coexists with upper oil phase (O) and lower water phase (W). The colour of the oil changed to dark brownish due to the addition of asphaltenes. The phase separation in the W/O emulsion might be caused by the sedimentation and coalescence of water droplets. Sedimentation is the downward movement of water droplets due to their higher density, in comparison to the surrounding oil phase, leading to an excess oil phase on top (McClements 2007). The coalescence is the process where water droplets come together to form a single larger droplet (McClements 2007), of which is prone to breaking, thus leading to the excess water phase at the bottom.

Asphaltene concentration   0 wt.%   0.25 wt.%   0.5 wt.%   1 wt.%   1.5 wt.%

Glass vial results
(1 day after emulsion preparation)
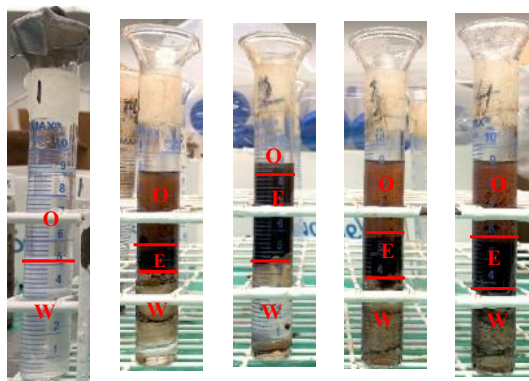
Figure 46—Glass vials containing 5 ml DIW and 5 ml model oil with various asphaltene concentrations 1 day after emulsion preparation where the red lines indicate phase interfaces and letters stand for different phases: O: Oil, E: Emulsion, W: Water.

The emulsion stability can be evaluated by calculating the relative volume of emulsion phase (E) to the total volume of the system (i.e., O+E+W) (Chen and Tao 2005). **Fig. 47** shows that the relative emulsion volume reaches a maximum of 43% at 0.5 wt.% asphaltene concentration, which was found to be the optimum asphaltene concentration for emulsion stabilization. Note that this optimal asphaltene concentration of 0.5 wt.% in model oil corresponds to the oil (7/3) composed of 70 vol.% mineral oil and 30 vol.% toluene and might be changed if the oil aromaticity was adjusted (Joseph D McLean and Kilpatrick 1997). As the asphaltene concentration increased, the aggregation state and size of asphaltene particles would increase until they formed large aggregates above 0.5 wt.% (e.g., 1 wt.% and 1.5 wt.%); due to its limited solubility in solvents (i.e., toluene), the emulsion became less stable (Xia et al. 2004). Additionally, when the asphaltene concentration was lower than 0.5 wt.% (i.e., 0.25 wt.%), there might not have been enough asphaltene particles to adsorb onto the water-oil interfaces, and the water droplets coalesced and sedimented (Xia et al. 2004).
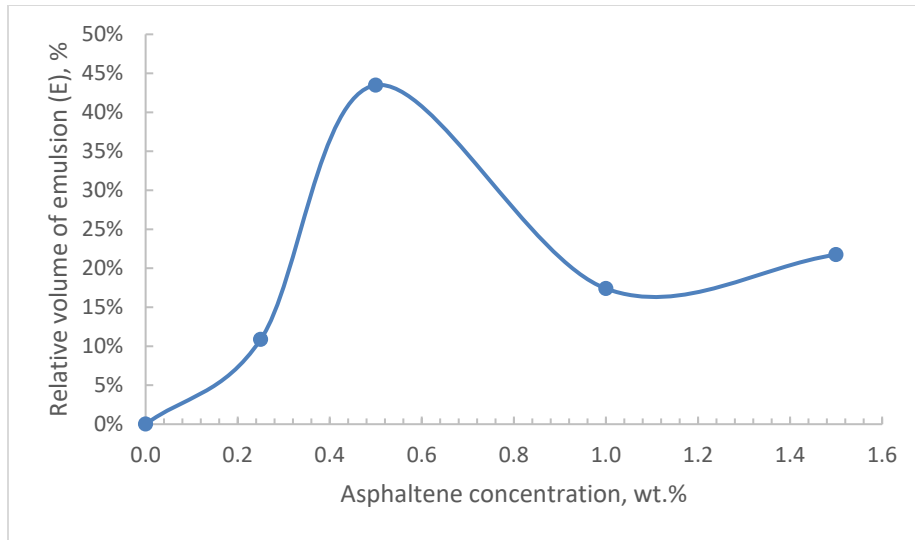
Figure 47—Effect of asphaltene concentration on W/O emulsion stability.

Fig. 48 shows that asphaltene particles were finely dispersed in the oil phase when the concentration was 0.5 wt.% and below (**Fig. 48a** and **48b**), and the finely dispersed asphaltenes not only adsorbed onto the water droplet surface as highlighted within the red circles, but also exist in the continuous phase as indicated by the red lines, accounting for the stabilization of W/O emulsion. Furthermore, more water droplets and excess asphaltene particles in the oil phase were observed at the concentration of 0.5 wt.% compared to those at concentration of 0.25 wt.%, which is consistent with the observed high emulsion stability with 0.5 wt.% asphaltenes. When the concentration was 1 wt.% and above, large asphaltene aggregates formed and less water droplets were observed as indicated by red lines in **Fig. 48c** and **48d**, which led to unstable emulsion.

a: 0.25 wt.% asphaltenes

b: 0.5 wt.% asphaltenes

c: 1 wt.% asphaltenes

d: 1.5 wt.% asphaltenes

85
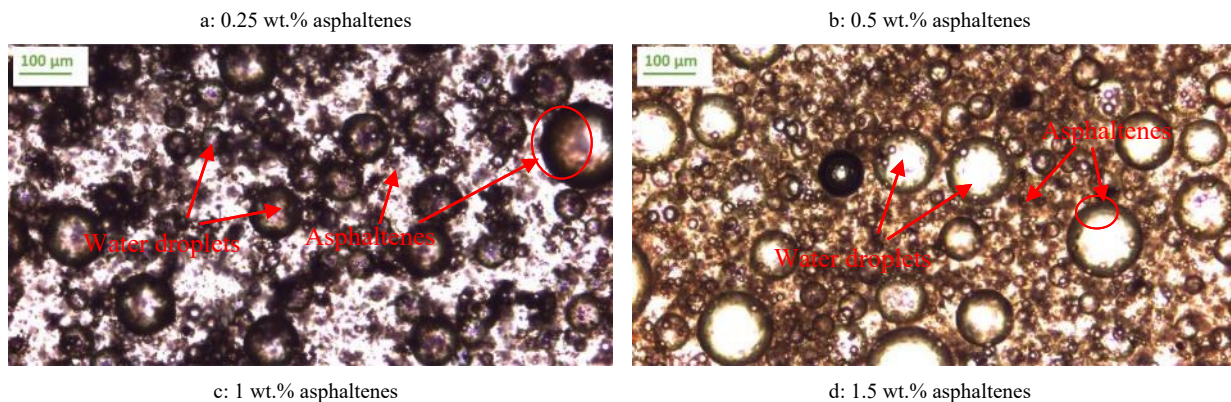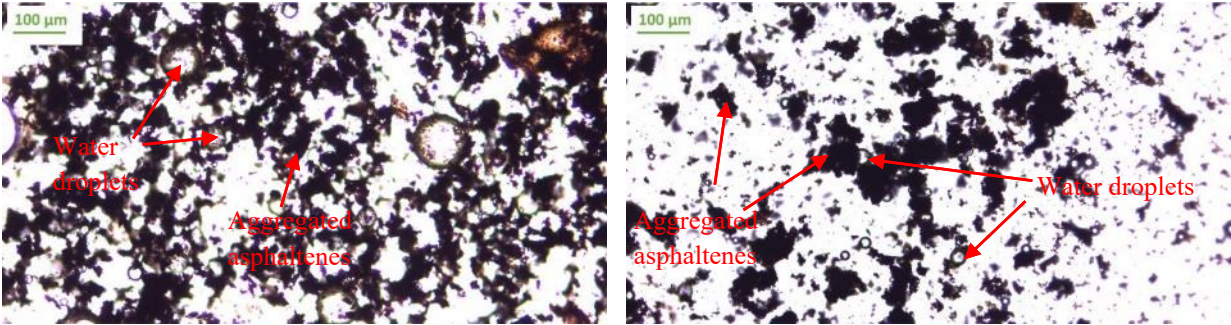
Figure 48—Microscopy images of W/O emulsion phase when adding different amounts of asphaltenes in the model oil (7/3): a: 0.25 wt.%, b: 0.5 wt.%, c: 1 wt.%, d: 1.5 wt.% asphaltenes. The red lines with arrow show examples of water droplets and asphaltenes in oil phase and the red circles highlight asphaltenes adsorbed on droplet surface.

Effect of water pH. To study the effect of water pH on the emulsion stability, 5 ml water solutions with various pH values (2, 4, 7, 10, and 12) were prepared and mixed with 5 ml model oil (7/3) containing 0.5 wt.% asphaltenes. **Fig. 49** shows that the emulsion type changed from Winsor type III (three phases) at pH=7 (and below) conditions to Winsor type I (two phases) conditions when the upper oil phase coexists with lower emulsion phase at pH=10 and 12 conditions. **Fig. 50** shows the emulsion stability improved as water pH increased from 2 to 12. This increased emulsion stability might be owing to the ionization of acidic components in the asphaltenes at high pH conditions, which makes asphaltenes more surface active and leads to lower interfacial tension (IFT) (Poteau et al. 2005). Note that asphaltenes used in this study were separated from a heavy crude oil sample with a total acid number (TAN) of 2.21 mg KOH/g (Wang et al. 2021), indicating the acidic property of the oil. The measured IFT values between this heavy oil and the water solutions also decreased with increasing water pH (Wang et al. 2021), which can also support the arguments made here.
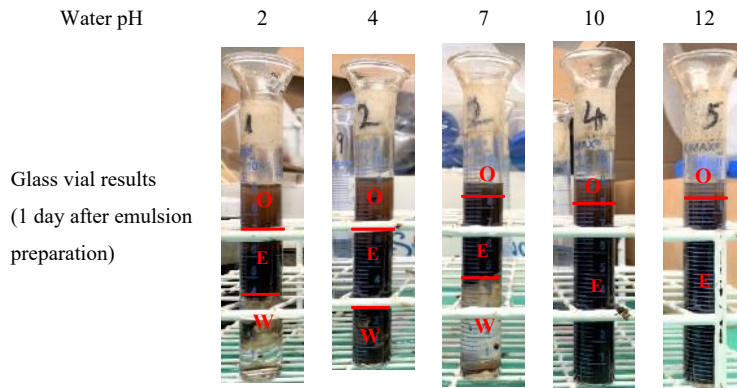
Figure 49—Glass vials containing 5 ml model oil (7/3) and 5 ml water solution with various pH values 1 day after emulsion preparation where the red lines indicate phase interfaces and letters stand for different phases: O: Oil, E: Emulsion, W: Water. The asphaltene concentration was 0.5 wt.%.
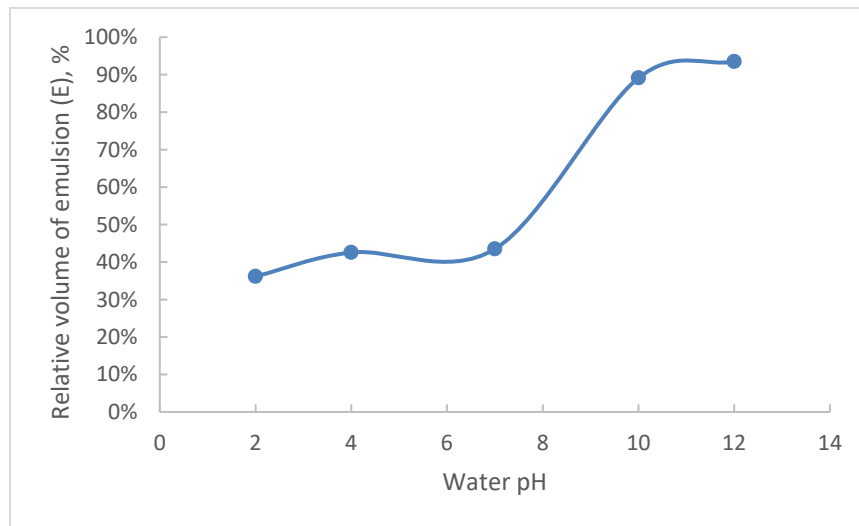
Figure 50—Effect of water pH on W/O emulsion stability.

Fig. 51 shows that within the tested pH range (from 2 to 7), the asphaltenes (0.5 wt.%) were all finely dispersed in the oil phase and stabilized the water droplets by forming a layer around them as indicated by the red lines and circles. The number of water droplets appears to be fewer in high pH conditions (i.e., above 7) than in low pH conditions (i.e., below 7), but this is a result of the field of view; when the field of view changes, the water droplets are more spatially spread out, and fewer remain within the scope of the view.
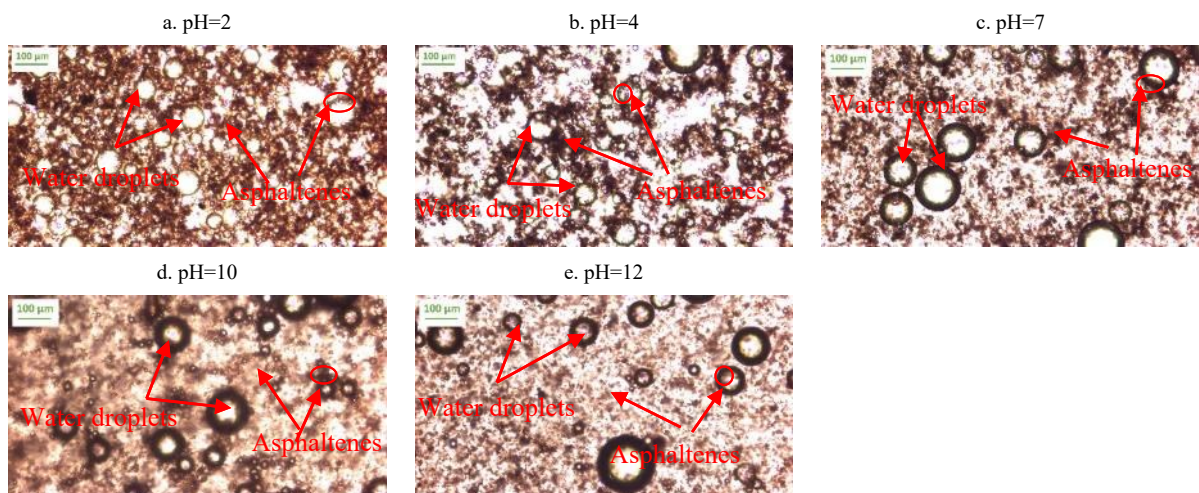
Figure 51—Microscopy images of W/O emulsion phase prepared with model oil (7/3) containing 0.5 wt.% asphaltenes and water solutions with various pH values: a: pH=2, b: pH=4, c: pH=7, d: pH=10, e:pH=12. The red lines with arrow show examples of water droplets and asphaltenes in oil phase and the red circles highlight asphaltenes adsorbed on droplet surface.

Effect of water salinity. In these tests, the water salinity was adjusted by adding various amounts of NaCl (i.e., 0, 1, and 5 wt.%) into DIW. **Fig. 52** shows clearly that the emulsion was most stable at intermediate salinity (i.e., 1 wt.% NaCl) condition where no water was separated from the emulsion after one day. When the salinity was either below (i.e., 0 wt.% NaCl) or above (i.e., 5 wt.% NaCl) this value, the W/O emulsion became unstable and a significant amount of water separated at the bottom of the glass vials. The improved emulsion stability with increasing salinity in the low salinity range (i.e., 0 to 1 wt.% NaCl) might be attributed to the enhanced accumulation of surface-active species (i.e., asphaltenes) at the water-oil interface driven by increasing salinity (Ling et al. 2018). While within the high salinity range (i.e., 1 to 5 wt.% NaCl), the aggregation and coalescence rate of water droplets increased with increasing salinity due to the electrostatic screening, leading to decreased emulsion stability (Maaref et al. 2017). **Fig. 53** shows, microscopically, that the water droplets were stabilized asphaltenes. The droplets look smaller at 1 wt.% NaCl condition in comparison to those at lower (0 wt.%) and higher (5 wt.%) salinity

conditions, which is consistent with the highest emulsion stability at intermediate salinity condition.

Salinity, wt.% NaCl   0   1   5

Glass vial results
(1 day after emulsion
preparation)

Figure 52—Glass vials containing 5 ml model oil (7/3) and 5 ml water solution with various salinity values 1 day after emulsion preparation where the red lines indicate phase interfaces and letters stand for different phases: O: Oil, E: Emulsion, W: Water. The asphaltene concentration was 0.5 wt.%.

a. 0 wt.% NaCl   b. 1 wt.% NaCl   c. 5 wt.% NaCl
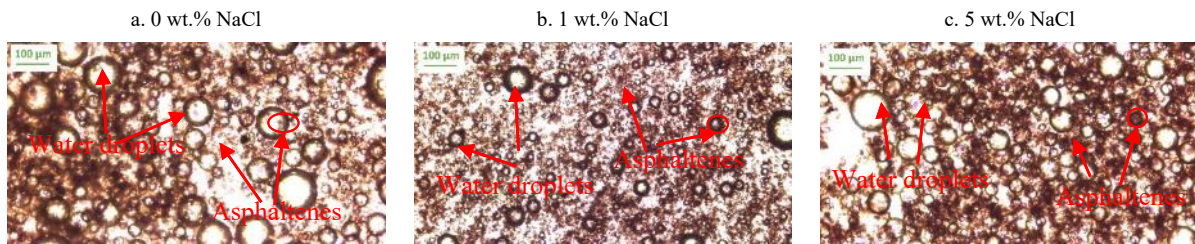
Figure 53—Microscopy images of W/O emulsion phase prepared with model oil (7/3) containing 0.5 wt.% asphaltenes and water solutions with various salinity conditions: a: 0 wt.% NaCl, b:1 wt.% NaCl, c: 5 wt.% NaCl. The red lines with arrow show examples of water droplets and asphaltenes in oil phase and the red circles highlight asphaltenes adsorbed on droplet surface.

Effect of water to oil ratio (WOR). In these tests, the model oil (7/3) was mixed with DIW solutions at different volume ratios. **Fig. 54** shows that the relative volume of emulsion phase decreased with increasing WORs, and thus the emulsion became less stable. This can be easily understood bas the water droplets becoming more tightly packed as the WOR increases (less oil), thus increasing the coalescence rate, leading to larger droplets as shown in **Fig. 55b**. At an extremely high WOR ratio (i.e., 9:1), some oil droplets were observed (black lines in **Fig. 55c**), indicating phase inversion occurs somewhere between a WOR of 7:3 and 9:1.

WOR, volume ratio   1:1   7:3   9:1

Glass vial results
(1 day after preparation)
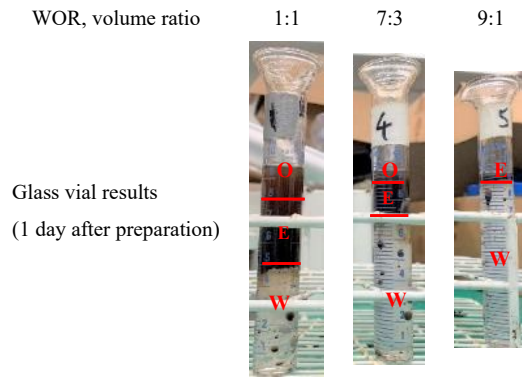
Figure 54—Glass vials containing model oil (7/3) and DIW solution at different WORs 1 day after emulsion preparation where the red lines indicate phase interfaces and letters stand for different phases: O: Oil, E: Emulsion, W: Water. The asphaltene concentration was 0.5 wt.%.
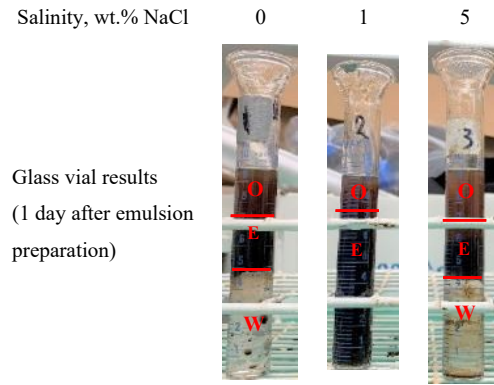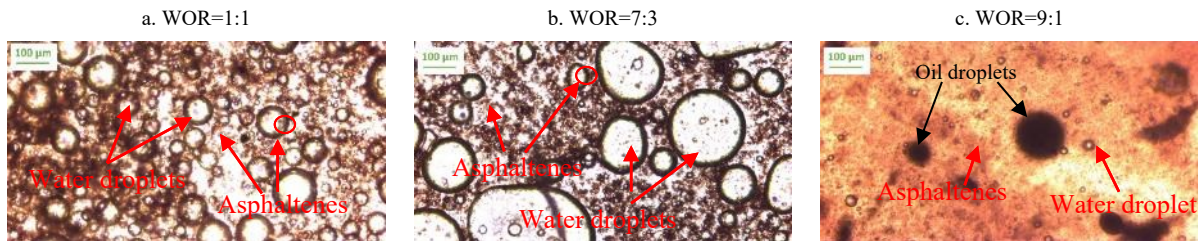

Figure 55—Microscopy images of W/O emulsion phase prepared with model oil (7/3) and DIW solutions at different WORs: a: WOR=1:1, b:wor=7:3, c: WOR=9:1. The red lines with arrow show examples of water droplets and asphaltenes in oil phase and the red circles highlight asphaltenes adsorbed on droplet surface. The black lines with arrow show examples of oil droplets. The asphaltene concentration was 0.5 wt.%.

4.4.2 Dynamic sandpack flooding tests

The purpose of these sandpack floods tests was to see if the asphaltenes were able to stabilize emulsions in a porous medium (i.e., reservoir) under flow conditions, and how it will affect the oil recovery. As shown in **Table 9**, these sandpack floods were designed to test three parameters: (1) asphaltene concentration, (2) water pH, and (3) water salinity, which were found to be important factors affecting the stability of asphaltene-stabilized emulsions in previous glass vial tests.

Asphaltene concentration effect. Sandpack floods SP1 to SP3 were designed to simulate the in-situ activation of asphaltenes occurring in the reservoir, where the sandpacks were initially saturated with model oils containing various amounts of asphaltenes (i.e., 0.25, 0.5, and 1wt.%) and an injection fluid of DIW (pH=7). **Table 10** shows that as more fluids were injected (horizontally comparison), the concentration of asphaltenes in the oil phase decreased—as

reflected by the color change of oil phase (from dark color to light color), which might be due to the asphaltene precipitation and adsorption onto sand grain surfaces in the porous medium (Khanifar et al. 2011). Also noted in **Table 10** is that after the pure oil production stages (i.e., 0.1 and 0.2 pore volume (PV) in SP1 and SP2 tests), the water was produced together with oil and no separate emulsion phase was observed even at optimal asphaltene concentration (i.e., 0.5 wt.%) which was determined through previous glass vial tests. In fact, the W/O emulsion was only observed at the interface between water and oil phase in the form of a single layer as highlighted within the red rectangle (**Table 10**). Since the emulsion layer was invisible to the naked eye, it was checked under a microscope. **Table 11** shows that the W/O emulsions were only produced in early stages after water breakthrough (i.e., 0.3 and 0.4 PV for SP1 and SP2, 0.2 and 0.3 PV for SP3). As more fluids were injected (e.g., after 0.4 PV), the WOR became so high that no W/O emulsion was observed. As shown in **Table 11**, at the concentration of 0.25 wt.% (SP1), asphaltenes were very finely dispersed in the oil phase (e.g., at 0.1 PV-SP1) and few water droplets were emulsified (i.e., at 0.3 and 0.4 PV-SP1). At the intermediate concentration (SP2) (i.e., 0.5 wt.%), the asphaltenes were finely dispersed (e.g., at 0.1 PV-SP2) and more water droplets were stabilized (i.e., at 0.3 and 0.4 PV-SP2); alternatively, if the asphaltene concentration reached 1 wt.% (SP3), large aggregations of asphaltene particles were produced (e.g., 0.1 PV-SP3), and water breaks through early at 0.2 PV (SP3) of the injected fluid. These observations were also consistent with previous glass vial tests in **Effect of asphaltene concentration**, where 0.5 wt.% was found to be the optimal concentration for emulsion stabilization.

After each sandpack flooding test, the sand grains from the sandpack were checked under the microscope to visualize the pore scale fluid distribution after flooding. **Fig. 56** shows the in-situ emulsification of W/O emulsion in pore space as reflected by the water droplets stabilized by asphaltenes when the asphaltene concentration was 0.5 wt.% and below. At a higher asphaltene concentration (i.e., 1 wt.%), large clusters of asphaltene particles deposited on the sand grain surface, some even plugging the pores as shown in the red rectangle in **Fig. 56c**. Also noted in **Fig. 56c** is that no emulsion droplets were observed after water flooding because the aggregated asphaltenes were too large to stabilize W/O emulsions. Since the shear energy of fluid flow in porous medium is much lower than that provided by the homogenizer, the in-situ emulsification as observed in **Fig. 56a** and **56b** might be largely owing to the spontaneous adsorption of asphaltenes at the water-oil interface (Joonaki et al. 2019).

Fig. 57 shows that the oil recoveries at low (i.e., 0.25 wt.%) and intermediate (i.e., 0.5 wt.%) asphaltene concentrations were similar and close to 30% after injecting 1 PV solutions. While at a high asphaltene concentration (i.e., 1 wt.%), the oil recovery was lower at 24%, which might be because the asphaltenes were more easily aggregated at high concentrations and such aggregates would plug the pores as shown in the red rectangle in **Fig. 56c**, causing the formation damage and lower oil recovery.

Table 10—Effluent samples collected in glass vials from sandpack flood tests SP1 and SP3 after injecting different amounts (in pore volume or PV) DIW solutions. The red lines indicate phase interfaces and letters stand for different phases: A: Air, O: Oil, E: Emulsion, W: Water. The red circle in dashed line shows evidence of water breakthrough at 0.3 PV for SP1 tests. The red rectangle highlights the water-oil phase interface where the emulsion layer was located.

Table 11––Microscopy images of the oil/emulsion phase (near the interface between water and oil phase) of effluent samples from sandpack tests SP1 to SP3 at different injection stages. The red arrows show examples of water droplets and asphaltenes in oil phase and the red circles highlight asphaltenes adsorbed on droplet surface.

Injection stage	0.1 PV	0.2 PV	0.3 PV	0.4 PV	0.6 PV and after
SP1					
SP2					
SP3					

a. SP1 (0.25 wt.% asphaltene) b. SP2 (0.5 wt.% asphaltene) c. SP3 (1 wt.% asphaltene)
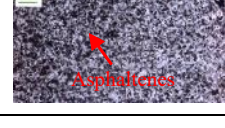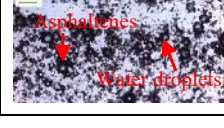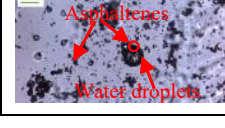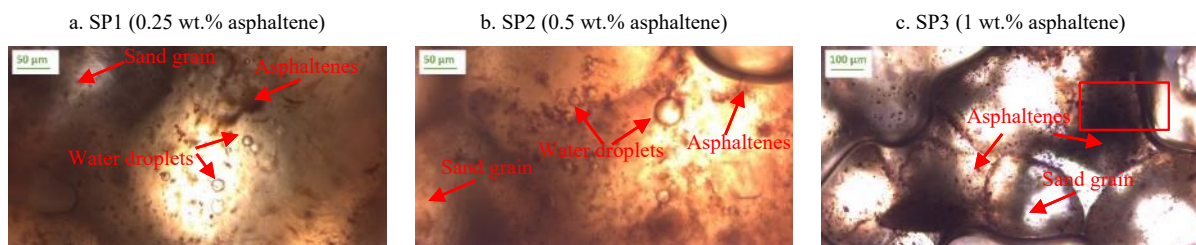
Figure 56––Microscopy images of sand grains flooded with 1 PV DIW from sandpacks initially saturated with various concentrations of asphaltenes: a: SP1-0.25 wt.%, b: SP2-0.5 wt.%, c: SP3-1wt.%. The red lines with arrow show examples of water droplets and asphaltenes as well as the sand grain. The red rectangle highlights the pore plugging by aggregated asphaltenes.
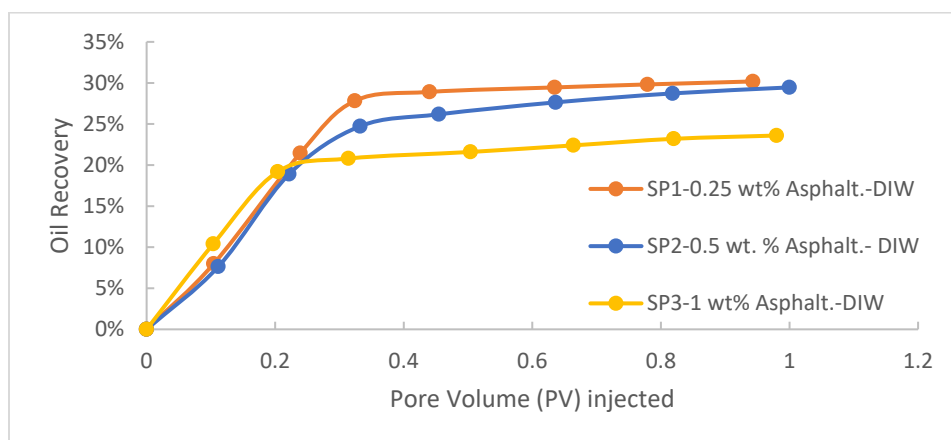
Figure 57—Effect of asphaltene concentration on oil recovery.

Water pH tests. For SP4 and SP5, alkaline solutions with pH=10 and 12, respectively, were injected into sandpacks initially saturated with model oil containing 0.5 wt.% asphaltenes. **Table 12** shows the similar trend as observed in **Table 11**, where the asphaltene concentration in the effluent sample decreased as more fluids were injected, and no single emulsion phase was observed in both high pH conditions, even though previous glass vial tests (**Effect of water pH**) showed that high pH solutions helped stabilize emulsions. This might be again because of the low shear energy in the porous medium which was too low to create enough oil-water interfaces for asphaltenes to adsorb on and thus less emulsion was generated in-situ. Other researchers also had similar observations. For example, Bryan and Kantzas (2007) observed stable O/W emulsions in the bottle tests by adding alkaline and surfactant and the activation energy was manual shaking, but they did not see any emulsions produced in the core flooding tests.

Table 13 shows that at pH=10 condition (SP4), the emulsion layer was produced at 0.4 PV injected solution, meanwhile occurring early at 0.2 and 0.3 PV at pH=12 condition. Besides, there are more water droplets in the emulsion phase at pH=12 condition (SP5-0.3 PV) than those at pH=10 condition (SP4-0.4 PV), which is consistent with the emulsion stability improving with increasing water pH as shown in **Fig. 50**. **Fig. 58** shows that W/O emulsions were formed in-situ in pore space as reflected by the water droplets stabilized by asphaltenes at both pH conditions. **Fig. 59** shows that the final oil recovery after injecting 1 PV of different pH solutions is 30% (SP2-pH=7), 32% (SP4-pH=10), and 27% (SP5-pH=12). The reduction of oil recovery at pH=12 condition was due to the early water breakthrough which happened after injecting 0.2 PV fluids, while the breakthrough times for SP2 (pH=7) and SP4 (pH=10) were 0.3 and 0.4 PV, respectively. The reason for the early breakthrough at high pH (i.e., 12) condition was probably because the W/O emulsion formed at pH=12 condition has a higher viscosity since more water droplets were present in the emulsion phase as shown in **Table 13** (SP5-0.3 PV) and the W/O emulsion viscosity was reported to increase with the volume fraction of dispersed phase (i.e., water), also called emulsion quality, in porous medium (Arhuoma et al. 2009). Therefore, it looks like the most stable emulsion (W/O) (i.e., emulsion formed at pH=12 condition) does not lead to highest oil recovery. Instead, intermediate emulsion stability such as the emulsions formed at pH=7 and 10 conditions, yields higher oil recovery, due to the viscosity differences of emulsions.

Table 12—Effluent samples collected in glass vials from sandpack flood tests SP4 and SP5 after injecting different amounts (in pore volume (PV)) alkaline solutions. The red letters stand for different phases: O: Oil, E: Emulsion, W: Water. The red rectangle highlights the water-oil phase interface where the emulsion layer was located.

Injected fluids, PV	0.1	0.2	0.3	0.4	0.6	0.8	1
SP4-pH=10							
SP5-pH=12							

Table 13—Microscopy images of the oil/emulsion phase (near the interface between water and oil phase) of effluent samples from sandpack tests SP4 and SP5 at different injection stages. The red lines with arrow show examples of water droplets and asphaltenes.

Injection stage	0.1 PV	0.2 PV	0.3 PV	0.4 PV	0.6 PV and after
SP4 pH=10					
SP5 pH=12					
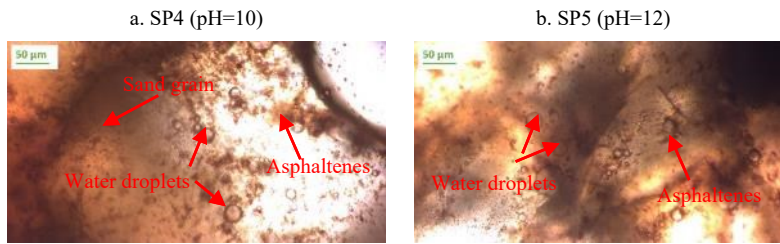
Figure 58—Microscopy images of sand grains flooded with 1 PV of water solutions with different pH values: a. SP4-pH=10, b. SP5-pH=12. The sandpacks were initially saturated with 0.5 wt.% asphaltenes. The red lines with arrow show examples of water droplets and asphaltenes as well as the sand grain.
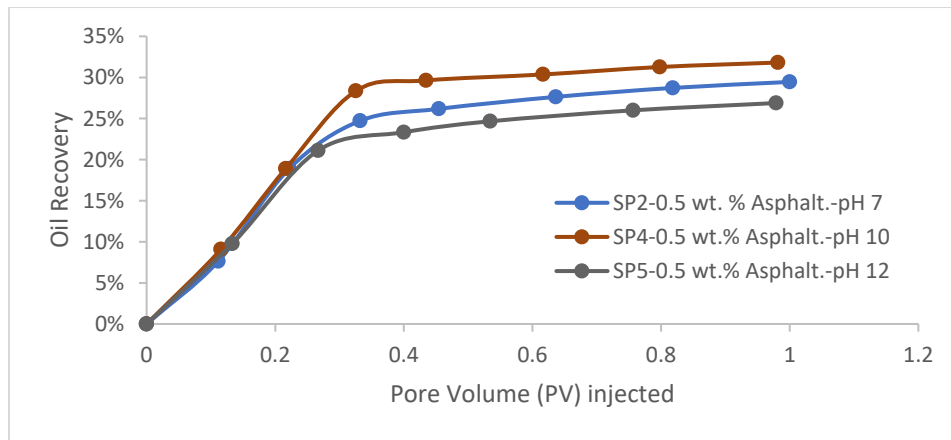
Figure 59—Effect of water pH on oil recovery.

Water salinity tests. In SP6 and SP7 tests, the sandpacks initially saturated with 0.5 wt.% asphaltenes were flooded by water solutions with 1 wt.% NaCl and 5 wt.% NaCl, which represented medium and high salinity conditions, respectively. **Table 14** shows that the water breaks through early after injecting 0.3 PV 1 wt.% NaCl solution compared to that at high salinity condition (i.e., 5 wt.% NaCl). This breakthrough happened after injecting 0.4 PV solution, which is the main reason leading to the higher oil recovery (i.e., 35%) at high salinity (5 wt.% NaCl) condition in comparison to the recoveries of 30% and 28% at low (0 wt.% NaCl) and intermediate (1 wt.% NaCl) salinity conditions as shown in **Fig. 61**. Two possible reasons might explain the increased oil recovery at high salinity condition. First, the asphaltenes were slightly more aggregated at 5 wt.% NaCl condition than that at 1 wt.% NaCl condition as shown in **Table 15** (SP7-0.1 PV), yet the slightly aggregated asphaltene size was still smaller than that observed in

the high asphaltene concentration case (i.e., SP3-1 wt.% asphaltenes) as shown in **Table 11**, so it did not cause significant pore plugging damage. The more slightly aggregated asphaltenes would increase the asphaltene deposition and alter the rock wettability to be more oil wet which improved the relative oil permeability at end point saturation (i.e., initial oil saturation) and thus improved the oil displacement efficiency as observed in work by Kamath et al. (1993), where they found the increased asphaltene deposition improved oil displacement efficiency by water flooding in both consolidated and unconsolidated cores owing to the improvement in relative oil permeability. The other reason might be due to the flow diverting effect of asphaltene deposition, which would plug the high permeability zone and divert the incoming water flow to the low permeability zone and thus improve water sweep efficiency and delay water breakthrough time (Kamath et al. 1993). **Fig. 60** also shows that the oil displacement efficiency at high salinity condition (**Fig. 60b**) was higher than that at intermediate salinity condition (**Fig. 60a**). Note that the asphaltene should not aggregate a lot, otherwise, the significant asphaltene aggregation would plug the pores and lead to low oil recovery as observed in SP3 test as shown in **Fig. 57**.

Table 14—Effluent samples collected in glass vials from sandpack flood tests SP6 and SP7 after injecting different amounts (in pore volume (PV)) of brine solutions. The red letters stand for different phases: O: Oil, E: Emulsion, W: Water. The red rectangle highlights the water-oil phase interface where the emulsion layer was located.

Table 15––Microscopy images of the oil/emulsion phase (near the interface between water and oil phase) of effluent samples from sandpack tests SP5 and SP6 at different injection stages. The red lines with arrow show examples of water droplets and asphaltenes.

Injection stage	0.1 PV	0.2 PV	0.3 PV	0.4 PV	0.6 PV and after
SP6 (1 wt.% NaCl)	Asphaltenes	Asphaltenes	Water droplets Asphaltenes	Asphaltenes Water droplets	Water droplets
SP7 (5 wt.% NaCl)	Slightly aggregated asphaltenes	Asphaltenes	Asphaltenes	Asphaltenes	Asphaltenes

a. SP6 (1 wt.% NaCl) b. SP7 (5 wt.% NaCl)
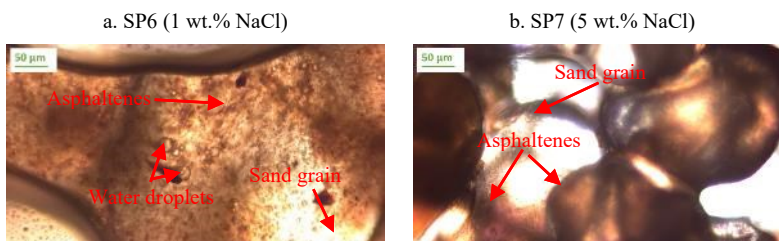
Figure 60––Microscopy images of sand grains flooded with 1 PV of water solutions with different salinities: a. SP6-1 wt.% NaCl, b. SP7-5 wt.% NaCl. The sandpacks were initially saturated with 0.5 wt.% asphaltenes. The red lines with arrow show examples of water droplets and asphaltenes as well as the sand grain.

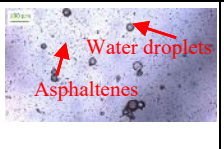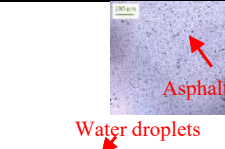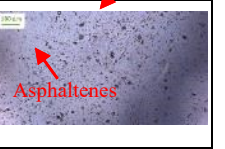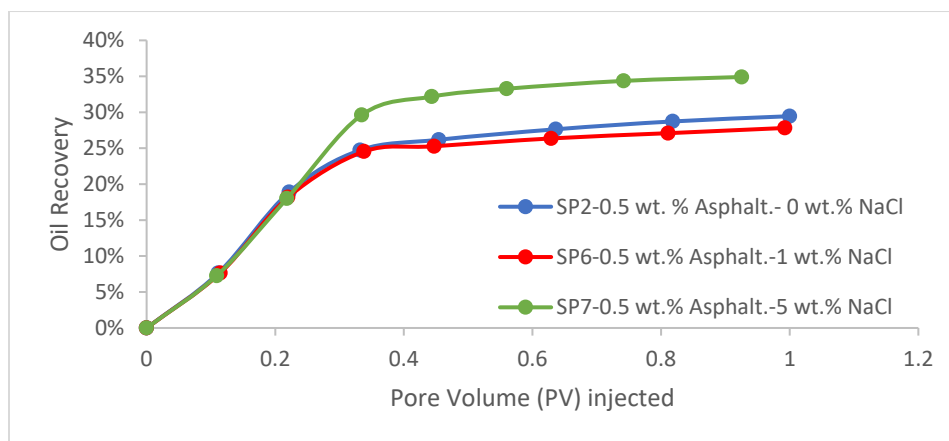**Figure 61––Effect of water salinity on oil recovery.**

4.5 Conclusions

In this study, the crude model oil (7/3) was first made by mixing 70 vol.% heavy mineral oil (653 cP) and 30 vol.% of toluene. Then the effects of asphaltene concentration, water pH and salinity on the stability of asphaltene-stabilized W/O emulsion and oil recovery were studied systematically through glass vial tests and sandpack flooding tests. The following conclusions can be drawn:

1. With the model oil (7/3) used in this study, an optimum asphaltene concentration of 0.5 wt.% exists which generated the most stable W/O emulsion and induced in-situ formation of W/O emulsion in pore space; above this concentration (e.g., 1 wt.%), asphaltenes would aggregate significantly and plug the pores in the porous medium leading to a lower oil recovery of 24% compared to that of 30% obtained when the oil contained 0.5 wt.% asphaltenes.

2. The emulsion stability increased with increasing water pH and in-situ formation of W/O emulsion was observed at pH values of 7 and above; however, the highest oil recovery of 32% was obtained when emulsions with intermediate stability were formed (i.e., emulsions formed at pH=10 condition), and the most stable emulsions formed at pH=12 condition led to a lower oil recovery of 27%, which might be due to the increased W/O emulsion viscosity since the volume fraction of dispersed phase (i.e., water) increased at pH=12 condition.

3. An optimum salinity of 1 wt.% NaCl yielded the highest emulsion stability and led to the in-situ formation of W/O emulsion; however, the highest oil recovery of 35% was obtained when injecting high salinity water solution (i.e., 5 wt.% NaCl). This was probably because the slightly aggregated asphaltenes formed at high salinity condition would increase the asphaltene deposition to some extent that it would on one hand, improve the oil displacement efficiency through changing the rock wettability toward more oil wet and improving relative oil permeability at end saturation point, on the other hand, improve the sweep efficiency by flow diverting effect.

Chapter 5: Conclusions, Contributions, and Future Work

5.1 General Conclusions and Contributions

Pickering emulsions could be an alternative to conventional surfactant-stabilized emulsions used for enhancing heavy oil recovery because of their low cost and high emulsion stability. Three groups of NPs were tested in this study on their emulsification capacity, which include commercial nanoparticles (i.e., cellulose nanocrystals (CNC), silica, alumina, magnetite, and zirconia), clays (i.e., bentonite and kaolinite), and asphaltenes. Effects of nanoparticle concentration, water salinity, and pH as well as WOR on Pickering emulsion stability were systematically studied through glass vial tests. Sandpack flooding experiments were performed to study the effect of two natural nanoparticles (i.e., clays and asphaltenes) on the in-situ emulsification and heavy oil recovery. From this study, some conclusions can be drawn as follows:

For commercial NPs:

1. Among five NPs (CNC, silica, alumina, magnetite, and zirconia) tested, CNC could act as an effective emulsifier for O/W emulsions either by adjusting the pH (3 or 11) or by adding an appropriate amount of salt (17 mM NaCl); although, the emulsion was not stable to creaming if only the pH was adjusted.

2. Two stabilization mechanisms account for the emulsion stability with the CNC; one is the formation of a dense particle layer around oil droplets impeding droplet coalescence, and the second is the formation of a CNC network structure in the continuous aqueous phase induced by relatively high salinity condition (175 mM NaCl).

3. Catastrophic phase inversion was observed when the oil content increased from 0.6 to 0.8 when the O/W emulsion was inverted to a W/O emulsion.

4. Emulsions stabilized with the CNCs were thermally stable up to 100°C.

5. Salinity had a great impact on the viscosity of the suspensions of the CNC, and O/W emulsions stabilized by the CNC displayed a shearing behavior showing yield stress due to droplet flocculation.

For clays:

1. Bentonite is a better O/W emulsifier compared to kaolinite. Stable O/W emulsions can be formed with 3 w/v.% of bentonite particles when the WOR is above 7:3 and the salinity is lower than 0.60 wt.% NaCl.

2. The formation of a thin layer around oil droplets by delaminated bentonite particles and the increase in aqueous phase viscosity by clay swelling are two emulsion stabilization mechanisms.

3. Waterflood experiments show that using low salinity water (e.g., DIW) could recover more oil compared to that when relatively high salinity water (e.g., 10 wt.% NaCl) was injected.

4. During the low salinity waterflood process, the presence of bentonite further improves oil recovery from 40% without bentonite clay to 49% with the presence of bentonite clay accompanied by a high displacement pressure. This improved oil recovery was probably due to the enhanced sweep efficiency caused by the swelling of bentonite when contacted with DIW as shown in the micromodel test.

5. No in-situ O/W emulsion was observed in the sandpack experiments; this is most likely because while the activation energy provided by the shear force when fluid is flowing in the porous medium was not high enough to generate O/W emulsion, the bentonite concentration in-situ was not high enough to stabilize O/W emulsion.

For asphaltenes:

1. An optimum asphaltene concentration of 0.5 wt.% exists to generate the most stable W/O emulsion and induced in-situ formation of W/O emulsion in pore space by using the model oil composed of 70 vol.% heavy mineral oil (653 cP) and 30 vol.% toluene.

2. The emulsion stability increased with increasing water pH and in-situ formation of W/O emulsion was observed at pH values of 7 and above; however, the highest oil recovery of 32% was obtained when emulsions with intermediate stability were formed (i.e., emulsions formed at pH=10 condition), and the most stable emulsions formed at pH=12 condition led to a lower oil recovery of 27% which might be due to the increased W/O emulsion viscosity since the volume fraction of dispersed phase (i.e., water) increased at pH=12 condition.

3. An optimum salinity of 1 wt.% NaCl yielded the highest emulsion stability and led to the in-situ formation of W/O emulsion; however, the highest oil recovery of 35% was obtained

when injecting high salinity water solution (i.e., 5 wt.% NaCl). This was probably because the slightly aggregated asphaltenes formed at high salinity condition would increase the asphaltene deposition to some extent that it would on one hand, improve the oil displacement efficiency through changing the rock wettability towards more oil wet and improving relative oil permeability at end saturation point, on the other hand, improve the sweep efficiency by flow diverting effect.

5.2 Future Works

The findings from this research work show that Pickering emulsions could be a very promising alternative to surfactant-stabilized emulsions to enhance heavy oil recovery. However, some limitations still exist for further field application of this new technique and further investigations are required. Potential future works include the following:

Core flooding experiments. Even though the sandpacks could simulate the porous medium to some extent, they could not represent the in-situ distribution of clays—which were supposed to be cemented in the rock formation instead of loosely packed in the sandpacks. Also, core flooding tests are necessary to investigate the applicability of commercial nanoparticles in porous medium, such as in-situ emulsification and pore plugging caused by injected nanofluid suspensions.

Brine composition effect. This research only studied the effect of NaCl concentration on the emulsion formulation. However, in a real reservoir, divalent cations such as Ca^{2+} and Mg^{2+} also exist, which may have great impact on the emulsion stability. Therefore, the brine composition also needs to be further investigated.

Crude oils for asphaltene study. The asphaltenes are very complex components in heavy oil and their properties might vary if they were separated from different oil samples. Also, other components in heavy oil, like resins, might have big impacts on the asphaltene's role on emulsion stabilization. Therefore, it is worthwhile to investigate effects of asphaltenes on emulsion generation and stability using real crude oil samples other than model oil.

Emulsion breakup. High emulsion stability is good for the displacement and sweep of oil in the reservoir, but undesirable for production and separation. Therefore, effective methods to break up the generated Pickering emulsions needs to be further investigated in future work. The emulsion stabilization mechanisms identified in this work could be used as the foundation for investigating emulsion breakup techniques, such as by adjusting water salinity and pH, of which were found to be key parameters affecting emulsion stability.

Testing binary and ternary mixtures of nano-particles. This research shows that CNC and bentonite nanoparticles alone can stabilize O/W emulsions under appropriate conditions (e.g., particle concentration, water pH and salinity)., while other nanoparticles (e.g., SiO_2, Al_2O_3, Fe_3O_4, and ZrO_2) failed. One potential way to further optimize the formulation of nanoparticles to stabilize

O/W emulsion is to mix one type of the effective emulsifiers (i.e., CNC and bentonite) with one type of the ineffective nano-particles (e.g., SiO_2, Al_2O_3, Fe_3O_4, and ZrO_2), the so called binary mixtures (e.g., CNC+SiO_2, CNC+Al_2O_3, bentonite+SiO_2, etc.). Another way of making such binary mixtures is to mix the positively charged nano-particles (i.e., Al_2O_3) with the negatively charged nanoparticles (i.e., SiO_2, Fe_3O_4, and ZrO_2). The rationality behind this is that the overall net charge of the mixtures (e.g., Al_2O_3+SiO_2) would be lowered compared to the single component system, which might modify the wettability of nanoparticles and stabilize Pickering emulsions. Furthermore, even ternary mixtures (e.g., CNC+SiO_2+Al_2O_3) can be tested depending on the testing results from ternary mixtures. One benefit of using binary or ternary mixtures of nano-particles is that the synergistic effects between different particles, if existed, would reduce the amount of each nano-particles alone used to stabilize emulsions, which therefore would lower the cost. Another benefit is that the advantages of various nano-particles can be combined, such as the environmentally friendly property of CNC and the abundance and low cost properties of silica, etc.

References

Chapter 1

Adams, D.M. 1982. Experiences with Waterflooding Lloydminster Heavy-Oil Reservoirs. J. Pet. Technol. 34, 1643–1650. https://doi.org/10.2118/10196-PA.

Agista, N.M., Guo, K., and Yu, Z. 2018. A State-of-the-Art Review of Nanoparticles Application in Petroleum with a Focus on Enhanced Oil Recovery. Appl. Sci. 8(6): 871. https://doi.org/10.3390/app8060871.

Arab, D., Kantzas, A., and Bryant, S.L. 2018. Nanoparticle stabilized oil in water emulsions: A critical review. J. Pet. Sci. Eng. 163, 217–242. https://doi.org/10.1016/j.petrol.2017.12.091

Arshad, M.W., Feilberg, K.L., Shapiro, A. et al. 2018. Characterization of Emulsion Formation with Nanoparticles for Enhanced Oil Recovery. SPE Kingdom Saudi Arab. Annu. Tech. Symp. Exhib. Dammam, Saudi Arabia, 23-26 April. https://doi.org/10.2118/192170-MS.

Aveyard, R., Binks, B.P., and Clint, J.H. 2003. Emulsions stabilized solely by colloidal particles. Adv. Colloid Interface Sci. 100–102, 503–546. https://doi.org/https://doi.org/10.1016/S0001-8686(02)00069-6.

Binks, B.P. 2002. Particles as surfactants - Similarities and differences. Curr. Opin. Colloid Interface Sci. 7, 21–41. https://doi.org/10.1016/S1359-0294(02)00008-0.

Binks, B.P., Philip, J., and Rodrigues, J.A. 2005. Inversion of silica-stabilized emulsions induced by particle concentration. Langmuir 21, 3296–3302. https://doi.org/10.1021/la046915z

Bragg, J.R. and Varadaraj, R. 2006. Solids-stabilized oil-in-water emulsion and a method for preparing same. US Patent No: US20060084581A1.

Bryan, J. and Kantzas, A. 2009. Potential for Alkali-Surfactant Flooding in Heavy Oil Reservoirs Through Oil-in-Water Emulsification. J. Can. Pet. Technol. 48, 37–46. https://doi.org/10.2118/09-02-37.

Cheraghian, G. and Hendraningrat, L. 2016. A review on applications of nanotechnology in the enhanced oil recovery part B: effects of nanoparticles on flooding. Int. Nano Lett. 6, 1–10. https://doi.org/10.1007/s40089-015-0170-7.

Chevalier, Y. and Bolzinger, M. 2013. Emulsions stabilized with solid nanoparticles: Pickering emulsions. Colloids Surfaces A: Physicochem. Eng. Asp. 439, 23–34. https://doi.org/10.1016/j.colsurfa.2013.02.054.

Joonaki, E., Buckman, J., Burgass, R. et al. 2019. Water versus Asphaltenes; Liquid–Liquid and Solid–Liquid Molecular Interactions Unravel the Mechanisms behind an Improved Oil Recovery Methodology. Sci. Rep. 9, 1–13. https://doi.org/10.1038/s41598-019-47782-5.

Kalashnikova, I., Bizot, H., Cathala, B. et al. 2012. Modulation of Cellulose Nanocrystals Amphiphilic Properties to Stabilize Oil/Water Interface. Biomacromolecules 13, 267–275. https://doi.org/10.1021/bm201599j.

Kim, I., Worthen, A.J., Lotfollahi, M. et al. 2017. Nanoparticle-stabilized Emulsions for Improved Mobility Control for Adverse-mobility Waterflooding. IOR 2017 - 19th Eur. Symp. Improv. Oil Recover. https://doi.org/10.3997/2214-4609.201700314.

Kumar, R., Dao, E., and Mohanty, K. 2012. Heavy-Oil Recovery by In-Situ Emulsion Formation. SPE J. 17, 326–334. https://doi.org/10.2118/129914-PA.

Levine, S., Bowen, B.D., and Partridge, S.J. 1989. Stabilization of emulsions by fine particles I. Partitioning of particles between continuous phase and oil/water interface. Colloids and Surfaces 38, 325–343. https://doi.org/https://doi.org/10.1016/0166-6622(89)80271-9.

Nallamilli, T., Binks, B.P., Mani, E. et al. 2015. Stabilization of Pickering Emulsions with Oppositely Charged Latex Particles: Influence of Various Parameters and Particle Arrangement around Droplets. Langmuir 31, 11200–11208. https://doi.org/10.1021/acs.langmuir.5b02443.

Pei, H., Zhang, G., Ge, J. et al. 2015. Investigation of synergy between nanoparticle and surfactant in stabilizing oil-in-water emulsions for improved heavy oil recovery. Colloids Surfaces A: Physicochem. Eng. Asp. 484, 478–484. https://doi.org/https://doi.org/10.1016/j.colsurfa.2015.08.025.

Pickering, S.U. 1907. CXCVI.—Emulsions. J. Chem. Soc. Trans. 91, 2001–2021. https://doi.org/10.1039/CT9079102001.

Sarma, H.K., Maini, B.B., and Jha, K. 1995. Evaluation of Emulsified Solvent Flooding For Heavy Oil Recovery. Annu. Tech. Meet. https://doi.org/10.2118/95-66.

Sharma, T., Kumar, G.S., Chon, B.H. et al. 2015. Thermal stability of oil-in-water Pickering emulsion in the presence of nanoparticle, surfactant, and polymer. J. Ind. Eng. Chem. 22, 324–334. https://doi.org/https://doi.org/10.1016/j.jiec.2014.07.026.

Xu, K., Zhu, P., Colon, T. et al. 2017. A Microfluidic Investigation of the Synergistic Effect of Nanoparticles and Surfactants in Macro-Emulsion-Based Enhanced Oil Recovery. SPE J. 22, 459–469. https://doi.org/10.2118/179691-PA.

Xu, M., Jiang, J., Pei, X. et al. 2018. Novel Oil-in-Water Emulsions Stabilised by Ionic Surfactant and Similarly Charged Nanoparticles at Very Low Concentrations. Angew. Chemie 130, 7864–7868. https://doi.org/10.1002/ange.201802266

Zhang, T., Davidson, D., Bryant, S.L. et al. 2010. Nanoparticle-Stabilized Emulsions for Applications in Enhanced Oil Recovery. SPE Improv. Oil Recover. Symp. https://doi.org/10.2118/129885-MS.

Chapter 2

Agista, N.M., Guo, K., and Yu, Z. 2018. A State-of-the-Art Review of Nanoparticles Application in Petroleum with a Focus on Enhanced Oil Recovery. Appl. Sci. 8(6): 871. https://doi.org/10.3390/app8060871.

Arab, D., Kantzas, A., and Bryant, S.L. 2018a. Nanoparticle stabilized oil in water emulsions: A critical review. J. Pet. Sci. Eng. 163: 217–242. https://doi.org/10.1016/j.petrol.2017.12.091.

Arab, D., Kantzas, A., and Bryant, S.L. 2018b. Nanoparticle-Fortified Emulsification of Heavy Oil. SPE EOR Conf. Oil Gas West Asia. Muscat, Oman, 26-28 March. SPE-190377-MS. https://doi.org/10.2118/190377-MS.

Arditty, S., Whitby, C.P., Binks, B.P. et al. 2003. Some general features of limited coalescence in solid-stabilized emulsions. Eur. Phys. J. E 11(3): 273–281. https://doi.org/10.1140/epje/i2003-10018-6.

Arshad, M.W., Feilberg, K.L., Shapiro, A. et al. 2018. Characterization of Emulsion Formation with Nanoparticles for Enhanced Oil Recovery. SPE Kingdom of Saudi Arab. Annu. Tech. Symp. Exhib. Dammam, Saudi Arabia, 23-26 April. SPE-192170-MS. https://doi.org/10.2118/192170-MS.

Aveyard, R., Binks, B.P., and Clint, J.H. 2003. Emulsions stabilised solely by colloidal particles. Adv. Colloid Interface Sci. 100–102: 503–546. https://doi.org/10.1016/S0001-8686(02)00069-6.

Binks, B.P. 2002. Particles as surfactants—similarities and differences. Curr. Opin. Colloid Interface Sci. 7(1-2): 21–41. https://doi.org/10.1016/S1359-0294(02)00008-0.

Binks, B.P., Clint, J.H., and Whitby, C.P. 2005. Rheological Behavior of Water-in-Oil Emulsions Stabilized by Hydrophobic Bentonite Particles. Langmuir 21(12): 5307–5316. https://doi.org/10.1021/la050255w.

Binks, B.P., Liu, W., and Rodrigues, J.A. 2008. Novel Stabilization of Emulsions via the Heteroaggregation of Nanoparticles. Langmuir 24(9): 4443–4446. https://doi.org/10.1021/la800084d.

Binks, B.P. and Lumsdon, S.O. 2000. Catastrophic Phase Inversion of Water-in-Oil Emulsions Stabilized by Hydrophobic Silica. Langmuir 16(6): 2539–2547. https://doi.org/10.1021/la991081j.

Binks, B.P. and Lumsdon, S.O. 1999. Stability of oil-in-water emulsions stabilised by silica particles. Phys. Chem. Chem. Phys. 1(12): 3007-3016. https://doi.org/10.1039/a902209k

Bragg, J.R. and Varadaraj, R. 2006. Solids-stabilized oil-in-water emulsion and a method for preparing same. US Patent No. USll/269,445. US20060084581A1.

Bryan, J. and Kantzas, A. 2009. Potential for Alkali-Surfactant Flooding in Heavy Oil Reservoirs Through Oil-in-Water Emulsification. J. Can. Pet. Technol. 48(2): 37–46. https://doi.org/10.2118/09-02-37.

Cheraghian, G. and Hendraningrat, L. 2016. A review on applications of nanotechnology in the enhanced oil recovery part B: effects of nanoparticles on flooding. Int. Nano Lett. 6(1): 1–10. https://doi.org/10.1007/s40089-015-0170-7.

Cherhal, F., Cousin, F., and Capron, I. 2016. Structural Description of the Interface of Pickering Emulsions Stabilized by Cellulose Nanocrystals. Biomacromolecules 17(2): 496–502. https://doi.org/10.1021/acs.biomac.5b01413.

Chevalier, Y. and Bolzinger, M.-A., 2013. Emulsions stabilized with solid nanoparticles: Pickering emulsions. Colloids Surfaces A Physicochem. Eng. Asp. 439: 23–34. https://doi.org/10.1016/j.colsurfa.2013.02.054.

Delamaide, E., Bazin, B., Rousseau, D. et al. 2014. Chemical EOR for Heavy Oil: The Canadian Experience. SPE EOR Conf. Oil Gas West Asia. Muscat, Oman, 31 March-2 April. SPE-169715-MS. https://doi.org/10.2118/169715-MS.

Hubbe, M.A., Tayeb, P., Joyce, M. et al. 2017. Rheology of Nanocellulose-rich Aqueous Suspensions: A Review. Bio Resources 12(4): 9556-9661. https://ojs.cnr.ncsu.edu/index.php/BioRes/article/view/BioRes_12_4_9556_Hubbe_Rheology _Nanocellulose_Aqueous_Suspension/5699.

Kalashnikova, I., Bizot, H., Cathala, B. et al. 2012. Modulation of Cellulose Nanocrystals Amphiphilic Properties To Stabilize Oil/Water Interface. Biomacromolecules 13(1): 267–275. https://doi.org/10.1021/bm201599j.

Kim, I., Worthen, A.J., Lotfollahi, M. et al. 2017. Nanoparticle-stabilized Emulsions for Improved Mobility Control for Adverse-mobility Waterflooding. IOR 2017 - 19th Eur. Symp. Improv. Oil Recover. Tulsa, Oklahoma, 24 April. https://doi.org/10.3997/2214-4609.201700314.

Lee, J. and Babadagli, T. 2018. Improvement of Microemulsion Generation and Stability Using New Generation Chemicals and Nano Materials during Waterflooding as a Cost-Efficient Heavy-Oil Recovery Method. SPE Trinidad and Tobago Sect. Energy Resour. Conf. Port of Spain, Trinidad and Tobago, 25-26 June. https://doi.org/10.2118/191171-MS.

Levine, S., Bowen, B.D. and Partridge, S.J. 1989. Stabilization of emulsions by fine particles I. Partitioning of particles between continuous phase and oil/water interface. Colloids and Surfaces 38(2): 325–343. https://doi.org/10.1016/0166-6622(89)80271-9.

Nallamilli, T., Binks, B.P., Mani, E. et al. 2015. Stabilization of Pickering Emulsions with Oppositely Charged Latex Particles: Influence of Various Parameters and Particle Arrangement around Droplets. Langmuir 31(41): 11200–11208. https://doi.org/10.1021/acs.langmuir.5b02443.

Oguzlu, H., Danumah, C., and Boluk, Y. 2017. Colloidal behavior of aqueous cellulose nanocrystal suspensions. Curr. Opin. Colloid Interface Sci. 29: 46–56. https://doi.org/10.1016/j.cocis.2017.02.002.

Pandey, A., Telmadarreie, A., Trifkovic, M. et al. 2018. Cellulose Nanocrystal Stabilized Emulsions for Conformance Control and Fluid Diversion in Porous Media. SPE Annu. Tech. Conf. Exhib. Dallas, Texas, 24-26 September. SPE-191609-MS. https://doi.org/10.2118/191609-MS.

Patel, A., Nihalani, D., Mankad, D., Patel, D., Chaudhari, R., Dhameliya, M., Tripathi, D., Bhui, U.K., 2017. Evaluating Feasibility of Hydrophilic Silica Nanoparticles for In-Situ Emulsion Formation in Presence of Co-Surfactant: An Experimental Study. SPE Kingdom Saudi Arab. Annu. Tech. Symp. Exhib. https://doi.org/10.2118/188141-MS

Pei, H., Zhang, G., Ge, J. et al. 2015. Investigation of synergy between nanoparticle and surfactant in stabilizing oil-in-water emulsions for improved heavy oil recovery. Colloids Surfaces A Physicochem. Eng. Asp. 484: 478–484. https://doi.org/10.1016/j.colsurfa.2015.08.025.

Pickering, S.U. 1907. CXCVI.—Emulsions. J. Chem. Soc. Trans. 91: 2001–2021. https://doi.org/10.1039/CT9079102001.

Prathapan, R., Thapa, R., Garnier, G. et al. 2016. Modulating the zeta potential of cellulose nanocrystals using salts and surfactants. Colloids Surfaces A Physicochem. Eng. Asp. 509: 11–18. https://doi.org/10.1016/j.colsurfa.2016.08.075.

Sarma, H.K., Maini, B.B., and Jha, K. 1995. Evaluation of Emulsified Solvent Flooding For Heavy Oil Recovery. Paper presented at the Petroleum Society of Canada Annual Technical Meeting Calgary, Alberta, 7-9 June. PETSOC-95-96. https://doi.org/10.2118/95-66.

Shafiei-Sabet, S., Hamad, W.Y., and Hatzikiriakos, S.G. 2014. Ionic strength effects on the microstructure and shear rheology of cellulose nanocrystal suspensions. Cellulose 21(5): 3347–3359. https://doi.org/10.1007/s10570-014-0407-z.

Sharma, T., Kumar, G.S., Chon, B.H. et al. 2014. Viscosity of the oil-in-water Pickering emulsion stabilized by surfactant-polymer and nanoparticle-surfactant-polymer system. Korea-Australia Rheol. J. 26(4): 377–387. https://doi.org/10.1007/s13367-014-0043-z.

Sharma, T., Kumar, G.S., Chon, B.H. et al. 2015. Thermal stability of oil-in-water Pickering emulsion in the presence of nanoparticle, surfactant, and polymer. J. Ind. Eng. Chem. 22: 324–334. https://doi.org/10.1016/j.jiec.2014.07.026.

Tang, J., Lee, M.F.X., Zhang, W. et al. 2014. Dual Responsive Pickering Emulsion Stabilized by Poly[2-(dimethylamino)ethyl methacrylate] Grafted Cellulose Nanocrystals. Biomacromolecules 15(8): 3052–3060. https://doi.org/10.1021/bm500663w.

Vignati, E., Piazza, R., and Lockhart, T.P. 2003. Pickering Emulsions: Interfacial Tension, Colloidal Layer Morphology, and Trapped-Particle Motion. Langmuir 19(17): 6650–6656. https://doi.org/10.1021/la034264l.

Winuprasith, T. and Suphantharika, M. 2015. Properties and stability of oil-in-water emulsions stabilized by microfibrillated cellulose from mangosteen rind. Food Hydrocoll. 43: 690–699. https://doi.org/10.1016/j.foodhyd.2014.07.027.

Xu, K., Zhu, P., Colon, T. et al. 2017. A Microfluidic Investigation of the Synergistic Effect of Nanoparticles and Surfactants in Macro-Emulsion-Based Enhanced Oil Recovery. SPE J. 22(2): 459–469. https://doi.org/10.2118/179691-PA.

Xu, M., Jiang, J., Pei, X. et al. 2018. Novel Oil-in-Water Emulsions Stabilised by Ionic Surfactant and Similarly Charged Nanoparticles at Very Low Concentrations. Angew. Chemie 130(26): 7864–7868. https://doi.org/10.1002/ange.201802266.

Zhang, T., Davidson, D., Bryant, S.L. et al. 2010. Nanoparticle-Stabilized Emulsions for Applications in Enhanced Oil Recovery. SPE Improv. Oil Recover. Symp. Tulsa, Oklahoma, 24-28 April. SPE-129885-MS. https://doi.org/10.2118/129885-MS.

Zhong, L., Fu, S., Peng, X. et al. 2012. Colloidal stability of negatively charged cellulose nanocrystalline in aqueous systems. Carbohydr. Polym. 90(1): 644–649. https://doi.org/10.1016/j.carbpol.2012.05.091.

Chapter 3

Abend, S., Bonnke, N., Gutschner, U. et al. 1998. Stabilization of emulsions by heterocoagulation of clay minerals and layered double hydroxides. Colloid Polym. Sci. 276: 730–737. https://doi.org/10.1007/s003960050303.

Abend, S. and Lagaly, G. 2001. Bentonite and double hydroxides as emulsifying agents. Clay Miner. 36(4): 557–570. https://doi.org/10.1180/0009855013640009.

Adams, D.M. 1982. Experiences with Waterflooding Lloydminster Heavy-Oil Reservoirs. J. Pet. Technol. 34(8): 1643–1650. SPE-10196-PA. https://doi.org/10.2118/10196-PA.

Arab, D., Kantzas, A., and Bryant, S.L. 2018. Nanoparticle stabilized oil in water emulsions: A critical review. J. Pet. Sci. Eng. 163: 217–242. https://doi.org/10.1016/j.petrol.2017.12.091.

Au, P.-I. and Leong, Y.-K. 2013. Rheological and zeta potential behavior of kaolin and bentonite composite slurries. Colloids and Surfaces A: Physicochem. Eng. Asp. 436: 530–541. https://doi.org/10.1016/j.colsurfa.2013.06.039.

Aveyard, R., Binks, B.P., and Clint, J.H. 2003. Emulsions stabilised solely by colloidal particles. Adv. Colloid Interface Sci. 100–102: 503–546. https://doi.org/10.1016/S0001-8686(02)00069-6.

Babadagli, T. 2020. Philosophy of EOR. J. Pet. Sci. Eng. 188. https://doi.org/10.1016/j.petrol.2020.106930.

Bartels, W.-B., Mahani, H., Berg, S. et al. 2019. Literature review of low salinity waterflooding from a length and time scale perspective. Fuel 236: 338–353. https://doi.org/10.1016/j.fuel.2018.09.018.

Bayliss, P. and Levinson, A.A. 1976. Mineralogical review of the Alberta oil sand deposits (Lower Cretaceous, Mannville Group). Bull. Can. Pet. Geol. 24(2): 211–224.

Bennion, D.B., Bennion, D.W., Thomas, F.B. et al. 1998. Injection Water Quality-A Key Factor to Successful Waterflooding. J. Can. Pet. Technol. 37(6). PETSOC-98-06-06. https://doi.org/10.2118/98-06-06.

Bernard, G.G. 1967. Effect of Floodwater Salinity on Recovery of Oil from Cores Containing Clays. SPE Calif. Reg. Meet., Los Angeles, California, 26-27 October. SPE-1725-MS. https://doi.org/10.2118/1725-MS.

Binks, B. and Lumsdon, S. 1999. Stability of oil-in-water emulsions stabilised by silica particles. Phys. Chem. Chem. Phys. 12(1): 3007–3016. https://doi.org/10.1039/A902209K.

Binks, B.P. 2002. Particles as surfactants—similarities and differences. Curr. Opin. In Colloid Interface Sci. 7(1-2): 21–41. https://doi.org/10.1016/S1359-0294(02)00008-0.

Binks, B.P., Liu, W., and Rodrigues, J.A. 2008. Novel Stabilization of Emulsions via the Heteroaggregation of Nanoparticles. Langmuir 24(9): 4443–4446. https://doi.org/10.1021/la800084d.

Binks, B.P. and Lumsdon, S.O. 2000. Catastrophic Phase Inversion of Water-in-Oil Emulsions Stabilized by Hydrophobic Silica. Langmuir 16(6): 2539–2547. https://doi.org/10.1021/la991081j.

Binks, B.P., Philip, J., and Rodrigues, J.A. 2005. Inversion of silica-stabilized emulsions induced by particle concentration. Langmuir 21(8): 3296–3302. https://doi.org/10.1021/la046915z.

Bragg, J.R. and Varadaraj, R. 2006. Solids-stabilized oil-in-water emulsion and a method for preparing same. United States Patent No. #. US20060084581A1.

Bryan, J. and Kantzas, A. 2009. Potential for Alkali-Surfactant Flooding in Heavy Oil Reservoirs Through Oil-in-Water Emulsification. J. Can. Pet. Technol. 48(2): 37–46. PETSOC-09-02-37. https://doi.org/10.2118/09-02-37.

Chevalier, Y. and Bolzinger, M.-A. 2013. Emulsions stabilized with solid nanoparticles: Pickering emulsions. Colloids and Surfaces A: Physicochem. Eng. Asp. 439: 23–34. https://doi.org/10.1016/j.colsurfa.2013.02.054.

Clem, A.G. and Doehler, R.W. 1961. Industrial Applications of Bentonite. Clays and Clay Minerals. 10: 272–283. https://doi.org/10.1346/CCMN.1961.0100122.

Delamaide, E., Bazin, B., Rousseau, D. et al. 2014. Chemical EOR for Heavy Oil: The Canadian Experience. SPE EOR Conf. Oil Gas West Asia, Muscat, Oman, 31 March-2 April. SPE-169715-MS. https://doi.org/10.2118/169715-MS.

Dusseault, M.B. 2001. Comparing Venezuelan and Canadian Heavy Oil and Tar Sands. Can. Int. Pet. Conf., Calgary, Alberta, 12-14 June. PETSOC-2001-061. https://doi.org/10.2118/2001-061.

Fu, X., Lane, R.H., and Mamora, D.D. 2012. Water-in-Oil emulsions: flow in porous media and EOR potential. SPE Can. Unconv. Resour. Conf., Calgary, Alberta, 30 October-1 November. SPE-162633-MS. https://doi.org/10.2118/162633-MS.

Heikola, T., Kumpulainen, S., Vuorinen, U. et al. 2013. Influence of alkaline (pH 8.3–12.0) and saline solutions on chemical, mineralogical, and physical properties of two different bentonites. Clay Minerals 48(2): 309–329. https://doi.org/10.1180/claymin.2013.048.2.12.

Isaacs, E.E. and Chow, R.S. 1992. Practical Aspects of Emulsion Stability. In Emulsions, Advances in Chemistry. Chapter 2: 51-77. https://doi.org/doi:10.1021/ba-1992-0231.ch002.

Jennings Jr., H.Y., Johnson Jr., C.E., and McAuliffe, C.D. 1974. A Caustic Waterflooding Process for Heavy Oils. J. Pet. Technol. 26(12): 1344–1352. SPE-4741-PA. https://doi.org/10.2118/4741-PA.

Kumar, R., Dao, E., and Mohanty, K. 2012. Heavy-Oil Recovery by In-Situ Emulsion Formation. SPE J. 17(2): 326–334. SPE-129914-PA. https://doi.org/10.2118/129914-PA.

Lagaly, G. 2006. Chapter 5 Colloid Clay Science. In Handbook of Clay Science, Volume 1, Bergaya, F., Theng, B.K.G., Lagaly, G.B.T.-D. in C.S. (Eds.), Chapter 5, pp. 141-245, Developments in Clay Science. Elsevier. https://doi.org/10.1016/S1572-4352(05)01005-6.

Lee, J. and Babadagli, T. 2018. Improvement of Microemulsion Generation and Stability Using New Generation Chemicals and Nano Materials During Waterflooding as a Cost-Efficient Heavy-Oil Recovery Method. SPE Trinidad Tobago Sect. Energy Resour. Conf., Port of Spain, Trinidad and Tobago, 25-26 June. SPE-191171-MS. https://doi.org/10.2118/191171-MS.

Lever, A. and Dawe, R.A. 1987. Clay migration and entrapment in synthetic porous media. Mar. Pet. Geol. 4(2): 112–118. https://doi.org/10.1016/0264-8172(87)90027-4.

Levine, S., Bowen, B.D., and Partridge, S.J. 1989. Stabilization of emulsions by fine particles I. Partitioning of particles between continuous phase and oil/water interface. Colloids and Surfaces 38(2): 325–343. https://doi.org/10.1016/0166-6622(89)80271-9.

Mandal, A. 2015. Chemical flood enhanced oil recovery: A review. Int. J. Oil, Gas Coal Technol. 9(3): 241. https://doi.org/10.1504/IJOGCT.2015.069001.

Miller, K.A. 2006. Improving the State of the Art of Western Canadian Heavy Oil Waterflood Technology. J. Can. Pet. Technol. 45(4). PETSOC006-04-GE. https://doi.org/10.2118/06-04-GE.

Muecke, T.W. 1979. Formation Fines and Factors Controlling Their Movement in Porous Media. J. Pet. Technol. 31(2): 144–150. SPE-7007-PA. https://doi.org/10.2118/7007-PA.

Nasralla, R.A., Alotaibi, M.B., and Nasr-El-Din, H.A. 2011. Efficiency of Oil Recovery by Low Salinity Water Flooding in Sandstone Reservoirs. SPE West. North Am. Reg. Meet., Anchorage, Alaska, 7-11 May. SPE-144602-MS. https://doi.org/10.2118/144602-MS.

Pickering, S.U. 1907. CXCVI.—Emulsions. J. Chem. Soc. Trans. 91, 2001–2021. https://doi.org/10.1039/CT9079102001.

Pratama, R.A. and Babadagli, T. 2019. Reconsideration of Steam Additives to Improve Displacement Efficiency: Can New Generation Chemicals be Solution for Steam Induced Unfavorable Wettability Alteration? SPE Annu. Tech. Conf. Exhib., Calgary, Alberta, 30 September-2 October. SPE-195833-MS. https://doi.org/10.2118/195833-MS.

Secor, R.B. and Radke, C.J. 1985. Spillover of the diffuse double layer on montmorillonite particles. J. Colloid Interface Sci. 103(1): 237–244. https://doi.org/10.1016/0021-9797(85)90096-7.

Sharma, T., Kumar, G.S., Chon, B.H. et al. 2015. Thermal stability of oil-in-water Pickering emulsion in the presence of nanoparticle, surfactant, and polymer. J. Ind. Eng. Chem. 22: 324–334. https://doi.org/10.1016/j.jiec.2014.07.026.

Tamiz Bakhtiari, M. 2015. Role of Sodium Hydroxide in Bitumen Extraction: Production of Natural Surfactants and Slime Coating. Doctor of Philosophy in Chemical Engineering Thesis, University of Alberta, Edmonton, Alberta.

Tamiz Bakhtiari, M., Harbottle, D., Curran, M. et al. 2015. Role of Caustic Addition in Bitumen–Clay Interactions. Energy & Fuels 29(1): 58–69. https://doi.org/10.1021/ef502088z.

Uddin, F. 2008. Clays, Nanoclays, and Montmorillonite Minerals. Metall. Mater. Trans. A 39: 2804–2814. https://doi.org/10.1007/s11661-008-9603-5.

Vittoratos, E., Kovscek, A.R., 2019. Doctrines and realities in viscous and heavy-oil reservoir engineering. J. Pet. Sci. Eng. 178, 1164–1177. https://doi.org/https://doi.org/10.1016/j.petrol.2019.03.044

Williams, D.J.A. and Williams, K.P. 1978. Electrophoresis and zeta potential of kaolinite. J. Colloid Interface Sci. 65(1): 79–87. https://doi.org/10.1016/0021-9797(78)90260-6.

Yan, N. and Masliyah, J.H. 1995. Characterization and demulsification of solids-stabilized oil-in-water emulsions Part 1. Partitioning of clay particles and preparation of emulsions. Colloids Surfaces A: Physicochem. Eng. Asp. 96(3): 229–242. https://doi.org/10.1016/0927-7757(94)03058-8.

Yan, Y. and Masliyah, J.H. 1993. Solids-stabilized oil-in-water emulsions: Scavenging of emulsion droplets by fresh oil addition. Colloids Surfaces A: Physicochem. Eng. Asp. 75: 123–132. https://doi.org/10.1016/0927-7757(93)80423-C.

Zhang, T., Davidson, D., Bryant, S.L. et al. 2010. Nanoparticle-Stabilized Emulsions for Applications in Enhanced Oil Recovery. SPE Improv. Oil Recover. Symp., Tulsa, Oklahoma, 24-28 April. SPE-129885-MS. https://doi.org/10.2118/129885-MS.

Chapter 4

Arhuoma, M., Dong, M., Yang, D. et al. 2009. Determination of water-in-oil emulsion viscosity in porous media. Ind. Eng. Chem. Res. 48: 7092–7102. https://doi.org/10.1021/ie801818n.

ASTM D6560-17. 2017. Standard Test Method for Determination of Asphaltenes (Heptane Insolubles) in Crude Petroleum and Petroleum Products, ASTM International, West Conshohocken, PA, www.astm.org

Aveyard, R., Binks, B.P., and Clint, J.H. 2003. Emulsions stabilised solely by colloidal particles. Adv. Colloid Interface Sci. 100–102: 503–546. https://doi.org/https://doi.org/10.1016/S0001-8686(02)00069-6.

Binks, B.P. 2002. Particles as surfactants - Similarities and differences. Curr. Opin. Colloid Interface Sci. 7: 21–41. https://doi.org/10.1016/S1359-0294(02)00008-0.

Binks, B.P. and Lumsdon, S.O. 1999. Stability of oil-in-water emulsions stabilised by silica particles. Phys. Chem. Chem. Phys. 12(1): 3007-3016. https://doi.org/10.1039/a902209k.

Bryan, J. and Kantzas, A. 2007. Potential for alkali-surfactant flooding in heavy oil reservoirs through oil-in-water emulsfication. Can. Int. Pet. Conf., Calgary, Alberta, 12-14 June. PETSOC-2007-134. https://doi.org/10.2118/2007-134.

Chen, G. and Tao, D. 2005. An experimental study of stability of oil-water emulsion. Fuel Process. Technol. 86: 499–508. https://doi.org/10.1016/j.fuproc.2004.03.010.

Chevalier, Y. and Bolzinger, M. 2013. Physicochemical and Engineering Aspects Emulsions stabilized with solid nanoparticles: Pickering emulsions. Colloids and Surfaces A: Physicochem. Eng. Asp. 439: 23–34. https://doi.org/10.1016/j.colsurfa.2013.02.054.

Eley, D.D., Hey, M.J., and Symonds, J.D. 1988. Emulsions of water in asphaltene-containing oils 1. Droplet size distribution and emulsification rates. Colloids and Surfaces 32: 87–101. https://doi.org/10.1016/0166-6622(88)80006-4.

Fan, Y., Simon, S., and Sjöblom, J. 2010. Interfacial shear rheology of asphaltenes at oil-water interface and its relation to emulsion stability: Influence of concentration, solvent aromaticity and nonionic surfactant. Colloids and Surfaces A: Physicochem. Eng. Asp. 366: 120–128. https://doi.org/10.1016/j.colsurfa.2010.05.034.

Joonaki, E., Buckman, J., Burgass, R., et al. 2019. Water versus Asphaltenes; Liquid–Liquid and Solid–Liquid Molecular Interactions Unravel the Mechanisms behind an Improved Oil Recovery Methodology. Sci. Rep. 9: 1–13. https://doi.org/10.1038/s41598-019-47782-5.

Kale, S.N. and Deore, S.L. 2016. Emulsion micro emulsion and nano emulsion: A review. Syst. Rev. Pharm. 8: 39–47. https://doi.org/10.5530/srp.2017.1.8.

Kamath, V.A., Yang, J., and Sharma, G.D. 1993. Effect of asphaltene deposition on dynamic displacements of oil by water. 1993 West. Reg. Meet., Anchorage, Alaska, 26-28 May. SPE-26046-MS. https://doi.org/10.2118/26046-ms.

Khanifar, A., Demiral, B., Alian, S.S. et al. 2011. Study of asphaltene precipitation and deposition phenomenon. 2011 Natl. Postgrad. Conf., Kuala Lumpur, Malaysia, 19-20 September. https://doi.org/10.1109/NatPC.2011.6136532.

Langevin, D. and Argillier, J.F. 2016. Interfacial behavior of asphaltenes. Adv. Colloid Interface Sci. 233: 83–93. https://doi.org/10.1016/j.cis.2015.10.005.

Lee, J. and Babadagli, T., 2020. Optimal design of pickering emulsions for heavy-oil recovery improvement. J. Dispers. Sci. Technol. 41: 2048–2062. https://doi.org/10.1080/01932691.2019.1650754.

Li, Z., Xu, D., Yuan, Y. et al. 2020. Advances of spontaneous emulsification and its important applications in enhanced oil recovery process. Adv. Colloid Interface Sci. 277: 102119. https://doi.org/https://doi.org/10.1016/j.cis.2020.102119.

Ling, N.N.A., Haber, A., Graham, B.F. et al. 2018. Quantifying the Effect of Salinity on Oilfield Water-in-Oil Emulsion Stability. Energy and Fuels 32: 10042–10049. https://doi.org/10.1021/acs.energyfuels.8b02143.

Maaref, S., Ayatollahi, S., Rezaei, N. et al. 2017. The Effect of Dispersed Phase Salinity on Water-in-Oil Emulsion Flow Performance: A Micromodel Study. Ind. Eng. Chem. Res. 56: 4549–4561. https://doi.org/10.1021/acs.iecr.7b00432.

Mandal, A. 2015. Chemical flood enhanced oil recovery: A review. Int. J. Oil, Gas Coal Technol. 9: 241. https://doi.org/10.1504/IJOGCT.2015.069001.

McClements, D.J. 2007. Critical review of techniques and methodologies for characterization of emulsion stability. Crit. Rev. Food Sci. Nutr. 47: 611–649. https://doi.org/10.1080/10408390701289292.

McLean, Joseph D. and Kilpatrick, P.K. 1997. Effects of asphaltene solvency on stability of water-in-crude-oil emulsions. J. Colloid Interface Sci. 189: 242–253. https://doi.org/10.1006/jcis.1997.4807.

McLean, Joseph D. and Kilpatrick, P.K. 1997. Effects of asphaltene aggregation in model heptane–toluene mixtures on stability of water-in-oil emulsions. J. Colloid Interface Sci. 196(1): 23–34. https://doi.org/10.1006/jcis.1997.5177.

Nenningsland, A.L., Gao, B., Simon, S. et al. 2011. Comparative study of stabilizing agents for water-in-oil emulsions. Energy and Fuels 25: 5746–5754. https://doi.org/10.1021/ef2014265.

Pickering, S.U. 1907. CXCVI.—Emulsions. J. Chem. Soc. Trans. 91: 2001–2021. https://doi.org/10.1039/CT9079102001.

Poteau, S., Argillier, J.F., Langevin, D. et al. 2005. Influence of pH on stability and dynamic properties of asphaltenes and other amphiphilic molecules at the oil-water interface. Energy and Fuels 19: 1337–1341. https://doi.org/10.1021/ef0497560.

Sharma, T., Kumar, G.S., Chon, B.H. et al. 2015. Thermal stability of oil-in-water Pickering emulsion in the presence of nanoparticle, surfactant, and polymer. J. Ind. Eng. Chem. 22, 324–334. https://doi.org/https://doi.org/10.1016/j.jiec.2014.07.026.

Wang, Z., Babadagli, T., and Maeda, N. 2021. Can we generate stable Pickering emulsions activating naturally occurring nanoparticles in the reservoir for cost effective heavy-oil recovery? Fuel 283: 118916. https://doi.org/10.1016/j.fuel.2020.118916.

Xia, L., Lu, S., Cao, G. 2004. Stability and demulsification of emulsions stabilized by asphaltenes or resins. J. Colloid Interface Sci. 271: 504–506. https://doi.org/10.1016/j.jcis.2003.11.027.

Zhang, T., Davidson, D., Bryant, S.L. et al. 2010. Nanoparticle-Stabilized Emulsions for Applications in Enhanced Oil Recovery. SPE Improv. Oil Recover. Symp., Tulsa, Oklahoma, 24-28 April. SPE129885-MS. https://doi.org/10.2118/129885-MS.

Zhou, Y., Yin, D., Chen, W. et al. 2019. A comprehensive review of emulsion and its field application for enhanced oil recovery. Energy Sci. Eng. 7(4): 1046-1058. https://doi.org/10.1002/ese3.354.